



TECHNISCHE
UNIVERSITÄT
WIEN
Vienna University of Technology



Diploma Thesis

Synthesis and Evaluation of Chiral Stationary Phases Derived from Natural Compounds for Enantiomer Separation

Submitted in satisfaction of the requirements for the degree of

Diplom Ingenieur

Under the supervision of

Univ.-Prof. Dipl.-Chem. Dr.rer.nat. DDr.h.c. Thomas Rosenau

Ass.Prof. Dr.nat.techn. Hubert Hettegger

(H77400 Institute of Chemistry of Renewable Resources, BOKU)

Assoc.Prof. Dipl.-Ing. Dr.techn. Michael Schnürch

(E163 Institute of Applied Synthetic Chemistry)

Submitted at the TU Wien

Faculty of Technical Chemistry

by

Agop Kabrelian, BSc

████████████████████

██

Vienna, January 2023

Agop Kabrelian

Declaration

I declare that I have authored this thesis independently, that I have not used other than the declared sources/resources, and that I have explicitly indicated all material that has been quoted either literally or by content from the sources used.

Date

Signature

Acknowledgments

First of all, I would like to thank my supervisor Hubert Hettegger for granting me the possibility to be part of his research group and work on such an interesting topic for my thesis. Not only his support and time investment in my thesis was appreciated but also his friendly personality, which assured a friendly atmosphere and gave me much motivation.

Especially I would like to thank my 2nd supervisor Anna Florentina Lehrhofer, MSc for her nonstop support and help whenever I needed it, and for always having an open ear to listen to any of my difficulties.

Many thanks to Prof. Thomas Rosenau and Prof. Antje Potthast for the ideas and the opportunities they provided during the past years. Because of them, I got a chance to meet many great scientists and discover my passion in the field of renewable resources.

Also, I would like to thank my supervisor Prof. Michael Schnürch for accepting to supervise from the TU Wien side and providing the ability to complete my thesis between 2 great universities. Without him, the success of this thesis would not be possible.

I also thank Cuong Viet Bui, MSc., Dr. Markus Bacher, and Ivan Melikhov, MSc. for sharing their knowledge and expertise in the field of HPLC, NMR, and synthesis and offering a helping hand, whenever difficulties arose.

I want to thank also all my friends, who have accompanied me on this challenging path.

Last but not least I want to express my deepest gratitude to my mother, sister, and girlfriend for their support, and for always believing in me in difficult times.

I dedicate this thesis to my late father Dr. Vasken Kabrelian, who was my ideal and inspiration to become a chemist from a young age.

Abstract

Living organisms represent a chiral environment: many natural but also synthetic molecules in nutrition, pharmaceuticals, agrochemicals, and fragrances are chiral. They can be found as racemic mixtures or even in their enantiopure form – for example, native homochiral L-amino acids and D-sugars. Enantiomers have different effects on biological systems in many cases. Selective isolation and identification of one of the enantiomers are challenging due to the structural similarity of enantiomers and identical physicochemical properties in an achiral environment. Within the last decades, there has been an increasing demand for highly efficient and universal separation techniques for chiral molecules in several medical and industrial fields. One of the most successful and important methods is high-performance liquid chromatography (HPLC) implementing chiral stationary phases (CSPs). CSPs based on derivatized polysaccharides, such as cellulose and amylose, gained high popularity in this field due to their natural abundance, the presence of stereocenters, and an overall chiral helical structure, making them highly suitable for enantiomer separation purposes. However, not only chiral biopolymers but also derivatives of small natural molecules like carbamoylated *Cinchona* alkaloids, *i.e.*, quinine, are efficiently used as separation materials in HPLC applications.

In the frame of this thesis, cello-oligomers were synthesized *in vitro* by cationic ring-opening polymerization (CROP) starting from glucose. After derivatization of the hydroxy groups of the oligosaccharide and other cellulose raw materials, the obtained chiral selectors (CSs) were coated onto silica for application as CSPs in HPLC. An additional stationary phase was prepared from a structural unit of quinine (*i.e.*, racemic aminoquinuclidine). All materials and their chemical structures were comprehensively characterized using analytical techniques such as liquid- and solid-state NMR spectroscopy, MALDI-TOF/MS, and elemental analysis. Different racemic and non-racemic mixtures of amino acid derivatives were subsequently synthesized and used as test analytes to evaluate the performance of the novel chiral and achiral stationary phases.

Kurzfassung

Lebende Organismen stellen eine chirale Umgebung dar: Viele natürliche, aber auch synthetische Moleküle in Lebensmitteln, Pharmazeutika, Agrochemikalien und Duftstoffen sind chiral. Sie können als racemische Mischungen oder sogar in ihrer Enantiomerenreinen Form gefunden werden – zum Beispiel native homochirale L-Aminosäuren und D-Zucker. Enantiomere haben in vielen Fällen unterschiedliche Wirkungen auf biologische Systeme. Die selektive Isolierung und Identifizierung eines der Enantiomere sind aufgrund der strukturellen Ähnlichkeit von Enantiomeren und identischen physikalisch-chemischen Eigenschaften in einer achiralen Umgebung eine Herausforderung. In den letzten Jahrzehnten gab es in mehreren medizinischen und industriellen Bereichen eine steigende Nachfrage nach hocheffizienten und universellen Trenntechniken für chirale Moleküle. Eine der erfolgreichsten und wichtigsten Methoden ist die HPLC mit CSPs. CSPs, die auf derivatisierten Polysacchariden wie Cellulose und Amylose basieren, wurden auf diesem Gebiet aufgrund ihrer natürlichen Häufigkeit, des Vorhandenseins von Stereozentren und einer insgesamt chiralen Helix Struktur bekannt, wodurch sie sich hervorragend für die Enantiomerentrennung eignen. Aber nicht nur chirale Biopolymere, sondern auch Derivate kleiner natürlicher Moleküle wie carbamoylierte Cinchona-Alkaloide, z. B. Chinin, werden effizient als Trennmaterialien in HPLC-Anwendungen eingesetzt.

Im Rahmen dieser Arbeit wurden Cello-Oligomere in vitro durch CROP ausgehend von Glucose synthetisiert. Nach der Derivatisierung der Hydroxygruppen des Oligosaccharids und anderer Cellulose-Rohmaterialien wurden die erhaltenen CSs zur Anwendung als CSPs in der HPLC auf Silica aufgetragen. Eine zusätzliche stationäre Phase wurde aus einer Struktureinheit von Chinin (d. h. racemischem Aminochinuclidin) hergestellt. Alle Materialien und ihre chemischen Strukturen wurden mit Analysetechniken wie Flüssig- und Festkörper-NMR-Spektroskopie, MALDI-TOF/MS und Elementaranalyse umfassend charakterisiert. Anschließend wurden verschiedene racemische und nicht-racemische Mischungen von Aminosäurederivaten synthetisiert und als Testanalyten verwendet, um die Leistung der neuartigen chiralen und achiralen stationären Phasen zu bewerten.

List of Abbreviations

ACN	acetonitrile
AIBN	azobisisobutyronitrile
AQ	aminoquinuclidine
AQ-AX	aminoquinuclidine anion-exchanger
ATR-FTIR	attenuated total reflectance – Fourier transform infrared
Bn	benzyl
Bz	benzoyl
CD	cyclodextrin
CE	capillary electrophoresis
CIP	Cahn-Ingold-Prelog
COSY	correlated spectroscopy
CROP	cationic ring-opening polymerization
CS	chiral selector
CSP	chiral stationary phase
DAD	photodiode array detector
DMAc	<i>N,N</i> -dimethylacetamide
DMF	<i>N,N</i> -dimethylformamide
DMSO	dimethyl sulfoxide
DNB	3,5-dinitrobenzoyl
EA	elemental analysis
Equiv	molar equivalent
GPC	gel permeation chromatography
HMBC	heteronuclear multiple bond correlation
HPLC	high-performance liquid chromatography
HSQC	heteronuclear single quantum coherence spectroscopy

MALDI	matrix-assisted laser desorption ionization
MP	microporous
MTPMS	(3-mercaptopropyl)trimethoxysilane
NP	normal-phase
Piv	pivaloyl
QD	quinidine
QN	quinine
R_f	retention factor
RP	reversed-phase
RT	room temperature
scH₂O	supercritical water
SFC	supercritical fluid chromatography
T₀	dead time
T_r	retention time
TOF	time of flight

List of Content

Declaration	i
Acknowledgments	ii
Abstract	iii
Kurzfassung	iv
List of Abbreviations	v
List of Content	vii
1. Introduction	1
1.1. Stereochemistry and Chiral Molecules	1
1.2. Separation of Enantiomers and Its Importance	3
1.3. Chiral Recognition and Separation Methods	5
1.3.1. Chiral Separation Using HPLC	8
1.4. Chiral Stationary Phases for HPLC	8
1.4.1. Ion-exchangers	10
1.4.2. 3-Aminoquinuclidine and Its Derivatives	13
1.4.3. Polysaccharide-based CSPs	14
1.4.4. Cellulose and Its Derivatives	16
2. Objective	19
3. Results and Discussion	20
3.1. Synthesis of D-Cellulose	20
3.2. Derivatization of Avicel® and sCH ₂ O-hydrolyzed cellulose	27
3.3. Pre-modification of Silica	28
3.4. Synthesis of AQ-AX Phase	28
3.5. Preparation of chiral test analytes	29
3.6. Evaluation of the AQ-AX Phase	30
4. Conclusion and Outlook	35
5. Experimental Part	36
5.1. Materials and Methods	36
5.2. Synthesis of D-Cellulose from D-Glucose	38
5.2.1. Precursor Synthesis and Polymerization	38

5.2.2. Derivatization of Avicel/scH ₂ O Cellulose	45
5.2.3. Derivatization of Silica Gel	46
5.3. Synthesis of AQ-AX Stationary Phase.....	46
5.4. Derivatization of Amino Acids.....	47
5.5. Evaluation of the AQ-AX Phase.....	48
6. References	49
7. Appendix	63

1. Introduction

1.1. Stereochemistry and Chiral Molecules

Stereochemistry describes the spatial arrangement of connected atoms forming a molecule. Many molecules, either naturally abundant or chemically synthesized, may be found in two or more different stereochemical forms. In chemistry, stereoisomerism is a fundamental phenomenon, where a set of substituents is directly bound to a stereocenter but is arranged differently relative to one another in space. If two of these molecules are non-superimposable and cannot be transformed into one another by simple rotation, this molecule is defined by the term “chiral” (Nguyen et al., 2006). The term derives from the ancient Greek word “χείρ” (*cheir*) meaning hand/handedness because chiral molecules come in so-called enantiomeric pairs, which, like our hands, are non-superimposable mirror images of each other (see **Figure 1**). Chiral molecules have at least one chiral center, mostly an asymmetric carbon atom containing four different substituents. Additionally, the absence of symmetry elements is characteristic. If symmetry elements such as a rotation axis, a plane of symmetry, or an inversion center are present, the molecule is considered achiral (Ouellette & Rawn, 2015; Roos & Roos, 2015). However, also molecules containing other chiral centers than classical asymmetric carbon atoms are considered chiral, *i.e.*, molecules exhibiting planar chirality, lone-pair-induced chirality, or axial chirality (Davankov V.A, 1997; López & Palomo, 2022; Wang et al., 2021; Xin & Pope, 1996).

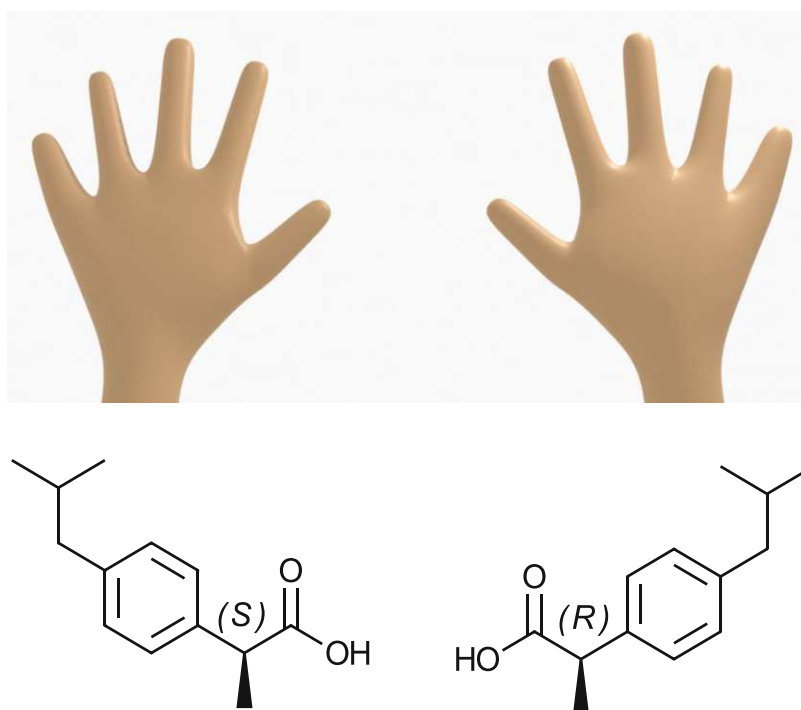


Figure 1: Examples of chiral structures (macroscopic hands and molecular ibuprofen enantiomers).

Meso compounds are examples of achiral stereoisomers (Ouellette & Rawn, 2015). When a molecule contains more than one chiral center, the molecule can form both, enantiomeric and diastereomeric pairs. Enantiomers are optical isomers, which are non-superimposable mirror images of each other, whereas diastereomers are geometric isomers and are non-mirror images (Chhabra et al., 2013; Grybinik & Bosakova, 2021a; Metcalfe & Reilly, 2010; Ouellette & Rawn, 2015).

Although many molecules are found in nature enantiopure, such as D-amino acids (except glycine) (Abdulbagi et al., 2021), other molecules and synthetic pharmaceuticals such as ibuprofen, are found as pairs of enantiomers (see **Figure 1**).

Enantiomeric pairs can be differentiated by either stating their absolute configuration (*R*) or (*S*) (*rectus* or *sinister*; assigned by Cahn-Ingold-Prelog (CIP) nomenclature), which is defined by their geometry, or by giving their rotational configuration D or L (*levo* or *dextro*, assigned by Fischer nomenclature), or by the overall rotation direction of polarized light by a chiral molecule (+ and -, clock- and anticlockwise). In many cases, such as after conventional achiral chemical synthesis, both enantiomers are obtained in equimolar amounts, which is referred to as a racemic mixture/racemate or not enantiopure (H. Brooks et al., 2011; Metcalfe & Reilly, 2010).

However, as most natural molecules are obtained from a precise synthesis involving highly efficient and specific enzyme catalysis, many of them are found in their enantiopure form, e.g., L-amino acids or D-sugars (Abdulbagi et al., 2021; Gu et al., 2021). As they consist of these naturally chiral molecules, living organisms, and ultimately also nature in general, provides a highly chiral environment. Thus, two enantiomers might have completely different effects on our biological system, such as a different smell or taste. In fragrance and flavor industries this often causes difficulties, as many metabolites, developed drugs, and synthetic molecules are typically obtained in their racemic form (Finefield et al., 2012).

Since enantiomers, unlike diastereomers, have, except for their optical rotation, identical physical and chemical properties, separation of the chiral molecules is very difficult and requires highly advanced separation techniques in a chiral environment (Guo-Qiang Lin, 2011; Ouellette & Rawn, 2015). As stated before, our human body is full of chiral biological receptors, providing a chiral environment for chiral molecules. This chirality allows not only the ability to distinguish two enantiomers from one another but also to interact differently with them, causing distinct effects on our bodies (Baykusheva et al., 2019). This chiral environment requires a better understanding of chirality since two enantiomers used as fragrances or pharmaceuticals frequently show different properties such as unpleasant effects, toxicity, dosage efficiency, and rate of metabolism. This can be explained by the highly specific biological receptors and active sites of enzymes in our body, which can easily distinguish two enantiomers. Their different interaction with these biological receptors leads to unequal reactions and responses in living organisms. Therefore, the separation of enantiomers with a good understanding of their stereochemistry is crucial to regulate the bioactivity of a chiral chemical molecule (Abate et al., 2005; Heuberger, 2001; McConathy & Owens, 2003; Nguyen et al., 2006).

One example of such different effects is the essential oil of citrus peels. This oil contains the molecule limonene (see chemical structure in **Figure 2**), which is found

as (*R*)-(+)- and (*S*)-(-)-limonene in its racemic mixture, due to one chiral center. The peel of oranges contains high amounts of the (*R*)-(+)-limonene giving orange peel its characteristic smell, whereas lemon peel contains only the (*S*) enantiomer, which causes the distinct smell of the latter (Isac-García et al., 2016). Another example in **Figure 2** is a pyranol (Florol®) used in the fragrance industry. This molecule contains two stereogenic centers, therefore having four different stereoisomers ((*RR*), (*RS*), (*SR*), and (*SS*)). Out of these, only two are used in the fragrance industry, since the other two stereoisomers are completely odorless in our perception (Abate et al., 2005).

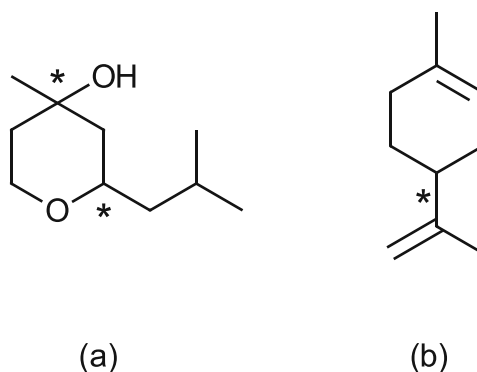


Figure 2: Molecular structures of Florol® and limonene.

1.2. Separation of Enantiomers and Its Importance

Although a lot of effort was and is put into the development of asymmetric syntheses, enantiomer separation persists to be the method of choice to obtain enantiopure products. This is mostly because asymmetric synthesis is still neither cost-efficient nor well-established for a broad range of substrates. Besides racemic products obtained from chemical synthesis, many molecules extracted from nature are obtained as mixtures of two enantiomers. Their similarity in physicochemical properties on the one hand and the difference in pharmacokinetic properties on the other hand lead to an increase in the importance of their identification and separation (Bingyun Li & Donald T. Haynie, 2005; Blackmond, 2019; P. Guo et al., 2022; Y. Liu et al., 2022).

In the history of mankind, due to a lack of knowledge and proper analytical methods, there are several examples where racemic mixtures were employed, although only one enantiomer had the desired effect on the human body, especially when talking about pharmaceutical applications. Although several methods for the characterization of enantiomers are well established, many drugs are still sold in their racemic form (carrying so-called “enantiomeric ballast”), even though it is known that in certain cases only one of the enantiomers is responsible for the desired or has a higher therapeutic effect and fewer side-effects in our body (so-called “eutomer), e.g. dexibuprofen (Evans, 2001). This can be done given that the other enantiomer is inactive or less active (so-called distomer), harmless, or can be transformed into the active one by, e.g., isomerases in our body. However, in some cases, the non-therapeutic enantiomer may cause severe side effects or puts an extra burden on specific organs (Fassihi, 1993).

One of the most famous yet tragic examples of racemic drugs in history is thalidomide (Contergan®) (see chemical structure in **Figure 3**). Its (*R*) isomer was a promising mild sedative for pregnant patients, whereas the (*S*) isomer was later found to be teratogenic. Since the drug requirements were not as severe as they are now before approval, it caused thousands of deformities in the children of pregnant women who took Contergan® (Cossy, 2012). Another example of the importance of enantiomer separation is dopamine. One of its isomers is used to treat Parkinson's disease (levodopa), whereas the other is toxic (Bingyun Li & Donald T. Haynie, 2005). Similar cases are found in the food industry. Fruit juices for example must contain only L-amino acids because D-amino acids can cause health problems upon bad preservation (Bui et al., 2021).

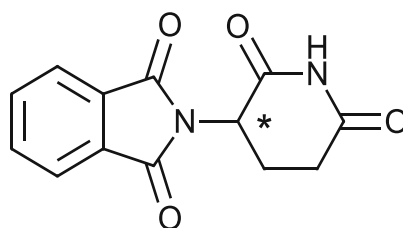


Figure 3: Chemical structure of thalidomide (Contergan®).

An additional reason for the application of enantiopure drugs, besides the potential harm the non-therapeutic enantiomer might cause, is the decreased potency of racemic mixtures. It was shown that, if more than 50% consists of inactive isomers, this makes an increase in the drug dosage necessary for the drug to still be efficient (Fassihi, 1993). When drugs are provided in their enantiopure form, however, they can be more efficient at lower drug dosages, preventing adverse effects and toxicity, while also improving the time of action (Hancu & Modroiu, 2022; Long et al., 2021; McConathy & Owens, 2003; Sekhon, 2013). To make enantiopure pharmaceuticals accessible, careful separation and characterization are required.

One general way to characterize absolute configuration and identify the enantiopurity of a mixture is to use a polarimeter. In the polarizer, unpolarized light is polarized. By passing the enantiomers in the polarimeter tube, polarized light is rotated depending on the optical activity of the molecules in the solution (see **Figure 4**). With different rotation directions, optical purity and enantiomeric excess can be determined (Ouellette & Rawn, 2015). Since chiral molecules are optically active, enantiomers rotate polarized light in the opposite direction. Hence, by measuring the rotation direction, and optical purity, the enantiomeric excess (*(R)* and *(S)* ratio) of the molecule can be determined. However, in racemic mixtures, enantiomeric pairs exist in a 1/1 ratio, showing no optical activity. This phenomenon occurs because one rotation cancels the other leading to zero rotation of the light, hence no optical activity is detected (Bougas et al., 2022; Gogoi et al., 2021; Hellwich, 2002; Nguyen et al., 2006; Shinoda et al., 2005).

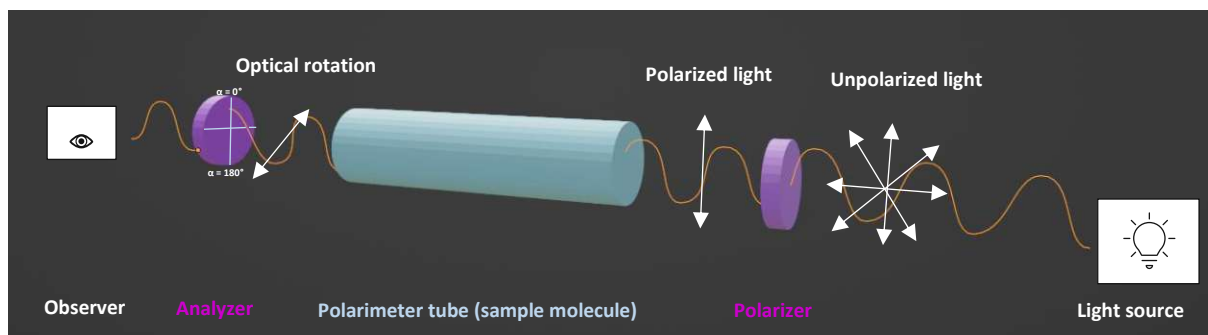


Figure 4: The concept of a polarimeter.

Two properties, determined by polarimetry, are optical purity (OP) and enantiomeric excess (ee). These values can be used as measures for the enantiopurity of a substance, for example, to evaluate if a synthesis or separation was effective. Their values are calculated according to the following equations:

$$\%OP = \frac{[\alpha]_{mixture}}{[\alpha]_{pure}} \times 100$$

$$\% ee = \frac{|[R]-[S]|}{[R]+[S]} \times 100$$

α = specific optical rotation

Within the last decades, the increasing demand for enantiopure chemical molecules triggered the development of novel chiral separation methods. Numerous techniques have been established and are still being improved to not only analytically, but also preparatively separate enantiomers. The main goal of recent developments is the reduction of material waste as well as a more universal applicability while still offering good separation efficiency and selectivity.

1.3. Chiral Recognition and Separation Methods

As mentioned above, enantiomers have identical physicochemical properties, except for their optical rotation. Therefore, they are difficult to distinguish and impossible to separate in an achiral environment. However, distinguishing enantiomers in an achiral environment is possible by NMR spectroscopy, either by forming true diastereomers or diastereoisomeric interactions. This is possible either by derivatization agents (e.g. Mosher's acid) (Allen et al., 2008) or by chiral solvating agents or enantiomerically pure chiral shift reagents (Balzano et al., 2018; Calvello & Soncini, 2020).

For enantiomeric separation, methods like kinetic resolution using enzymatic hydrolysis/esterification or crystallization implementing chiral auxiliary agents can be used. However, these methods are highly complex and the enantiopurity of the separated products is sometimes not satisfactory (Harada, 2016; José et al., 2016; Viedma et al., 2015).

The most popular strategy to (analytically but also preparatively) separate enantiomers is the use of different kinds of chromatography since they are fast, efficient, and consume only small amounts of analytes. In chromatography, separation is achieved either by transforming enantiomers into diastereomers or by achieving transient

diastereomeric interactions, based on the vivid (but often discussed and challenged) three-point interaction model (Berthod, 2010a; Didier et al., 2008; Geoffrey B. Cox, 2005; Hellwich, 2002).

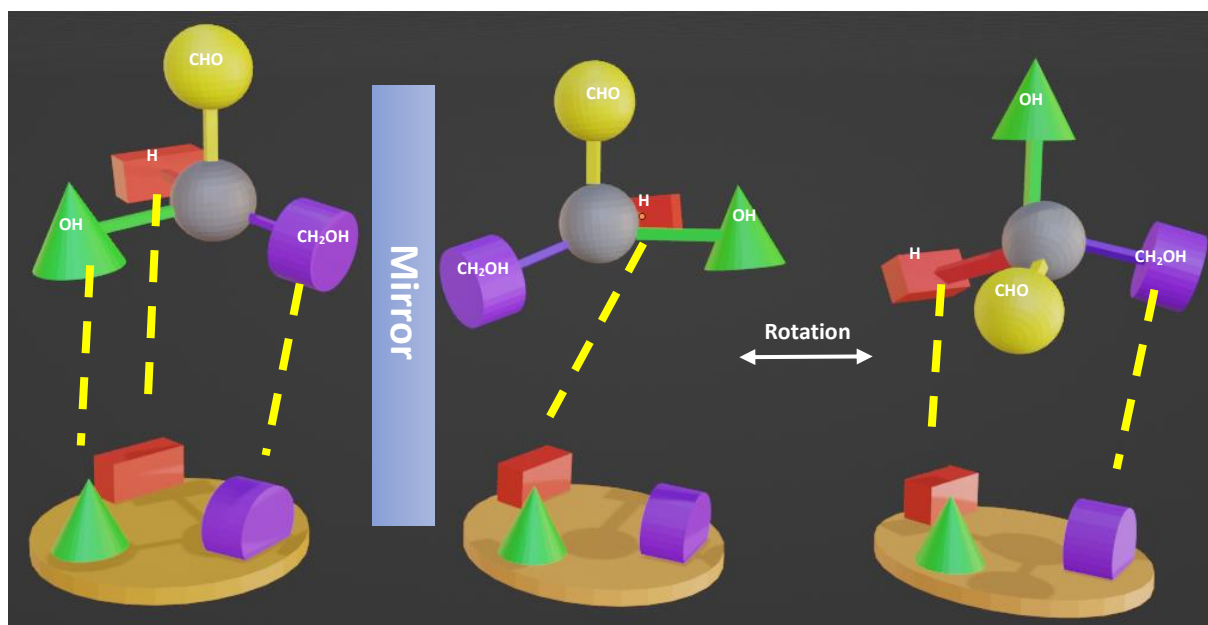


Figure 5: Visualization of stereoselectivity by a three-point interaction (McConathy & Owens, 2003).

Figure 5 shows a schematic visualization of the three-point interaction model. In the example, one enantiomer of glyceraldehyde achieves the three-point interactions with the receptor, while the other enantiomer lacks two (matching) interactions. After multiple rotations, the latter still lacks one interaction (McConathy & Owens, 2003). The three-point interaction is one model to explain the stereoselective interaction of chiral molecules with a chiral receptor or selector, which can also be applied to natural stereoselective processes. This model is adapted to separate enantiomers using a chromatograph, since a three-point interaction could provide strong interactions, hence longer retention of one enantiomer on the stationary phase. The chiral recognition in the case of the three-point interaction model can be explained by different forces, such as Coulomb forces, hydrogen bonding, steric hindrance, van der Waals forces, π -bond interactions, etc. A combination of the latter causes the difference in retention and thus separation of enantiomers (Armstrong et al., 1994; Berthod, 2010a).

Thermodynamics is another parameter, which plays a crucial role in the recognition and separation of enantiomers since the binding of each enantiomer to a chiral selector (CS) is related to the standard Gibbs free energy. This relationship can be derived from the following equation, where the binding constant of each enantiomer is related to the standard Gibbs free energy change:

$$\Delta G^{\circ}_{R/S} = -RT \ln K_{R/S}$$

R = gas constant

T = absolute temperature (K)

K = binding constant

If the binding of one of the enantiomers to the CS is exothermic (*i.e.*, the Gibbs free energy change is negative) compared to its unbound counterpart, this will lead to strong interaction and longer retention of the enantiomer. However, since the Gibbs free energy is dependent on enthalpy and entropy changes, then the dependency can be defined by the following equation:

$$\Delta G^{\circ}_{R/S} = \Delta H^{\circ}_{R/S} - T \Delta S^{\circ}_{R/S} \quad [*]$$

ΔH° = enthalpy (measurement for the binding)

ΔS° = entropy (disorder magnitude upon complex formation)

By combining the previous equations, the *van't Hoff* equation is obtained:

$$\ln K_{R/S} = -\frac{1}{T} \frac{\Delta H^{\circ}_{R/S}}{R} + \frac{\Delta S^{\circ}_{R/S}}{R}$$

This equation allows us to determine how enantiomers form a complex with the chiral selector through the slopes and intercepts when $\ln K_{R/S}$ is plotted against $1/T$.

When assuming that one enantiomer is bound to the selector by strong interactions but the other is free, a difference appears in Gibbs free energy changes ($\Delta\Delta G^{\circ}$) of each enantiomer. This difference helps us define the enantioselectivity (α) of a chiral selector towards a certain enantiomer. For example, if enantiomer (*R*) is bound stronger to the CS than its (*S*) form ($K_R > K_S$), then the first equation can be transformed into:

$$\Delta\Delta G^{\circ}_{S,R} = \Delta G^{\circ}_R - \Delta G^{\circ}_S = -R \cdot T \ln \frac{K_R}{K_S} = -R \cdot T \ln \alpha$$

$\Delta\Delta G^{\circ}$ = Gibbs free energy difference

α = chromatographic selectivity factor

This equation is then combined with equation [*] and subsequently, $\ln \alpha$ is plotted against $1/T$. In this way, enantioselectivity is calculated by the enthalpy and entropy differences (Ahuja, 2010; Barth G. H., 2018; Castells & Carr, 2000; Lämmerhofer, 2010; Oberleitner et al., 2002).

Most applied chromatographic methods based on three-point interaction are supercritical fluid chromatography (SFC), GC, and HPLC. Capillary electrophoresis (CE) is another non-chromatographic method. CE, in comparison to chromatographic separation methods, can separate enantiomers based on their different interaction with the mobile CS when an electrical field is applied. This mobile CS causes a difference in migration times in CE, whereas in chromatographic techniques the CS is usually immobilized as a CSP – however, also chiral mobile phase additives are also possible (Berthod, 2010b; B. Li & Haynie, 2005). Although CE is proven to be more cost-efficient, simpler, and faster compared to chromatography, their sample volumes, success rates, and reproducibility rates are relatively low and require more method development.

Chromatographic methods are generally well-established in the field of chiral separations; however, each form has its advantages and disadvantages. For example, in GC a broad variety of solvents can be used for sample dissolution. However, not all

chiral analytes are volatile and thermally stable, limiting the use of GC. HPLC is frequently the method of choice for enantioseparation since various analytes are well separated with high reproducibility and it is applicable to both, analytical as well as preparative scales. Additionally, its dependency on three main parameters (mobile phase, CS or chiral stationary phase (CSP), and analyte) makes it flexible for method adjustments (B. Li & Haynie, 2005).

1.3.1. Chiral Separation Using HPLC

In general, there are three main strategies for chiral separation using HPLC, which can be classified into direct and indirect methods. When the CS is incorporated into/onto the stationary phase, *i.e.*, a chiral stationary phase, these are considered direct methods. On contrary, when an enantiopure derivatizing agent is added to the mobile phase to form (transient) diastereomers, this is called an indirect separation. It is important to note that in the case of an indirect method or mobile phase chiral addition an achiral separation material can be used (Arenas et al., 2021; Berthod, 2010a; Grybinik & Bosakova, 2021a).

When the above-mentioned additional interactions are neglected, one enantiomer will stereoselectively bind to the CS on the stationary phase by strong three-point interaction, whereas the other enantiomer will elute faster due to weaker interaction, leading to a difference in retention time. By this, the separation and isolation of the two enantiomers can be achieved.

To achieve successful separation, the difference between the retention factors of the enantiomers should be as high as possible within a short retention time. Therefore, the choice of CSP and mobile phase plays a crucial role in efficient separation. However, many other parameters, such as additional interactions (mentioned above), counter ions, buffers, temperature, and mobile phase pH affect the retention time (Davankov V.A, 1997).

Indirect separation by derivatization into diastereomeric molecules is not only complicated since additional steps are required for preparation, but also limited by the fact that the auxiliary derivatization agents have to be highly enantiopure and should be easily cleaved off after separation, especially on preparative scales. On the contrary, little optical impurities of CSPs in the direct method do not affect the enantioseparation dramatically (Bargmann-Leyder et al., 2000; Berthod, 2010a; Betzenbichler et al., 2022; Robards et al., 2004; J. Zhang et al., 2022), therefore making the latter much more applicable and efficient. Additionally, it is the most investigated method since there is a huge number of CSPs commercially available (Sanganyado et al., 2017).

1.4. Chiral Stationary Phases for HPLC

Nowadays, the development of CSPs is intensively studied and many new CSPs are being designed. The main goals are to achieve better functional group specificity, applicability to a wider substrate scope of chiral molecules, and to improve the resolution in the separation of racemic mixtures (Wahab et al., 2018). CSPs are

prepared either from naturally abundant molecules or chemically synthesized to design specific interaction sites and in turn, enhance enantiomer separation. Although synthetic selectors may be advantageous, as elution orders can be well controlled and different interactions can be established by careful designing (Berthod, 2010a; Pirkle et al., 1981; Wahab et al., 2018), they have several drawbacks. Nowadays mostly natural (homochiral and thus enantiopure) molecules are derivatized or modified to improve their properties for chiral separation and add interaction sites (Berthod, 2010a).

The classification of CSPs is quite difficult since they can be categorized by various properties such as the type of interaction they induce, the molecular weight of the chiral selector, or the functional groups they offer. Additionally, many novel groups of selectors have been introduced within the last decades (Lough, 2014). The two classifications which are most commonly used are based on size and interactions according to the Wainer Types I-V classifications. The latter are shown in **Table 1** below (Arenas et al., 2021; Boratyński et al., 2019; Grybinik & Bosakova, 2021a; Hettegger et al., 2020; Lämmerhofer, 2010; Lough, 2014; Sharp et al., 2014; Teixeira et al., 2019).

Table 1: Different classifications of CSPs.

Classification according to the size		Classification according to the main mode of interaction	
Size	Types of chiral selectors	Main interactions	Types of chiral selectors
Macromolecule-based	Polysaccharide-based, protein-based, molecularly imprinted polymer-based	Attractive interactions (π - π bond, dipole, hydrogen bonds, ionic interactions)	Chiral ion exchangers (QN-AX, QD-AX), Pirkle type
Macrocyclic molecule-based	Cyclodextrin-based, crown ether-based	Attractive interactions and inclusion	Polysaccharides (cellulose derivatives), crown ethers
Small molecule-based	Ion exchanger (<i>Cinchona</i> alkaloids), Pirkle type	Inclusion in cavities	Cyclodextrins (CD), crown ethers, helical polymers

		Hydrophobic and polar interactions	Proteins
--	--	------------------------------------	----------

For a chiral selector to be used commercially, its analyte-CS complex formation needs to have a high kinetics and thermodynamics profile, it should be universal for a wide scope of analytes, be cheap, and be suitable for different chromatography modes. Also, its application should be efficient not only in analytical but also on a preparative scale (Chankvetadze, 2012).

One type of CSPs, which is very popular and abundantly used, is the macrocyclic cyclodextrin-based (CD) selectors. The CD's glucose units exhibit many OH groups allowing hydrophilic interactions and hydrogen binding outside of the macrocycle, whereas the inner side is hydrophobic allowing hydrophobic interactions (Patil et al., 2018). However, the applicability of CDs is limited when complex or big analytes are used due to the limited cavity sizes of the different CDs. Since their main separation mechanism is based on their rather small structural cavities, only small molecules can enter them (Yu & Quirino, 2019). Another popular CSP type is synthetic polymer-based selectors since many different properties and structures can be finely tuned. One example of such optically active helical polymers is polymethacrylates (Nakano, 2001). However, the drawback of these synthetic polymers is that most of them either swell or shrink in the mobile phases during measurements and their column efficiency is very low (J. Guo et al., 2020). Other CSPs, which are well established and commercially available, are the ion-exchanger-based and the polysaccharide-based types.

1.4.1. Ion-exchangers

Since many chiral analytes are also charged, such as peptides, amino acids, amines, and acids, ion exchangers have been widely used as CSPs to efficiently separate charged chiral enantiomers. The concept of this approach is that the CS on the stationary phase is either ionized or contains an ionic unit, which can interact with the counter ion on the chiral analyte forming an ion-pair (Piette et al., 2003; Wolrab et al., 2021). Many different CSPs, such as proteins, amino acids, or macrocyclic molecules can be classified as ion-exchanger if they contain charged functional groups and are capable of forming ionic interactions (J. Guo et al., 2020).

In the class of ion exchangers, one can distinguish three different types, *i.e.*, cation-, zwitterion-, and anion-exchangers (AX). Cation-exchangers are charged molecules based on negatively charged carboxylic (weak) or sulfonic acid (strong) groups and interact with positively charged analytes, such as bases and amines. AXs on the contrary contain positively charged groups, like protonated amine groups with quaternary ammonium ions being the strongest type of AXs. These interact electrostatically with negatively charged ionized analytes, mainly organic acids, and thus cause longer retention times for the analyte on the CSP. AXs show excellent chiral discrimination with many chiral analytes, especially when *N*-protected amino acids are used (Grinberg & Carr, 2017). In the case of cation-/anion-exchangers, the ionic pairing between analyte and selector can sometimes be very strong, in which counter-ions are

required as competitors to elute the retained analyte faster, hence significantly shortening the analysis time (Cavazzini et al., 2011; Hoffmann et al., 2007).

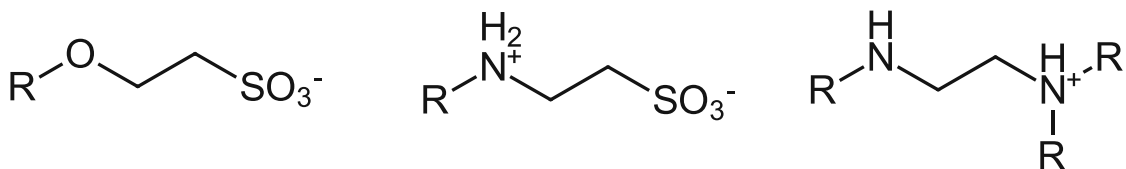


Figure 6: Example of cation- (left), zwitterion- (middle), and anion-exchangers (right) (Wolrab et al., 2021).

In case both, cation- and anion-exchanger units, are present in the CS, this type of CSP is called a zwitterion-exchanger. One example of the latter is a derivatized *Cinchona* alkaloid (a type of AX), in which a cation-exchanger group is added. Zwitterion-exchangers can attract and repulse two different enantiomers at the same time. This parallel attraction and repulsion are achieved due to the contribution of the oppositely charged groups, making the zwitterion exchangers not only applicable to acidic but also basic and zwitterionic analytes. Additionally, they are less sensitive to mobile phase changes and require no additional displacers in the mobile phase as one of the groups acts as the counter-ion. This automatically improves the speed of the elution and analysis time (Bajtai et al., 2018; Hoffmann et al., 2009).

In the case of ion-exchanger-based CSPs, the main interactions are ionic, however, the mobile phase composition also plays a role in providing additional hydrophobic and hydrophilic interaction sites if long chains, aromatic rings, or carbonyl groups are present. Further, the addition of acidic or basic units in the mobile phase can act as a co- or counter-ion and therefore affect analysis times (Wolrab et al., 2021). All three types of ion-exchanger-based CSPs share the same mobile phase compatibility, in which reversed-phase and polar-organic modes with the addition of buffers are well investigated (Hoffmann et al., 2009; Mandl et al., 1999; Teixeira et al., 2019; Wolrab et al., 2021). However, one major limitation of ion-exchanger-based CSPs is that they all require charged or ionized analytes, otherwise, a neutral analyte leads to instant elution without any interaction.

Recently, two or three types of selectors were combined to achieve additional interactions besides the main interaction mode. For instance, long hydrophobic chains, which are typically used for reversed-phase chromatography, and/or polar units such as amides, which are frequently found in normal-phase type stationary phases, are combined with an ion-exchanger-type selector to form mixed-mode chromatographic phases. In this type, the three different modes of interaction (hydrophobic, ionic, hydrophilic) are on the same level of importance, leading to high resolution and unique selectivity not only for charged analytes but also for inorganic and polar organic analytes (K. Zhang & Liu, 2016).

To transform a CS into a CSP, it usually needs to be brought onto a (mechanically robust) chromatographic support such as microporous silica (MP silica), either by coating or by chemical immobilization. When the selector is coated, the scope of solvents applicable as the mobile phase is significantly limited. Thus, most of the AX-based selectors are immobilized onto silica, which can be done by radical polymerization, coupling agents, polycondensation or click chemistry, etc. (Fernandes et al., 2021). Within these methods, click chemistry using radical-mediated thiol-ene addition (see **Figure 7**) to a double bond, *i.e.* Michael addition, and alkyne-azide

cycloaddition are the most popular ones (Lowe, 2010; Sun et al., 2018). An alternative approach is the amidation of carboxylic-acid type selectors onto 3-aminopropyl silica (e.g., with a coupling agent) (Cavazzini et al., 2011; Fernandes et al., 2021; Kohout et al., 2018). In the thiol-ene addition method, azobisisobutyronitrile (AIBN) is frequently used as a radical thermal- or photoinitiator. First, a thiol is transformed into the radical thiyl, which in turn hydrothiolates double or triple bonds (ene or yne) by a Michael addition mechanism. Chain transfer takes place until the termination is achieved by radical-radical coupling. Via this coupling mechanism, stable bonds between the CS and the chromatographic support (e.g., mercaptopropyl-modified silica) are formed, leading to highly solvent-resistant CSPs.



Figure 7: Radical mediated thiol-ene addition.

1.4.2. 3-Aminoquinuclidine and Its Derivatives

Although all kinds of molecules can be modified to be ion-exchanger, mainly *Cinchona* alkaloids, such as quinines (shown in **Figure 8**) containing a quinuclidine ring and their derivatives are used due to their high abundance in nature and low cost. They are used as AX due to the charged amine groups. However, also a zwitterion-exchanger is accessible by introducing cationic exchanger groups on the *Cinchona* alkaloid. *Cinchona* alkaloid-based CSPs do not only achieve high enantioselectivity but also interact with various ionized analytes at low-molecular weights (Cavazzini et al., 2011) and are already commercially available under the names CHIRALPAK® QN-AX and CHIRALPAK® QD-AX (Tanács et al., 2021).

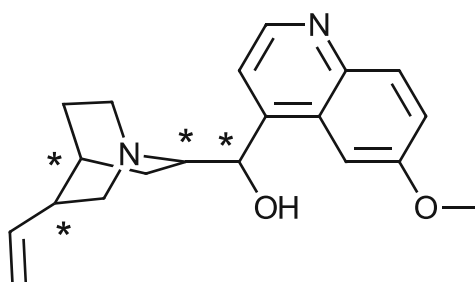


Figure 8: Chemical structure of quinine.

Cinchona alkaloids, such as quinines, quinidines, cinchonines, cinchonidines, and dihydroquinidines, are chiral molecules and found naturally in many stereoisomers due to the presence of four chiral carbon centers and one stereogenic pyramidal nitrogen in their structure (Sharma & Anand, 1997). One advantage of quinine and quinidine is that they are *pseudo*-enantiomeric to each other and often give different elution orders of enantiomeric analytes. This makes it possible to analyze trace molecules or

impurities, which is difficult in the case of using other macromolecules (Lämmerhofer & Lindner, 1996).

Besides their use in stereochemistry and asymmetric synthesis, *Cinchona* alkaloids have been found to be a good choice for CSPs. Cinchonidine and other modifications are capable of inducing interactions necessary for chiral discrimination of acidic chiral analytes, e.g., amino acids (Boratyński et al., 2019; Geoffrey B. Cox, 2005; Sarasamkan et al., 2016).

Cinchona alkaloids like quinine and quinidine have an asymmetric carbon in the 9-position, which plays a main role in chiral discrimination. Further, this position is an attractive site for several kinds of derivatizations to fine-tune its properties (Hoffmann et al., 2009). One example is carbamoylated quinine, which is available commercially and a good choice to separate acidic chiral enantiomers, such as *N*-acylated peptides or *N*-derivatized amino acids. Its interactions are based on quinuclidine's ability to interact with the acidic analytes since the nitrogen of its tertiary amine is more basic than other nitrogen atoms in the *Cinchona* alkaloids. Therefore, it forms a cation upon protonation in a polar, acidic mobile phase (Czerwenka et al., 2003), which can further form ion pairs with negatively charged analytes, such as carboxylate groups (Piette et al., 2003). Other interactions, such as hydrogen bonding, dipole-dipole interactions, π - π , van der Waals forces, and steric interactions are accompanied by ionic interaction. Thus, derivatizing ionic analytes like amino acids with groups providing additional interaction sites leads to stereoselectivity enhancement. For example, when derivatizing amino acids with 3,5-dinitrobenzoyl or benzoyl groups, the electron-deficient aromatic ring interacts with the electron-rich quinoline ring by π - π interactions. Additionally, the carbonyl groups of the analyte or the carbamate of the chiral selector form weak hydrogen bonds with the NH group of the selector or the amino acid analyte, respectively. The absence of these additional interactions may dramatically affect stereoselectivity (Boratyński et al., 2019; Mandl et al., 1999; Piette et al., 2002).

To load quinine and quinidine-based ion-exchangers on CSPs, mostly immobilization is performed according to the above-mentioned click chemistry strategies (thiol-ene and alkyl-azide reactions).

Since the 3-aminoquinuclidine (QA) ring is present in most *Cinchona*-based AXs, many novel CSPs have been developed based on this structure. Nogueira and colleagues developed a mixed-mode stationary phase based on a 3-aminoquinuclidine ring, namely *N*-(10-undecenoyl)-3-aminoquinuclidine. This brush-type selector has been developed as a mixed weak AX- and RP-type stationary phase (Nogueira et al., 2005).

1.4.3. Polysaccharide-based CSPs

Polysaccharide-based CSPs gained much interest and are widely investigated, not only because they meet most of the requirements mentioned above. The presence of several stereogenic centers, the well-aligned polymer chains allowing supramolecular chirality, its helical structure allowing conformational chirality and their ability to separate a huge number of enantiomers with high selectivity, sensitivity, and reproducibility make them a convenient choice for the development of CSPs. Further, their high natural abundance as well as their typically low cost make them attractive for

utilization as a starting material. Many polysaccharide-based selectors using chitin and chitosan are in development, however, the most successful polysaccharides used as CSPs are cellulose and amylose. The choice of one of them over the other relies merely on the chiral analyte type (Arenas et al., 2021; Bui et al., 2021; Lämmerhofer, 2010; Petrie et al., 2019; Ribeiro et al., 2017).

Since natural polysaccharides are typically characterized by only limited chiral resolution, cellulose and amylose are mostly derivatized to improve their properties. A great variety of substituent groups, such as alkyls, esters, ethers, or cyclic substituents such as benzyl carbamates, phenyls, benzoates, or aryls were attached to the hydroxy groups of the polysaccharides. In this way, modified polysaccharides with improved properties, in addition to their natural advantages, were obtained. However, two of the most successfully derivatized polysaccharides for use as CSPs are aromatic esters and carbamates, e.g., 3,5-dimethylphenyl carbamate derivatives. These groups provide further interaction sites by hydrogen bonding between the NH and CO groups of the carbamates, whereas the phenyl ring allows for interactions *via* π - π and van der Waals forces (Chankvetadze, 2012; Ikai & Okamoto, 2009; Okamoto & Kaida, 1994; Petrie et al., 2019; Qiu et al., 2013; Scriba, 2019; Teixeira et al., 2019).

However, it has been proven that the type, number, and position of the substituents on the phenyl groups play a crucial role in the ability of chiral recognition (Shen et al., 2014). For example, an electron-withdrawing or donating substituent on the carbamate group causes better chiral recognition by disrupting the carbamate polarity and thus enhancing the analyte-selector interaction. When a non-polar electron-donating substituent is introduced to the carbamate group, the electron density of the carbonyl oxygen is increased. Hence, the analytes are retained more through stronger hydrogen bonding with the carbonyl groups of the CS. Regarding the substituent position, it was shown that ortho-substitution on the phenyl group causes weak chiral recognition. Substituents in the ortho-position of the phenyl ring prevent the formation of a liquid crystalline phase, which is a requirement for efficient chiral recognition (Hettegger et al., 2020; Ikai & Okamoto, 2009; Okamoto et al., 1987). Another factor affecting chiral separation performance is the degree of polymerization (DP) of the polysaccharide. It was shown that only long polysaccharides with a minimum DP = 18 are suitable for good chiral recognition (Hettegger et al., 2020).

Initially, these polysaccharide selectors have been tested without chromatographic support, but this showed problems regarding the thermodynamic and kinetic properties of the selectors. Thus, coating them onto the surface of microporous silica beads was tested, leading to higher mechanical stability and better accessibility of the interaction sites (Lämmerhofer, 2010). The coating is done by dissolving the CS in an organic solvent and subsequently mixing the solution with 3-aminopropyl-functionalized silica. Upon evaporation, the selector is coated onto the silica surface. However, many eluents disrupt the coating, leading to significant mobile phase limitations (Fernandes et al., 2021; Qiu et al., 2013). For example, solvents such as DCM, toluene, or acetone are usually not compatible with coated selectors, since they, depending on the type of substituents on the CS, might dissolve and elute the latter. Immobilization, as mentioned earlier, is another method, which allows enhanced resistance of the CSP and compatibility with a wider range of mobile phases. Nevertheless, immobilization in the case of cellulose or amylose reduces the flexibility and alters the stereoselective conformation. This, in turn, disrupts the supramolecular structure and optimal

secondary structure, which might affect the resolution. Additionally, polar amino groups might disappear upon cross-linking and the synthesis of active sites prone to form linkages requires additional derivatization steps, making immobilization less popular than coating (Hettegger et al., 2020; Qiu et al., 2013; Scriba, 2019; Teixeira et al., 2019).

1.4.4. Cellulose and Its Derivatives

Cellulose is a biopolymer based on cyclic anhydroglucopyranose monomer units linked by glycosidic linkages. As seen in **Figure 9**, glucose is naturally found in the D-form. When D-glucose is cyclized by hemiacetal formation, two diastereomers/anomers are distinguished, α and β , due to the newly formed chiral carbon C1 (the previously *prochiral* carbonyl), but only the β -form is found in cellulose since it is strictly linked in a β -(1 \rightarrow 4) manner (Rosanoff, 1906). Cellulose is naturally optically active and can be found in highly ordered crystalline forms. It exhibits right-handed chirality due to five asymmetric carbon centers (C1-C5) and usually forms helical secondary structures (Lehrhofer et al., 2022). These properties, as well as their low cost due to the extremely high natural abundance, make cellulose a good choice for stereochemical applications. One example is the commercial use of microcrystalline cellulose in asymmetric synthesis as a chiral catalyst (Kaushik et al., 2015; Khandelwal & Windle, 2014; Usov et al., 2015).

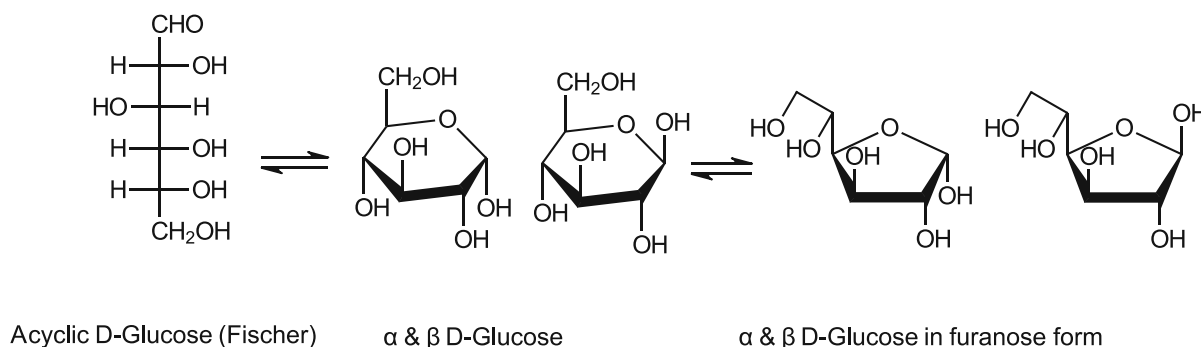


Figure 9: Different structural isomers of D-glucose.

Cellulose is usually derivatized to obtain a CS (Kato et al., 2011; L. Li et al., 2020). However, mostly, ordinary pulp or microcrystalline cellulose, such as commercially available Avicel[®], has been used for the preparation of CSPs. Cellulose chains should ideally be long (DP > 100), since short polysaccharide chains or oligosaccharides may dissolve in the organic mobile phases. It has also been proven that partial dissolution of the microcrystalline oligomers, which have low DP (< 18), causes a lower performance compared to longer ones (DP > 18) (Aburatani et al., 1990; Chankvetadze, 2012; Kasuya et al., 2002; R.-Q. Liu et al., 2013; Okada et al., 2016).

To obtain (microcrystalline) cellulose with slightly shorter, defined DP, hydrolysis with acids is mostly applied, which is used in the preparation of the commercially available Avicel[®] cellulose (Holtzapfle & Humphrey, 1983). However, an alternative green and homogenous method is the use of supercritical water (scH₂O) to hydrolyze conventional cellulose and obtain shorter chains or prepare microcrystalline cellulose

with smaller, well-defined DPs. The method uses scH_2O to break glycosidic bonds, where DPs above 6 show low solubility or no solubility in water after the reaction, which leads to precipitation and separation according to the chain length. Recently, microcrystalline cellulose with different DPs (from 12 to 24) has been prepared using the green scH_2O hydrolysis method (Buffiere et al., 2016).

Pure cellulose as CS can already discriminate chiral analytes, due to its hydrophobic helical conformation, multiple stereogenic centers, and its ability to form hydrogen bonds. Nevertheless, as mentioned in the case of polysaccharides, derivatization enhances chiral recognition. One of the most popular cellulose derivative-based CSPs is cellulose *tris*(3,5-dimethylphenylcarbamate) since it meets many requirements for high chiral resolution, e.g., proper electron donating substituents as well as ideal number and location of the substituents (Bui et al., 2021, 2022a; Witte et al., 1993). This cellulose derivative is typically synthesized by reacting a 3,5-dimethylphenyl isocyanate with the free OH groups at the 2-, 3-, and 6-positions of cellulose. By the introduction of the 3,5-dimethylphenylcarbamate substituents, several interaction sites for chiral analytes are established, as discussed earlier (*vide supra*). Hydrogen bonding, hydrophobic interactions, and π - π interactions become accessible due to the derivatization. Also, steric interactions are possible thanks to the helical structure and aromatic rings (Peluso et al., 2020; Yu & Quirino, 2019). By combining all these potential interactions, longer retention times and better chiral discrimination by a three-point interaction become accessible (Scriba, 2019).

This chiral selector, cellulose *tris*(3,5-dimethylphenylcarbamate), is already commercially available as CSP and typically coated onto silica-gel (see **Figure 10**). One highly successful application is the separation of enantiomeric drugs, like antidepressants, proton inhibitors, Fluoxetine, and other β -receptor blocking drugs (J. Zhou et al., 2007; Y. Zhou et al., 2012).

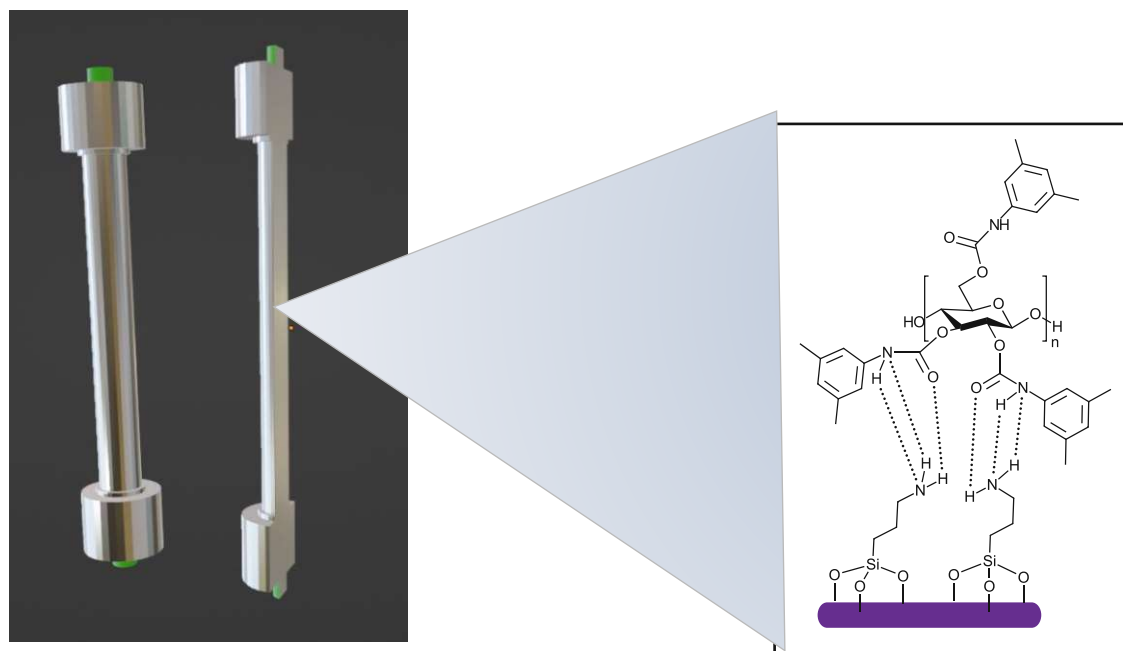


Figure 10: The molecular structure of cellulose *tris*(3,5-dimethylphenylcarbamate)-type CSPs.

Since cellulose is used in many chiral applications, such as chiral catalysts and CS for CSPs (Ikegami et al., 2021), several approaches are being made to precisely fine-tune or even alter its properties. Since its macromolecular heterogeneity renders precise control of the DP and specific and regioselective modification/substitution difficult, an alternative approach is to start CS synthesis from the monomer. Cellulose can be obtained by the polymerization of glucose in a so-called bottom-up approach. Many strategies have been documented such as the enzymatic polymerization (Kobayashi et al., 1991), or the polycondensation method, where glucose acts as both, a donor and acceptor by hydroxy and anomeric leaving groups (Xiao & Grinstaff, 2017).

Another strategy is pure cellulose synthesis starting from glucose by cationic ring-opening polymerization (CROP). This reaction requires multiple steps of monomer synthesis, where homogenous regio- and stereoselective substitution patterns are obtained throughout the whole polymer chain (Lehrhofer et al., 2022). CROP is a chain-growth polymerization, where the polymer itself is active for ionic propagation, it promotes the addition of a cyclic molecule to it, donating its charge to the added molecule, which in turn is again ready for ionic propagation (Takasu & Hayashi, 2015). The monomer initiation is done by acids and cations (Nuyken & Pask, 2013). In the course of the development of this highly advanced synthetic pathway, it has been shown that the choice of protecting groups selectively added to the free hydroxy groups is crucial for proper stereo- and regioselective glycosylation. For example, *O*-benzyl at position C3 is crucial for high yield and stereoregularity, whereas the pivaloyl group at C2 achieves the β -configuration during later polymerization (Kamitakahara et al., 1996; Nakatsubo et al., 1996).

2. Objective

In the last decade, many attempts have been conducted to develop CSPs that are not only highly efficient in enantioseparation but also applicable to a wide number of chiral analytes. Many polysaccharide-based CSPs have shown a good ability to discriminate chiral molecules. There are already various commercial cellulose-based chiral stationary phases available. However, most cellulose used in CSPs comes from chemical pulp and is broken down into lower MW cellulose by hydrolysis. Thus, this represents a so-called “top-down” method to obtain shorter chain cellulose molecules with specific DP ranges. In this thesis, a new approach will be used to synthesize a CSP material based on a commonly known cellulose derivative, *i.e.* cellulose *tris*(3,5-dimethylphenyl carbamate). This novel method will involve the *in-vitro* synthesis of cellulose by CROP starting from D-glucose representing a bottom-up construction of the CSP. Using this method, we hope to not only be able to control the DP of the cellulose more precisely but also achieve regioselective substitution, which is not accessible starting from the conventional derivatization of cellulose. For comparison purposes, commercially available microcrystalline cellulose and cellulose hydrolyzed by scH_2O will also be derivatized.

Further, *Cinchona* alkaloid-based CSPs have also shown high enantioselectivity for charged chiral analytes. Many CSPs based on *Cinchona* alkaloid motifs are already commercially available such as CHIRALPAK® QN-AX and QD-AX. Therefore, in parallel, a cationic stationary phase (= anion exchanger) based on a 3-aminoquinuclidine ring will be synthesized and subsequently immobilized onto 3-aminopropyl-modified silica. After packing into a column, the retention behavior based on ionic interaction with the (racemic) CS will be tested and evaluated using different *N*-protected amino acids.

Additionally, L- & D-amino acids will be *N*-protected by derivatization to serve as chiral test analytes. Further, microporous silica gel will be functionalized to serve as chromatographic support for the CSPs. The synthesis of (3-aminopropyl)triethoxysilane is crucial for coating or immobilizing chiral selectors onto microporous silica.

With these multiple steps including the synthesis of cellulose, the derivatization of the latter to obtain chiral selectors, the derivatization of silica to serve as chromatographic support, the coating and/or immobilization onto silica to obtain CSPs, the synthesis of chiral test analytes as well as the final testing and evaluation of the CSPs by HPLC the whole process of chiral separation from designing novel CSPs to the evaluation step will be dealt with in the frame of this thesis.

3. Results and Discussion

3.1. Synthesis of D-Cellulose

The first aim of this work was the *in-vitro* synthesis of cellulose starting from its monomer D-glucose. This synthesis was done based on the procedures established by Nakatsubo and colleagues (Nakatsubo et al., 1996) and further developed by Yagura and colleagues (Yagura et al., 2020). However, some modifications have been implemented.

All compounds were thoroughly characterized, and their purity was determined using NMR spectroscopy (^1H , ^{13}C , COSY, HSQC, HMBC). Also, IR spectroscopy (ATR-FTIR) and MALDI-TOF/MS have been used to characterize some products. The final product, the synthetic cello-oligomers, was characterized using solid-state ^{13}C NMR spectroscopy due to difficulties dissolving them in conventional NMR solvents. All spectra can be found in the **Appendix** section.

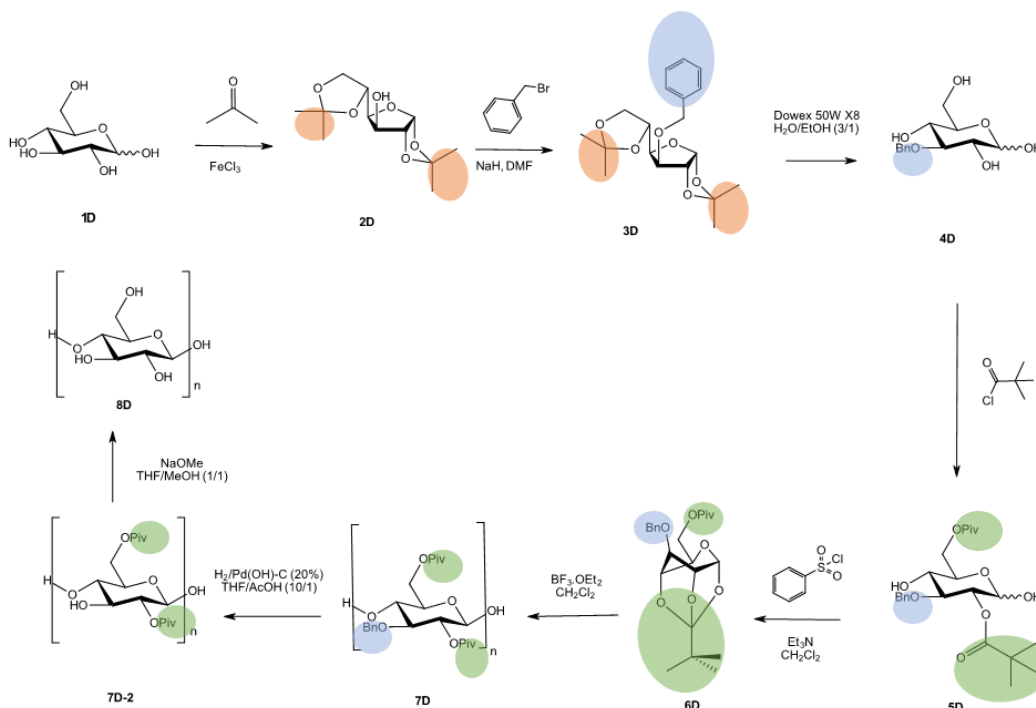


Figure 11: Chemical pathway for the synthesis of D-cellulose (8D) starting from D-glucose (1D).

The *in-vitro* synthesis of cellulose is conducted in eight steps as shown in **Figure 11**. First, the OH groups at positions C1, C2, C5, and C6 of D-glucose were acetal-protected using acetone and FeCl_3 as a Lewis-acidic catalyst under water-free conditions. Due to the rigidity of the protecting groups during this reaction, the resulting di-isopropylidene glucose-derivative isomerizes from mainly pyranose to furanose. Thereafter, the C3-OH as the only free OH group left was regioselectively protected by benzylation since protecting this position with an O-benzyl group significantly increases

the polymer yield (Kamitakahara et al., 1996; Nakatsubo et al., 1996). This is done by deprotonation of the OH using NaH as a strong base followed by nucleophilic substitution at the benzyl-CH₂ by the addition of benzyl bromide. NMR spectra of **2D** (see **Figures 32, and 33**) agree with the literature (Yagura et al., 2020), however, the ¹³C NMR spectrum shows many additional peaks, indicating the presence of carbonaceous impurities. In the case of **3D** (see **Figures 34, and 35**), the C4 and C5 shift signals were correctly assigned as those were wrongly displayed in the literature. To confirm this, HSQC and COSY spectra were well studied in detail and the findings were verified. As the NMR measurements are in good agreement with the literature, they confirm the successful synthesis of compounds **2D** and **3D**. The two different peaks for C6 were observed in most of the steps due to the α and β diastereomers. When the yield is compared, for the synthesis of **3D**, high yields of around 88% were achieved, however, **2D** synthesis only reached a yield of up to 50%. To improve this in the future, longer drying of the acetone and better exclusion of both, moisture and O₂, will be conducted, since yield loss through workup is not avoidable.

In the third step, the acetonide-protecting groups were removed using a strongly acidic ion exchange resin. Compound **4D** was obtained in acceptable yield (70%) after purification by column chromatography and recrystallization. Its identity and purity were confirmed by ¹H and ¹³C NMR measurements (see **Figures 36, 37**). However, due to the products' limited solubility in D₂O, the measurements were conducted in MeOD, resulting in shifts and signals slightly different from the literature values. Additionally, in ¹H NMR the α-H on C1 (noted as H-1a in the spectra) is not as clearly visible as in the literature, since only 5% of the product is in α-configuration in deuterated methanol. To visualize the different configurations at C1, the ¹³C spectrum has been used (Yagura et al., 2020).

The protection of C2- and C6-OH with pivaloyl groups was subsequently done to yield **5D** (47%). For the initial activation of the hydroxy groups, a complex with Bu₂SnO is formed. The subsequent esterification was conducted according to an Einhorn acylation-type protocol, a variant of the classical Schotten-Baumann reaction, with pyridine acting as both an acid capturing agent as well as a nucleophilic catalyst for the reaction with a reactive acid chloride, *i.e.*, pivaloyl chloride. The yield of this step was relatively low; also, Yagura and colleagues did not obtain yields higher than 65%. This might be due to the high water sensitivity of the tin complex as well as the need for precise control of temperature during the esterification to obtain mainly the di-pivaloylated product, as there are 3 free OH groups available in total. Finely ground K₂CO₃ was added to the silica for column chromatography to remove the organotin compounds from the product, which were hard to remove in other ways according to Yagura and co-workers. NMR spectroscopy measurements of **5D** (see **Figures 38, 39**) are in good agreement with the literature. Further, except for C5, two signals are observed for each carbon due to the anomers being present in α or β configuration. Additionally, to increase the yield, a highly pure substrate is needed for the polymerization. Since the complex formation before polymerization is very sensitive and unstable, an additional second column chromatography purification step was needed since the products' purity was insufficient. The high purity of the intermediates during the further steps is crucial since impurities significantly affect the polymerization degree (Orofino & Wenger, 1961).

Compound **6D** was successfully synthesized by the formation of an ortho-pivalate. The addition of benzenesulfonyl chloride was crucial to form a sulfonate ester with Et₃N, which catalyzes the cyclization. The NMR spectra (see **Figures 40, and 41**) show a pure product. The yield reached only 51%. The pivaloyl carbonyls react with the free OH groups forming the corresponding 1,2,4-orthopivalate. This formation is a crucial step to enable polymerization, as the opening of the strained ring is the driving force during CROP. Since this complex is very reactive, a fast purification using chromatography was performed. Contact with acid or moist air significantly affects the yield, since the highly strained ring is prone to decomposition (Yagura et al., 2020).

Due to the sensitivity of the polymerization reaction towards quenching by moisture or oxygen, the reaction was carried out under strictly inert conditions. For this reaction step, the standard Schlenk technique under an N₂ atmosphere was used. Different parameters have been tuned to achieve a higher degree of polymerization, such as purity and dryness of the solvent CH₂Cl₂, purity and concentration of the catalyst as well as the monomer, and different temperatures. Adding fresh concentrated catalyst directly to the reaction mixture, using commercially bought absolutely dry CH₂Cl₂ as the solvent, and stirring at room temperature (RT) gave the best results. Heating the mixture was unnecessary since high viscosity upon polymerization was achieved after a couple of hours, indicating successful polymerization. This step was conducted yielding compound **7D**. However, some aromatic impurities were still detectable in the ¹³C and ¹H NMR spectra (see **Figures 42, 43**) since the integrals of the aromatic signal are bigger than five protons. Also, a successful polymerization can be assumed by the polymer's ¹H NMR spectra shown in **Figure 12**, in which the broad signals around 1.2 ppm are characteristic of the pivaloyl end groups, whereas the wide multiple peaks are characteristic of the pivaloyl groups in the middle of the polymer. The bigger the difference between these characteristic peaks, the higher the DP.

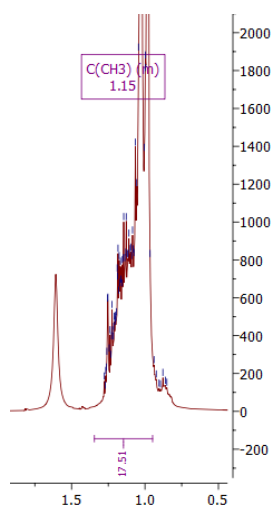


Figure 12: Characteristic peaks of the pivaloyl groups in the polymerization product 7D.

The polymerization step was recorded also by photographs to see the phase change, in which compound **6D** was a liquid before drying under a high vacuum. Upon application of vacuum, the product crystallized to form pure white crystals. Crystals

were then dissolved in CH_2Cl_2 . After polymerization, a highly viscous, partly solid white-to-brown product was formed as shown in **Figure 13**.



Figure 13: The different stages of the CROP during the synthesis of 7D.

To determine the length of the polymer, the DP was estimated using MALDI-TOF/MS (see **Figure 14**). The polymer embedded in the matrix was ionized at different voltages, at 362 mV (green) and 1142 (red). The DP obtained from the MALDI-TOF/MS spectra (see **Figure 45**) is approximately 6, which is comparably low to the literature value of 32. Although it is lower than desired, it is believed that MALDI-TOF/MS might not be the method of choice to determine the DP, since bigger polymer molecules may be discriminated against the smaller ones, therefore only small oligomers are detected.

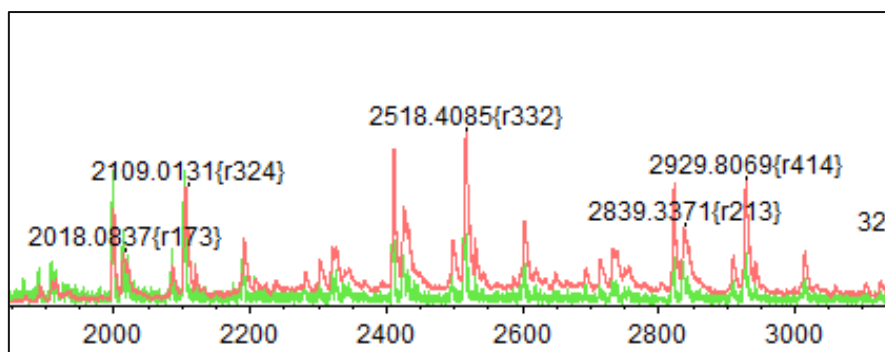


Figure 14: MALDI-TOF/MS spectra of 7D.

Finally, to obtain the cellulose, the removal of the protecting groups was performed. Deprotection of the benzyl group was done using two different approaches: heterogeneous hydrogenation using H_2 gas at atmospheric pressure and flow chemistry (H-cube[®]) as shown in **Figure 15**. The latter is the more automated and convenient method.



Figure 15: The H-cube[®] apparatus with an external pump and reaction chamber containing the Pd hydroxide catalyst circled in red.

As a catalyst, 10% palladium(II)hydroxide on activated carbon was used in the H-cube[®], and as a solvent, a mixture of THF/acetic acid (1/1 v/v) was used. The system was heated to 25°C under 4 bar pressure. The reaction mixture was injected into the capillary and upon contact with the Pd(OH)₂ catalyst the benzyl groups were reductively cleaved off. However, due to capillary leakage, a big amount of the product was lost during the initial tests. This complication led us to the first option using H₂ gas. This step was repeated twice since the benzyl groups could not be cleaved off quantitatively during the first cycle.

For tracking the dehydrogenation reactions, ¹H NMR measurements of the debenzylated products **7D** in THF were performed (see **Figures 46, 47**). THF was chosen due to the insolubility of protected cellulose in many conventional solvents. The NMR spectra after a first and second heterogeneous reductive debenylation are shown in **Figure 16**. The first hydrogenation was not quantitative, since aromatic signals are still present. When a second hydrogenation cycle was performed, only negligible aromatic peaks were present.

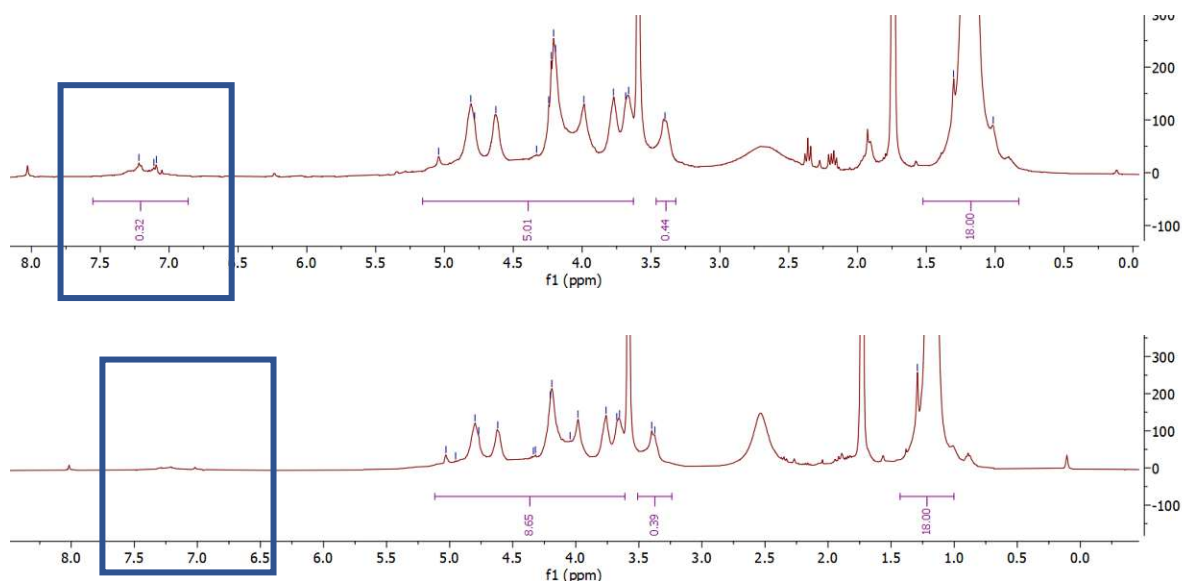


Figure 16: ^1H NMR spectra of 7D after one and two debenzoylation steps.

The pivaloyl groups were removed by heating the mixture at 50°C under base addition. However, it was observed that adding a higher amount of NaOMe in the mixture yielded more product (= oligomeric cellulose) as a precipitate. Contrary to the literature, several washing steps with water were avoided, since the DP was not high and oligomers/short polymers were soluble in the water, hence loss of the product was possible. After multiple MeOH washings, white crystals were obtained. However, the yield was comparably low (29%). This is mostly due to the washing steps, and several deprotecting steps, where most of the product was lost. The deprotection steps need further optimization to avoid product loss. Although the synthesis of cellulose by CROP has been described in quite several publications, it was far from being trivial to reproduce the individual synthesis steps.

To qualitatively determine the residual amount of protecting groups in the case of product 8D, products were characterized by ATR-FTIR (see **Figures 44, 48, 49**) after each step of the debenzoylation reactions and pivaloyl removal. In **Figure 17**, the red box highlights the characteristic benzyl group absorption bands, whereas the blue box highlights the pivaloyl carbonyl group. The orange box refers to the OH absorption band.

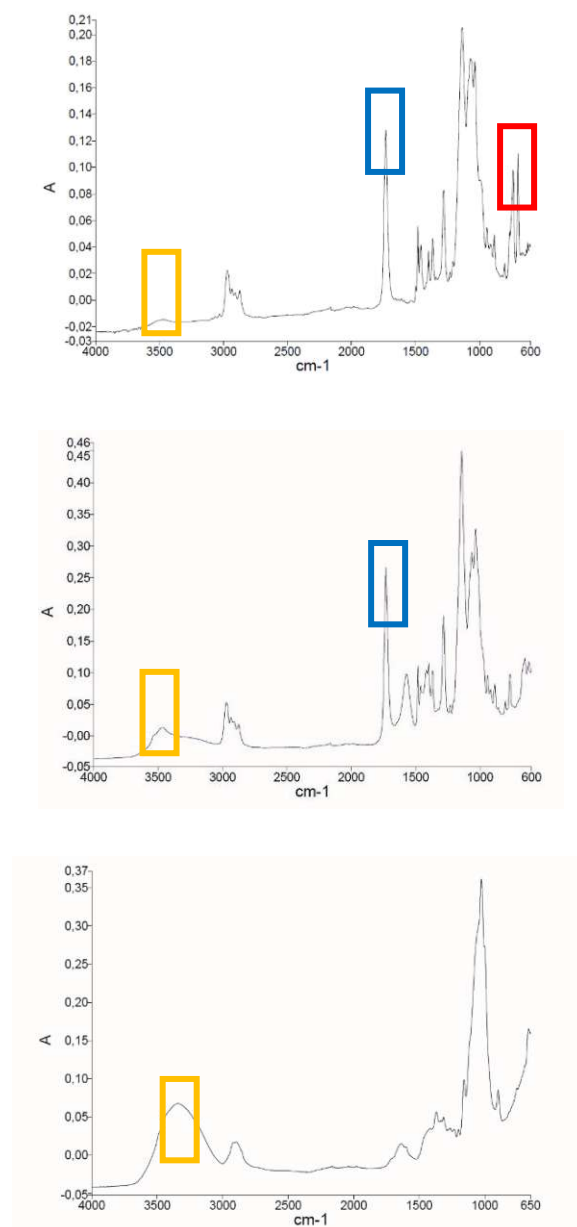


Figure 17: IR spectra of 7D (top), 7D-2 (middle), and 8D (bottom) during cellulose synthesis. The spectrum of 8D is comparable to a typical cellulose spectrum qualitatively indicating a successful synthesis of (oligomeric) cellulose.

The ATR-FTIR measurements indicate a successful deprotection. In the fully protected cellulose absorption bands around 700-600 cm^{-1} are characteristic for benzyl groups, while bands around 1700-1600 cm^{-1} are characteristic for the pivaloyl C=O groups. Also, the OH band is relatively small. With debenzilation, the absorption band around 700-600 cm^{-1} was not present anymore and the OH absorption was significantly increased. After removing the pivaloyl group, its characteristic absorption band was also absent accompanied by a high increase in the OH band.

For characterization, solid-state ^{13}C NMR spectroscopy has been used, since fully deprotected cellulose is not readily soluble in conventional solvents. The measurement results (see **Figure 50**) show the successful deprotection of **7D-2** since the signal shifts

correspond to the values of cellulose reported in the literature (Wei et al., 2020). If signals below 50 ppm are observed, these correspond to amorphous polymer, whereas sharp signals imply high crystallinity (Haslinger et al., 2019). In the measured NMR spectrum, sharp peaks with the absence of peaks at lower shift values were observed. Eventually, the end product **8D** was a white solid as shown in **Figure 18**.



Figure 18: The fully deprotected compound **8D**, (1 → 4)-β-D-glucopyranan.

Although the CROP was successfully carried out, the DP and yield were low compared with the starting sugar amount.

3.2. Derivatization of Avicel® and sCH₂O-hydrolyzed cellulose

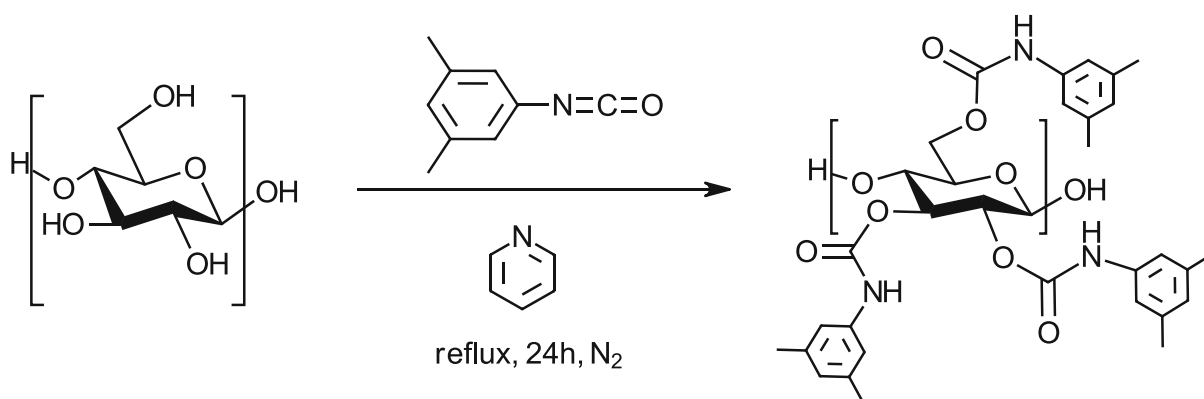


Figure 19: Carbamylation of cellulose to form cellulose tris-(3,5-dimethylphenyl carbamate).

Derivatization of Avicel® microcrystalline cellulose was done according to the previous derivatization method established by Bui and co-workers (Bui et al., 2022b), however, the nitrogen content according to EA measurements was higher than the expected value. For an ideal substitution with the 3,5-dimethylphenyl carbamate at the three OH groups, the maximum w-% of nitrogen should be 6.96, which in turn corresponds to the maximum degree of substitution of 3.0. By back calculations, the N = 7.23 w-% corresponds to the degree of substitution of 3.1. It is true that this substitution value is higher than the theoretical value. Impurities or side-products such as 3,5-dimethylaniline or urea-type products upon reaction with water and decarboxylation etc. cause an increase in nitrogen mass percent.

On the other hand, the derivatization of cellulose previously hydrolyzed by sCH_2O and the subsequent isolation were not successful, since the EA results show an even higher nitrogen content than the theoretical value. The amount of strongly adsorbed water at the surface or bulk phase of the (dried) sCH_2O hydrolyzed cellulose was probably too high still. Thus, alternative methods such as sequential solvent exchange are necessary (ongoing work).

Both derivatizations were achieved with high yields. For characterization purposes, solid-state NMR (see **Figure 51, 52**) was used, in which successful derivatization was proven since the peak shifts correspond to literature values of cellulose *tris*(3,5-dimethylphenyl carbamate) (Bui et al., 2022b). When comparing the signals of Avicel® and sCH_2O -hydrolyzed cellulose, the latter shows higher resolution. To determine purity, EA measurements were carried out (*vide supra*).

3.3. Pre-modification of Silica

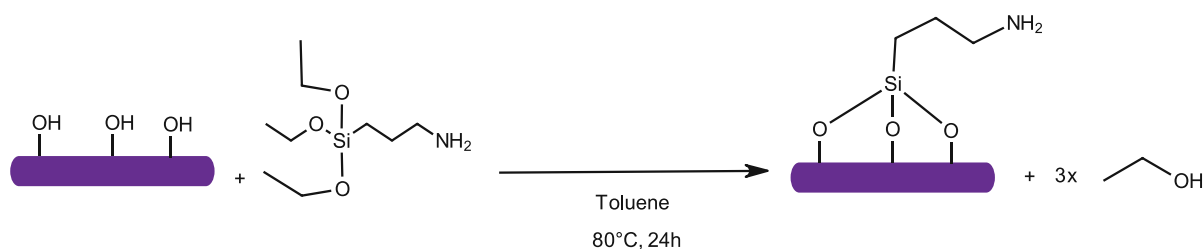


Figure 20: Synthesis of 3-aminopropyl-modified silica.

To pre-functionalize silica, (3-aminopropyl)triethoxysilane was reacted with the bare silica. This reaction is water-sensitive, therefore the use of a very dry solvent is required. To achieve that, dry HPLC-grade toluene was additionally distilled *in-situ* to remove water azeotropically. The pre-modified silica was characterized by solid-state NMR and EA measurements.

EA results proved the successful synthesis of the 3-aminopropyl-modified silica. The amine group loading, calculated based on the elemental nitrogen content was 393 $\mu\text{mol/g}$.

3.4. Synthesis of AQ-AX Phase

Besides the cellulose-type selectors, also a weak AX-type CSP was developed. The derivatization of aminoquinclidine was done at its primary amine by reacting it with allyl isocyanate. The urea-type selector was subsequently immobilized onto 3-mercaptopropyl-modified silica through thiol-ene addition. This (racemic) selector was used to evaluate the influence of ionic interaction on the retention of *N*-protected amino acids (protected with benzoyl (Bz) or 3,5-dinitrobenzoyl (DNB) groups). As mentioned above, these derivatizations are crucial for additional interactions and also provide acidity to the analyte, which in turn improves the retention and stereoselectivity (Boratyński et al., 2019; Mandl et al., 1999; Piette et al., 2002).

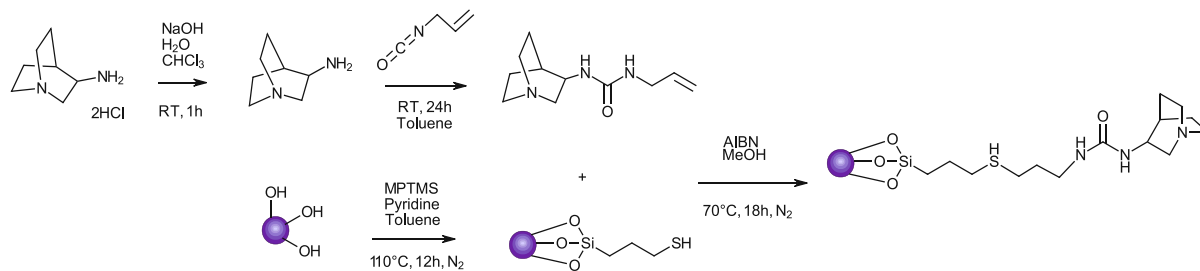


Figure 21: The synthesis route towards the AQ-AX phase and the immobilization of it by thiol-ene addition onto 3-mercaptopropyl-modified silica.

For silica modification with (3-mercaptopropyl)trimethoxysilane (MPTMS), the reaction is also O₂ and water sensitive, therefore silica drying and reaction in an inert gas atmosphere were crucial. Multiple washing steps were crucial for product purity.

Desalting of the dihydrochloride (shown in **Figure 21**) was performed by NaOH. Some loss of product was observed (67% yield). This was caused by the washing step. NMR spectroscopic measurements indicated a successful reaction since characteristic signals of the AQ are present. Nevertheless, the product was not obtained in completely pure form, however, the impurities do not significantly affect the next step of the synthesis. Hence the product was directly used in the subsequent step.

For the thiol-ene addition, double bonds are required, therefore allyl isocyanate was reacted with AQ. This step is very water sensitive, hence azeotropic distillation of the solvent was performed. The synthesis was successful with an acceptable yield (78%). The derivatized AQ was also characterized by NMR spectroscopy. The successful synthesis was also confirmed by the presence of the characteristic signals (see **Figures 55, 56**). However, impurities are still present.

After the implementation of the double bond, thiol-ene addition was done by radical-mediated click chemistry. AIBN was used as a radical initiator and was activated by heating it to 70°C. Since the radical reaction is water and O₂-sensitive, an inert atmosphere was crucial. The product purity determination and characterization were done using EA and NMR methods.

EA results prove the successful synthesis of the AQ-AX phase. The measurements were performed to determine the loading of the product. The calculations are based on the nitrogen and sulfur contents determined by EA measurements. N loading was 0.15 mmol/g and S loading was 0.63 mmol/g.

After the successful synthesis, AQ-AX was packed into a stainless steel HPLC column.

3.5. Preparation of chiral test analytes

N-protection of AAs is a crucial strategy since the protecting group provides additional interaction sites available for testing of the reference stationary phase. Additionally, in many peptide syntheses, *N*-protection is performed, therefore, amino acids are

frequently present in *N*-protected form during the crucial chromatographic purification/enantioseparation step. Within the framework of this thesis, two β -leucine derivatives with different protecting groups were synthesized.

- Synthesis of (*R,S*)-*N*-acetyl- β -leucine

The carbonyl group of the acyl-protecting group provides additional interaction sites with the AX phase. The Ac-group is one of the most frequently used protecting groups for NH functionalities and was added using one of its activated forms, *i.e.* acetic anhydride. According to NMR spectroscopy measurements (see **Figure 54**), the synthesis of (*R,S*)-*N*-acetyl- β -leucine was conducted successfully since the signals are in good agreement with the literature (Naturale et al., 2012). The product was obtained as white crystals (28.2 mg, 70%).

- Synthesis of (*R,S*)-*N*-benzoyl- β -leucine

Since the benzoyl group has the ability to form additional π - π interactions during chromatography, it was selected for derivatization. The NMR spectrum (see **Figure 53**) shows successful derivatization. The yield in the case of the (*R,S*)-*N*-benzoyl- β -leucine synthesis was lower than the (*R,S*)-*N*-acetyl- β -leucine (31.4 mg, 58%).

3.6. Evaluation of the AQ-AX Phase

In many fields, peptide synthesis is always accompanied by side products, impurities, or degradation by hydrolysis. To purify or separate chiral/achiral desired peptides or amino acids, chromatographic chiral or achiral methods, such as HPLC, are required (Nogueira et al., 2005). For this purpose, the newly synthesized AQ-AX phase was evaluated by using racemic *N*-protected amino acids (see **Figure 22**), since comparable AX-type columns were reported to be capable of separating similar peptides (Lämmerhofer et al., 2011). Although the AQ-AX phase has many chiral centers, a racemic phase was used, since the main aim was the observation of ionic properties and interactions in pilot experiments. Therefore, chiral separation of racemic analytes is not possible.

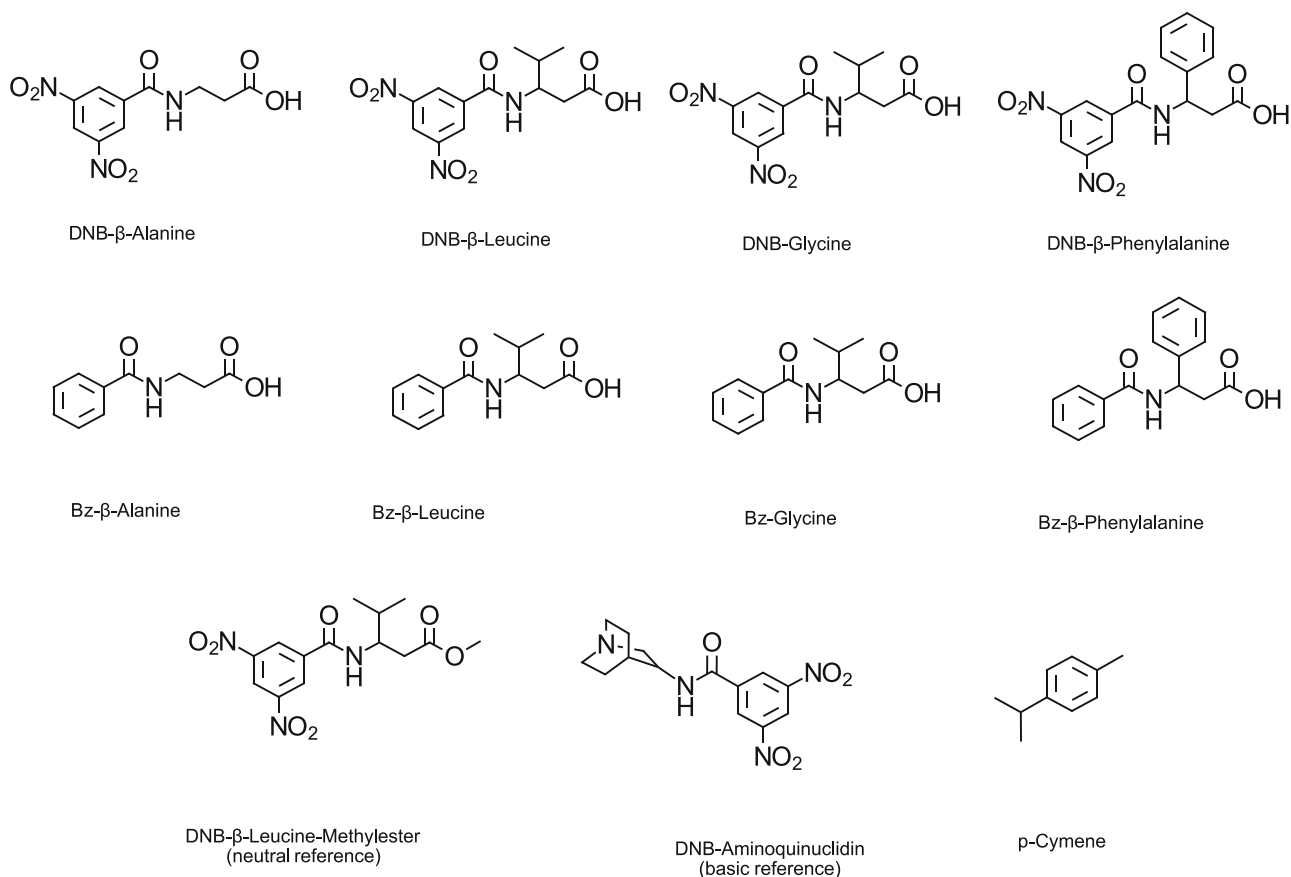


Figure 22: The eight different N-protected AAs and three references (dead time marker, neutral and basic reference).

The AQ-AX phase consists of cationic/polar/hydrophilic and hydrophobic parts and the retention is mainly based on ionic interactions, thanks to the tertiary amine. Therefore, in this work, AQ-AX was used to study the ionic interactions with ionic analytes, the role of additional interactions, and how the retention of specific AAs is affected. A representative selection of AAs with different lipophilicity and acidity was used to determine their retention times on the new CSP using different mobile phase compositions. To observe the ionic interactions and other hydrophobic and Coulomb interactions or steric effects, mobile phases with and without salt were used (Lämmerhofer & Lindner, 1996; Maier et al., 1999).

A small amount of salt (NH_4OAc) was used as an additive in the mobile phase to verify the presence of ionic interaction due to competitive interaction. This hypothesis was confirmed since analytes eluted much faster when the salt was added to the mobile phase. In the case of salt absence, very strong interactions caused high retention times (longer than 1 h). Therefore, only test runs with salt are presented in this thesis. Small salt concentrations also showed good linearity of the k' against mobile phase composition and high peak resolution.

A neutral reference (see **Figure 22**) was used as a control and was expected to elute without any ionic interaction. Additionally, also a basic reference (see **Figure 22**) was used and was anticipated to elute faster than the neutral one since the reference and

stationary phase may be charged positively in the solvent, causing a repulsion, in which results in a faster elution. As hypothesized, the basic reference eluted with the dead time marker. The neutral reference, however, showed an unexpected result. Instead of eluting fast due to its neutral character, it was retained even longer than the analytes. This phenomenon was also observed when high concentrations of NH_4OAc were used, in which neutral analytes were retained longer. This could be explained by the water volume increase on the stationary phase layer by the used salt (McCalley V. D., 2019).

A MeOH/ H_2O mobile phase with an H_2O proportion higher than 20 vol-% caused pressures higher than 400 bar, which might disrupt the stationary phase, therefore these measurements were avoided. In the case of the ACN/ H_2O mobile phase, a higher H_2O fraction than 30 vol-% caused the same and was thus also avoided. Further, measurements in pure ACN were not possible due to the insolubility of the salt in the pure organic phase.

Increasing the ACN fraction in the ACN/ H_2O from 70% to 90% showed (see **Table 2**) an increase in the retention time of the AAs. Similar phenomena were observed in the case of MeOH/ H_2O (see **Table 3**), however, DNB-Ala, DNB-Leu, and DNB-Leu-Me-ester were retained longer at 90% MeOH than in 100%.

Further, it has been observed that the Bz group caused higher retention time by increasing the organic phase content compared to the DNB group.

Table 2: Evaluation of AQ-AX as a stationary phase for HPLC using ACN/H₂O as a mobile phase.

	ACN content (vol-%)	90	80	70
Retention factors (k')	DNB-β-Ala	1.615	0.386	0.420
	DNB-β-Leu	1.189	0.313	0.434
	DNB-Gly	2.073	0.454	0.362
	DNB-β-Phe	1.078	0.313	0.398
	Bz-β-Ala	3.076	0.743	0.585
	Bz-β-Leu	2.260	0.683	0.637
	Bz-Gly	3.946	0.888	0.583
	Bz-β-Phe	2.051	0.612	0.636
	DNB-β-Leu-Me-ester	6.653	2.948	2.819
	DNB-AQ	-0.143	-0.187	-0.065

Table 3: Evaluation of AQ-AX as a stationary phase for HPLC using MeOH/H₂O as a mobile phase.

Retention factors (k')	MeOH content (vol-%)	100	90	80
	DNB-β-Ala	0.766	0.830	0.654
	DNB-β-Leu	0.707	0.739	0.697
	DNB-Gly	0.835	0.748	0.609
	DNB-β-Phe	0.836	0.750	0.757
	Bz-β-Ala	0.902	0.702	0.558
	Bz-β-Leu	0.889	0.702	0.627
	Bz-Gly	1.096	0.768	0.640
	Bz-β-Phe	1.047	0.792	0.743
	DNB-β-Leu-Me-ester	1.131	1.747	1.698
	DNB-AQ	0.075	0.059	0.045

4. Conclusion and Outlook

The main goal of this thesis was the *de-novo* synthesis of cellulose, which should subsequently be used to synthesize a novel CSP based on cellulose *tris*(3,5-dimethylphenyl carbamate). Additionally, a racemic AX-type stationary phase was synthesized and evaluated. All products were well characterized with diverse analytical techniques, such as NMR and EA.

Oligomeric cellulose was successfully synthesized starting from its D-glucose monomer implementing CROP. Each synthesis step was optimized, and several modifications were implemented. Additionally, the applicability of a novel reductive debenzoylation method using an H-Cube[®] Pro flow reactor was tested. However, both the yield of the single reaction steps as well as the DP of the final cello-oligomers were lower with respect to the values reported in the literature. Before further derivatization, the DP and yield still have to be optimized. However, this is subject to ongoing work. In parallel, 3-aminopropyl-modified silica was synthesized, which is required as chromatographic support for the coating of the CSs. Further, commercially available Avicel[®] microcrystalline cellulose and scH₂O-hydrolyzed cellulose were derivatized to form cellulose *tris*(3,5-dimethylphenyl carbamate) and will be used in later studies for comparative purposes to study the influence of the DP on chiral separation.

Additionally, an AX-type stationary phase was successfully synthesized starting from racemic 3-aminoquinuclidine. The derivatized AQ was immobilized onto silica as chromatographic support by a click chemistry-type thiol-ene reaction. For its evaluation different *N*-protected AAs were used, in which the ionic interactions and additional forces were studied. In parallel, β -leucine was derivatized using different *N*-protecting groups, which will be used for future CSP/AQ-AX evaluations.

Although synthetic cello-oligomers were obtained, many parameters, especially during polymerization, require more optimization. More specifically, the use of more advanced equipment is required to achieve full exclusion of moisture and oxygen, since a Schlenk line may not be efficient enough for small-scale polymerization. Also, freshly prepared chemicals are recommended to minimize the impurity or moisture factor. In the case of the DP, additional determination methods need to be investigated to better characterize the products. In the case of derivatization, Avicel[®] gave better results than the scH₂O-hydrolyzed cellulose. This might be attributed to the high amount of residual water in the latter one. The remaining water from hydrolysis needs to be carefully removed before future syntheses.

5. Experimental Part

5.1. Materials and Methods

All reagents and solvents used were purchased commercially from Fluka, Sigma-Aldrich, Fisher Scientific, Acros Organics, Roth, Merck, as well as Honeywell and used without further purification. Solvents intended for dry reactions were either purchased as absolute solvents or were dried using activated 4 Å molecular sieves for at least one week and degassed by bubbling through the solutions with dry N₂. Extra-dry CH₂Cl₂ was dried by refluxing over CaCl₂ and subsequent distillation. Inert reactions were performed under N₂ or Ar atmosphere implementing the standard Schlenk technique. For purification of the products, column chromatography was performed, using either pure silica gel 60 (0.063 – 0.200 mm) or silica gel with 10% finely ground solid K₂CO₃. Different mobile phase compositions were used depending on the product and are specified in the corresponding procedures.

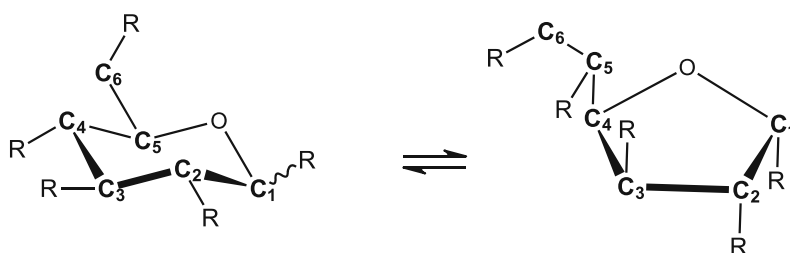
TLC silica plates with UV indicator (ALUGRAM[®] SIL G/UV254) were used for reaction and product monitoring. Visualization of aromatic compounds was assisted by UV light and *p*-anisaldehyde staining in the case of sugar compounds and ninhydrin staining for AQ derivatization. Staining was performed similarly to literature procedures (Metier et al., 2021; Pirrung C. M., 2017; Sinhababu et al., 2015).

In the case of D-cellulose synthesis and H-Cube[®] Pro (ThalesNano) equipped with 10% palladium(II)hydroxide on activated carbon as a catalyst (CatCart[®]) was used for debenzylolation besides classical hydrogenation using H₂ gas.

All product characterizations and purity determinations were done using ¹H and ¹³C liquid-state NMR and ¹³C solid-state NMR spectroscopy (Avance II and III 400 MHz instruments, Bruker, Rheinstetten) at RT. Data analysis was performed using TopSpin 4.2.0 from Bruker and MestreNova 14.3.1 software. Chemical shifts (δ) are given in ppm.

¹H NMR signals of derivatized AAs and the AQ-AX selector are defined by numbers according to the atom in the molecule shown in the spectrum.

¹H NMR signals of D-glucopyranose and D-glucofuranose are labeled from 1 to 6, according to the cyclic sugar structure numbering system shown below:



Also (a) and (b) signs in the spectrum are used to specify alpha and beta anomer configurations.

ATR-FTIR measurements were performed on a Frontier IR single-range spectrometer obtained from PerkinElmer Inc., USA. The system was composed of a diamond/ZnSe crystal, LiTaO₃ detector, and KBr windows. The wavenumber range was 4000-500 cm⁻¹. The spectra were evaluated using PerkinElmer® Spectrum software (Version 10.03.02).

Like Yagura and colleagues (Yagura et al., 2020) the DP determination of synthesized cellulose was done by MALDI-TOF, autoflexer, and Brucker. After samples were coated on the 2,5-dihydroxybenzoic acid matrix, spectra were measured upon ionization with a laser beam.

Elemental analysis was performed using the EURO EA 3000 CHNS-O instrument (HEKAtech, Wegberg, Germany) at the microanalytical laboratory of the University of Vienna.

The synthesized AQ-AX phase was coated and subsequently packed in the HPLC column. The surface area of the DAISOGEL SP-120-3P spherical ultra-pure packaging material obtained from OSAKA SODA is 300 m²/gg.

5.2. Synthesis of D-Cellulose from D-Glucose

5.2.1. Precursor Synthesis and Polymerization

- Synthesis of 1,2;5,6-di-O-isopropylidene- α -D-glucofuranose (**2D**)

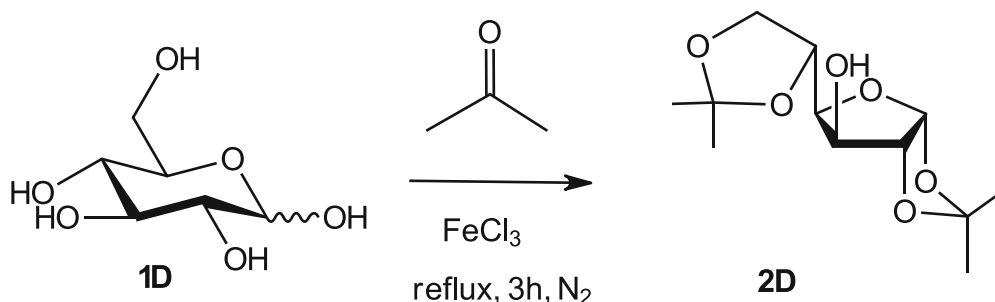


Figure 23: Synthesis of **2D**.

In an inert N_2 atmosphere pre-dried anhydrous D-glucose (4.10 g, 22.8 mmol, 1.0 equiv.) and anhydrous FeCl_3 (1.32 g, 8.1 mmol, 0.36 equiv., 35 mol%) were mixed and subsequently dry acetone (200 mL) was added. The dark grey/orange suspension was heated to refluxing temperature and stirred at this temperature for 3 h, whereupon its color changed from light brown to a black solution. The reaction mixture was cooled to RT and neutralized using an excess of saturated NaHCO_3 solution, whereupon a brown precipitate was formed. After filtration and washing with EtOAc, the orange filtrate was concentrated *in vacuo*. The concentrate was extracted with DCM (5 x 20 mL) and the combined organic phases were washed with brine (10 mL) and water (10 mL) yielding the crude product as an orange slurry after removal of the solvent *in vacuo*. The crude product was recrystallized from *n*-hexane to yield compound **2D** as beige crystals (2.91 g, 49% yield).

^1H NMR spectrum of **2D** (400.13 MHz, CDCl_3): 5.94 (d, $J = 3.6$ Hz, 1H, H-1), 4.53 (dd, $J = 3.6, 0.6$ Hz, 1H, H-2), 4.34 (m, 1H, H-3), 4.32 (m, 1H, H-5), 4.16 (dd, $J = 8.6, 6.2$ Hz, 1H, H-6a), 4.06 (dd, $J = 7.6, 2.8$ Hz, 1H, H-4), 3.98 (dd, $J = 8.6, 5.4$ Hz, 1H, H-6a), 2.60 (d, $J = 3.7$ Hz, 1H, OH), 1.69 (s, 1H, H_2O), 1.49 1.44 1.36 1.31 (d, $J = 0.7$, 12H, $-\text{C}(\text{CH}_3)_2$).

^{13}C NMR spectrum of **2D** (100.26 MHz, CDCl_3): 111.8, 109.6 ($-\text{C}(\text{CH}_3)_2$), 105.2 (C-1), 85.0 (C-2), 81.1 (C-4), 75.0 (C-5), 73.4 (C-3), 67.6 (C-6), 26.8, 26.7, 26.1, 25.1 ($-\text{C}(\text{CH}_3)_2$).

- Synthesis of 3-O-benzyl-1,2;5,6-di-O-isopropylidene- α -D-glucofuranose (**3D**)

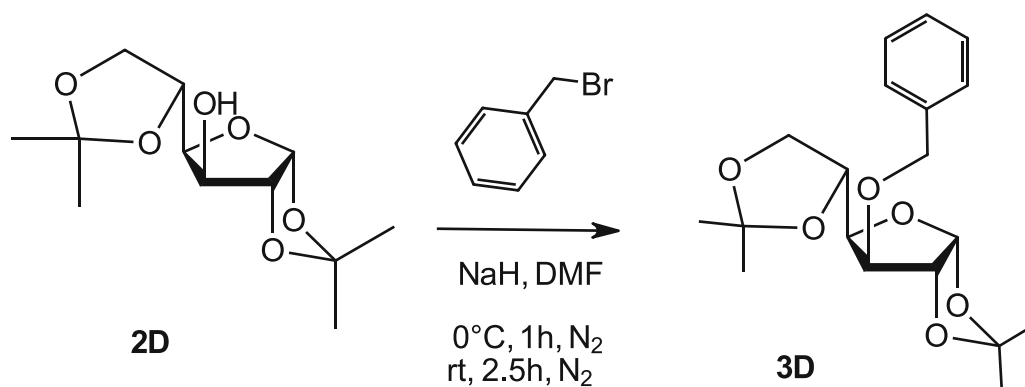


Figure 24: Synthesis of **3D**.

NaH (1.0 g, 60% oil suspension, 25.0 mmol, 2.2 equiv.) was washed using dry *n*-hexane (4 x 15 mL). In an inert N₂ atmosphere, compound **2D** (2.91 g, 11.2 mmol, 1.0 equiv.) was dissolved in anhydrous DMF (50 mL), cooled to 0°C, and added to the base. The reaction mixture was stirred at 0°C for 30 min before a solution of benzyl bromide (1.7 mL, 2.45 g, 14.3 mmol, 1.3 equiv.) in anhydrous DMF (12 mL) was added dropwise over a period of 5 min. After stirring the mixture at 0°C for 1 h, it was stirred at RT for another 2.5 h. Thereafter, MeOH (5 mL) was added dropwise until the foaming had stopped. Subsequently, deionized H₂O (100 mL) was added, yielding a yellowish, milky suspension. The mixture was extracted with EtOAc/*n*-hexane (1/4 v/v) (3 x 50 mL), and the combined organic phases were washed with saturated brine. After drying the solvent with MgSO₄, it was concentrated *in vacuo* yielding the crude product as a yellow oil. To obtain the pure product, flash column chromatography was performed (eluent: EtOAc/*n*-hexane (1/5 v/v), R_f = 0.33) to afford compound **3D** as a slightly yellowish oil (3.41 g, 88% yield).

¹H NMR spectrum of **3D** (400.13 MHz, CDCl₃): 7.34 (d, *J* = 4.5 Hz, 5H, -CH₂-Ph), 5.90 (d, *J* = 3.7 Hz, 1H, H-1), 4.65 (m, 2H, -CH₂-Ph), 4.59 (d, *J* = 3.7 Hz, 1H, H-2), 4.37 (dt, *J* = 7.7, 6.0 Hz, 1H, H-5), 4.18 – 4.14 (m, 1H, H-4), 4.13 – 4.09 (m, 1H, H-6a), 4.04 – 4.02 (m, 2H, H-3), 4.01 – 3.98 (m, 1H, H-6b), 1.49 1.43 1.38 1.31 (d, *J* = 0.7, 12H, -C(CH₃)₂).

¹³C NMR spectrum of **3D** (100.26 MHz, CDCl₃): 137.6, 128.4, 128.4, 27.8, 127.6 (-CH₂-Ph), 111.8, 108.9 (-C(CH₃)₂), 105.3 (C-1), 82.6 (C-2), 81.7 (C-3), 81.3 (C-4), 72.5 (C-5), 72.4 (-CH₂-Ph), 67.4 (C-6), 26.8, 26.8, 26.2, 25.4 (s, -C(CH₃)₂).

- Synthesis of 3-O-benzyl-D-glucopyranose (**4D**)

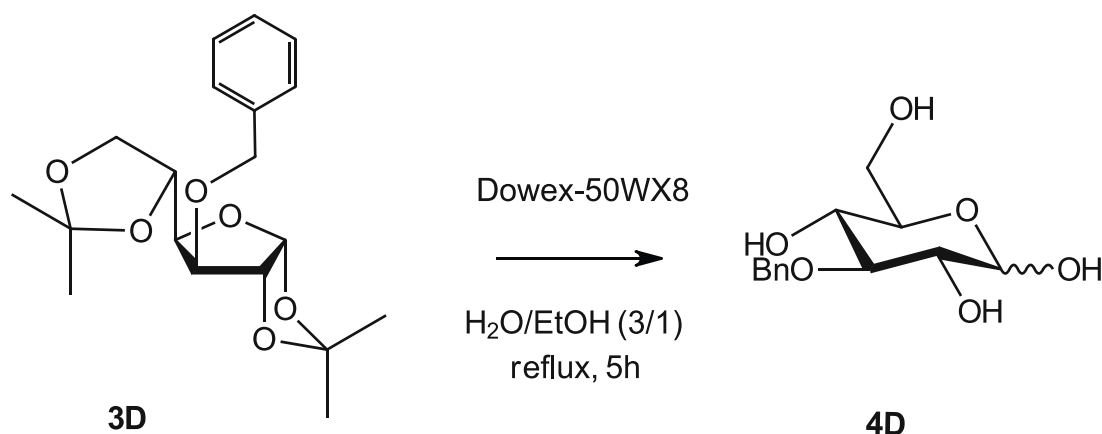


Figure 25: Synthesis of **4D**.

To **3D** (3.41 g, 9.7 mmol, 1 equiv.) EtOH/H₂O (1/3 v/v) (12 mL) and Dowex-50WX8 (100-200 mesh, Sigma-Aldrich) (2.40 g) were added and the mixture was stirred at refluxing temperature for 5 h. The reaction mixture was neutralized using 25% NaOMe in MeOH, filtered, and the resin was washed with water (2 x 5 mL) and EtOH (3 x 5 mL). Subsequently, the filtrate was concentrated *in vacuo* and lyophilized. The off-white crude product was purified by flash column chromatography (dry application by coating onto silica, eluted with MeOH/DCM (15/85 v/v), *R_f* = 0.44). Subsequently, the semi-pure product was recrystallized from EtOAc to yield pure compound **4D** as white crystals (1.84 g, 70% yield).

¹H NMR spectrum of **4D** (400.13 MHz, CD₃OD): 7.43 (x2), 7.31 (x2), 7.26 (m, *J* = 7.2 Hz, 5H, -CH₂-Ph), 4.88 (d, 2H, *J* = 5.4 Hz, -CH₂-Ph), 4.50 (d, 1H, *J* = 7.7 Hz, H-1β), 3.86 (dd, 1H, *J* = 11.8, 2.3 Hz, H-6a), 3.65 (dd, 1H, *J* = 11.8, 5.9 Hz, H-6b), 3.43 (dd, 1H, *J* = 9.7, 8.7 Hz, H-4), 3.35 (t, 1H, *J* = 8.8 Hz, H-3), 3.29 (d, 1H, *J* = 5.8 Hz, H-5), 3.26 (m, 1H, H-2).

¹³C NMR spectrum of **4D** (100.26 MHz, CD₃OD): 140.5, 129.2 x2, 129.1 x2, 128.5 (-CH₂-Ph), 98.3 (C-1b), 86.4 (C-3), 78.0 (C-5), 76.5 (C-2), 76.0 (-CH₂Ph), 71.7 (C-4), 62.9 (C-6).

- Synthesis of 3-O-benzyl-2,6-di-O-pivaloyl-D-glucopyranose (**5D**).

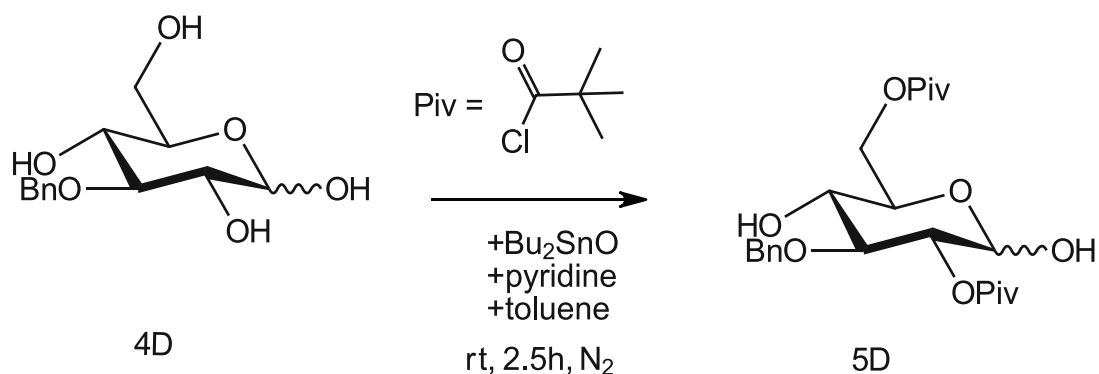


Figure 26: Synthesis of **5D**.

To compound **4D** (1.84 g, 6.8 mmol, 1.0 equiv.) Bu₂SnO (3.90 g, 15.7 mmol, 2.3 equiv.), and molecular sieves 4Å (4.00 g) were added and dried *in vacuo* overnight. Anhydrous toluene (50 mL) was added, and the mixture was stirred at refluxing temperature in an inert N₂ atmosphere for 20 min, whereupon the solid dissolved to yield a clear brown solution. After cooling to RT, anhydrous pyridine (1.6 mL, 19.8 mmol, 2.9 equiv.) was added before carefully adding pivaloyl chloride (1.85 mL, 14.9 mmol, 2.2 equiv.) dropwise at 0°C. Afterward, the mixture was stirred RT for another 2.5 h. MeOH (5 mL) was added, the mixture was filtered, and the beige powder was washed with EtOAc. The filtrate was concentrated azeotropically with EtOH giving a yellow slurry. The crude product was purified using flash column chromatography (silica with 10 wt% K₂CO₃, eluted with EtOAc/*n*-hexane (1/2 v/v), R_f = 0.33-0.41) yielding compound **5D** as a slightly yellowish oil (1.42 g, 47% yield).

¹H NMR spectrum of **5D** (400.13 MHz, CDCl₃): 7.39 – 7.27 (m, 5H, -CH₂-Ph), 5.43 (m, *J* = 3.7 Hz, 1H, H-1-α), 4.85 (d, *J* = 11.0 Hz, 1H, -CH₂-Ph-α), 4.81 (d, *J* = 11.6 Hz, 1H, -CH₂-Ph-β), 4.78 (d, *J* = 11.6 Hz, 1H, -CH₂-Ph-α), 4.78 (m, 1H, H-2-β), 4.74 (d, *J* = 11.0 Hz, 1H, -CH₂-Ph-β), 4.73 (q of d, *J* = 3.7 Hz, 1.1 Hz, 1H, H-2-α), 4.60 (dd, *J* = 9.60, 8.3 Hz, 1H, H-1-β); 4.48 (dd, *J* = 12.3, 3.2 Hz, 1H, H-6a-β), 4.44 (dd, *J* = 12.2, 2.3 Hz, 1H, H-6a-α), 4.28 (dd, *J* = 12.2, 2.3 Hz, 2H, H-6b-α+β), 4.02 (m (q of d), *J* = 9.9 (d), 1.9 (q), 1H, H-5-α), 3.92 (dd, *J* = 9.9, 9.0, 1H, H-3-α), 3.60 (dd, *J* = 9.1, 9.0, 1H, H-3-β), 3.53 (m, 1H, 1-OH-β), 3.52 (m, 1H, H-4-α), 3.51 (m, 1H, H-5-β), 3.49 (m, 1H, H-4-β), 2.83 (d, *J* = 2.9, 1H, 4-OH-β), 2.81 (dd, *J* = 3.8, 1.3, 1H, 1-OH-α), 2.69 (s, *J* = 4.2, 1H, 4-OH-α), 1.24–1.20 (d, 18H, -C(CH₃)₃).

¹³C NMR of **5D** (100.26 MHz, CDCl₃): 179.5, 179.3, 179.2, 177.9 (C=O), 138.2, 137.9, 128.7, 128.6, 128.2, 128.0, 127.9, 127.8 (-CH₂-Ph), 96.3 (C-1-β), 90.4 (C-1-α), 81.5 (C-3-β), 78.8 (C-3-α), 75.6 (C-2-β), 75.4 (-CH₂-Ph-α), 75.1 (-CH₂-Ph-β), 74.3 (C-4-β), 73.6 (C-2-α), 70.2 (C-5-β), 70.1 (C-4-α), 69.8 (C-5-α), 62.8 (C-6-α), 62.6 (C-6-β), 39.0, 38.7, (-C(CH₃)₃), 27.2, 27.1, 27.0 (-C(CH₃)₃).

- Synthesis of 3-O-benzyl-2,6-di-O-pivaloyl- α -D-glucopyranose-1,2,4-orthopivalate (**6D**)

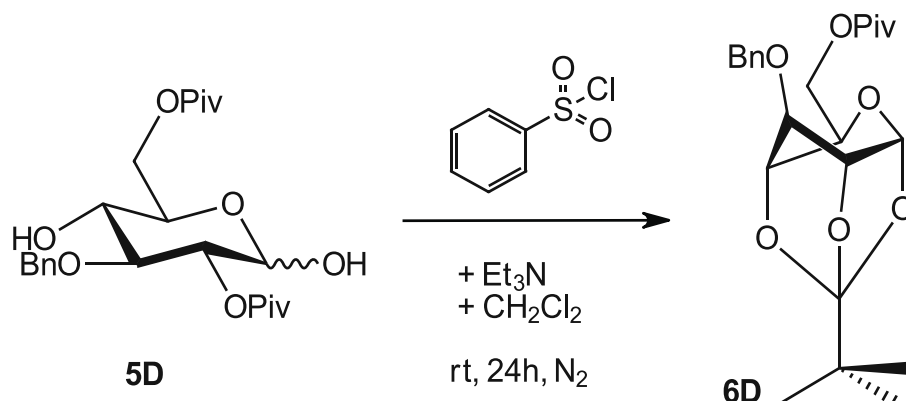


Figure 27: Synthesis of **6D**.

Compound **5D** (0.470 g, 1.1 mmol, 1.0 equiv.) was dried in a vacuum desiccator at RT for 3 days. Dried **5D** was dissolved in anhydrous CH_2Cl_2 (10 mL). In the inert N_2 atmosphere, Et_3N (0.30 mL, 2.2 mmol, 2.0 equiv.) and benzene sulfonyl chloride (0.15 mL, 1.2 mmol, 1.1 equiv.) were added. The reaction mixture was stirred at RT overnight and concentrated *in vacuo* yielding a yellow oil. The crude product was purified using flash column chromatography (eluted first with $\text{CH}_2\text{Cl}_2/n$ -hexane (1/2 v/v) and then with pure CH_2Cl_2 , $R_f = 0.55$ in CH_2Cl_2) yielding colorless crystals after evaporation of the solvent (0.23 g, 51% yield).

^1H NMR spectrum of **6D** (400.13 MHz, CDCl_3): 7.35 (m, 5H, $-\text{CH}_2\text{-Ph}$), 5.77 (d, $J = 4.9$ Hz, 1H, H-1), 4.63 (d, $J = 1.0$ Hz, 2H, $-\text{CH}_2\text{-Ph}$), 4.49 (d, $J = 6.4$ Hz, 1H, H-5), 4.41 (m, 2H, H-2, H-6a), 4.34 (dd, $J = 11.1, 6.2$ Hz, 1H, H-6b), 4.16 (dd, $J = 4.7, 2.2$ Hz, 1H, H-3), 3.95 (dt, $J = 4.7, 1.5$ Hz, 1H, H-4), 1.23 (s, 9H, $-\text{C}(\text{CH}_3)_3$), 1.03 (s, 9H, $-\text{C}(\text{CH}_3)_3$).

^{13}C NMR spectrum of **6D** (100.26 MHz, CDCl_3): 178.2 (C=O), 137.4, 128.6, 128, 127.6 ($-\text{CH}_2\text{-Ph}$), 123.1 ($(-\text{O}_3)\text{C}(\text{CH}_3)_3$), 97.5 (C-1), 75.3 (C-5), 72.2 ($-\text{CH}_2\text{-Ph}$), 72.0 (C-2), 71.5 (C-3), 71.2 (C-4), 64.4 (C-6), 38.8 (pivaloyl- $\text{C}(\text{CH}_3)_3$), 35.7 (orthopivalate- $\text{C}(\text{CH}_3)_3$), 27.2 (pivaloyl- $\text{C}(\text{CH}_3)_3$), 24.9 (orthopivalate- $\text{C}(\text{CH}_3)_3$).

- Synthesis of 3-O-benzyl-2,6-di-O-pivaloyl-(1→4)-β-D-glucopyranose (**7D**)

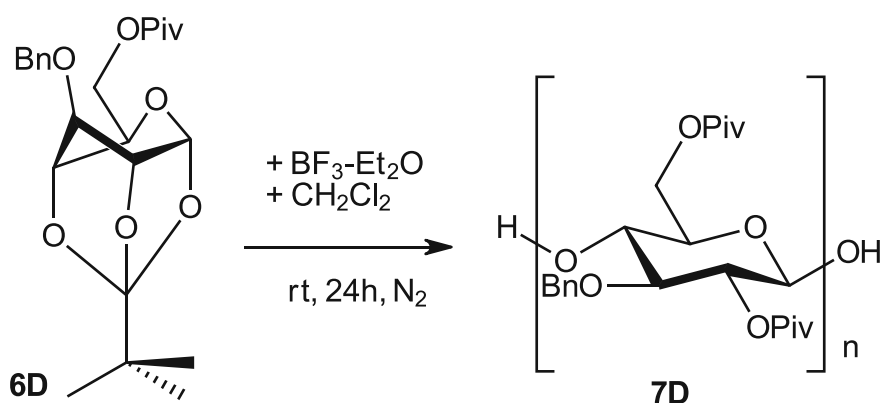


Figure 28: Synthesis of **7D**.

Compound **6D** (0.230 g, 0.5 mmol, 1.0 equiv.) was dried under high vacuum using a Schlenk vacuum line over a period of 3 days. Subsequently, the Schlenk flask was flushed with N₂, **6D** was dissolved in extra-dry CH₂Cl₂ (227 μL) and BF₃·Et₂O (5 mol%) (3.3 μL) was added to the colorless solution. The mixture was stirred under atmospheric pressure at RT overnight, whereupon it solidified. The off-white reaction product was dissolved in CH₂Cl₂ (10 mL), washed with water (10 mL), saturated NaHCO₃ (10 mL), brine (10 mL), and concentrated *in vacuo* yielding **7D** as a colorless solid (0.110 g, 50% yield).

¹H NMR spectrum of protected **7D** (400.13 MHz, CDCl₃): 7.18 (m, 5H, -CH₂-Ph), 4.95 (m, 1H, -CH₂-Ph), 4.83 (s, 1H, H-2), 4.41 (d, 1H, *J* = 11.4 Hz, -CH₂-Ph), 4.27 (s, 1H, H-1), 4.08 (s, 1H, H-6α), 3.82 (s, 1H, H-6β), 3.64 (s, 1H, H-4), 3.46 (d, 1H, *J* = 8.6 Hz, H-3), 3.33 (s, 1H, H-5), 1.12 (m, 18H, -C(CH₃)₃).

¹³C NMR spectrum of protected **7D** (100.26 MHz, CDCl₃): 177.6, 176.3 (C=O), 138.6, 128.0, 127.1, 126.7 (-CH₂-Ph), 100.1 (C-1), 80.7 (C-3), 76.7 (C-4), 74.7 (-CH₂-Ph), 73.1 (C-5), 72.1 (C-2), 62.3 (C-6), 26.8 (-C(CH₃)₃).

- Synthesis of (1 → 4)-β-D-glucopyranan (cellulose, **8D**)

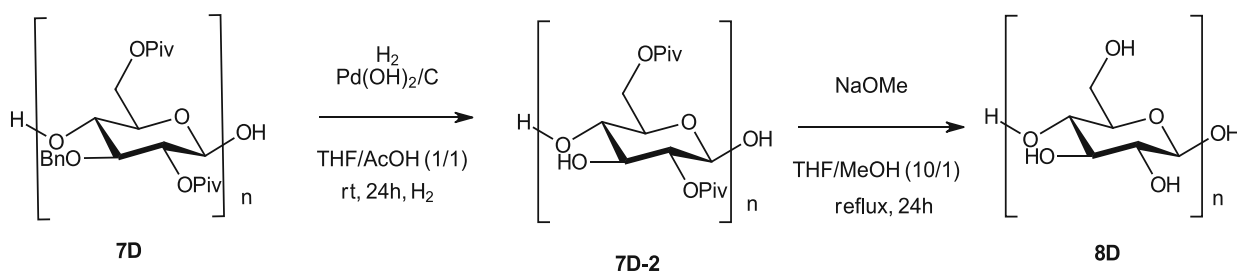


Figure 29: Deprotection of 7D yielding oligomeric cellulose 8D.

Compound **7D** (0.110 g, 0.3 mmol) was dissolved in THF/acetic acid (1/1 v/v, 5 mL). Pd(OH)₂ on carbon (200 mg, 1.4 mmol, 20 wt.%) was added as the catalyst and the reaction mixture was stirred under an inert atmosphere. After flushing the reaction apparatus with H₂ gas using a balloon, the mixture was stirred under a hydrogen atmosphere overnight. Thereafter, the mixture was filtered over Celite® 535 to remove the catalyst and the product was eluted using THF/acetic acid (50 mL, 1/1 v/v). Subsequently, the solvent was removed *in vacuo* azeotropically by repetitive addition of absolute EtOH yielding the debenzylated product. This procedure was repeated twice to yield a white/colorless solid.

Additionally, reductive debenzylation using a flow reactor system with an *in-situ* generation of H₂ in an H-Cube Pro® (ThalesNano) equipped with a 10% Pd(OH)₂/C CatCart® was performed. Compound **7D** (0.110 g) was dissolved in THF/acetic acid (20 mL, 1/1 v/v) and the mixture was degassed by bubbling through Ar for 5 min. The colorless solution was injected into the reactor using a flow rate of 1 mL/min, an H₂ pressure of 4 bars as well as a reaction temperature of 50°C and was cycled for 2 h to ensure efficient hydrogenation. Subsequently, the solvent was evaporated *in vacuo* azeotropically by repetitive addition of EtOH yielding the debenzylated product as a white/colorless solid.

The debenzylated product (0.110 g) was subsequently dissolved in THF/MeOH (10/1 v/v, 60 mL) and NaOMe 25% (1.0 mL) was added. The reaction mixture was stirred at 50°C overnight. After 16 h, the mixture was neutralized with HCl (1 M) and the product was isolated by centrifugation. After several steps of washing with MeOH, the fully deprotected product was isolated as a colorless powder (**8D**, 0.0127 g, 29% yield).

Solid-state ¹³C NMR spectrum of (**8D**): 104.8 (C-1), 87.4 (C-4), 74.7 (C-2, C-3, C-5), 62.2 (C-6).

5.2.2. Derivatization of Avicel/sCH₂O Cellulose

- Synthesis of cellulose *tris*(3,5-dimethylphenyl carbamate) using Avicel® PH-101

Pre-dried Avicel® PH-101 microcrystalline cellulose (0.50 g, 3.1 mmol, 1.0 equiv.) was suspended in dry pyridine (10 mL) in an inert N₂ atmosphere and subsequently heated to 110°C. At this temperature, 3,5-dimethylphenyl isocyanate (2.50 mL, 17.8 mmol, 5.7 equiv.) was added to the reaction mixture and stirred at 110°C overnight. After 24 h, the yellow/orange viscous solution was cooled to RT. The product was precipitated by adding EtOH (50 mL) and pouring the suspension into EtOH (1.0 L). Thereafter, it was isolated by filtration and multiple washing steps with EtOH and H₂O. The product was dried in a vacuum oven overnight. For further purification, the crude product (colorless/white solid) was dissolved in pyridine (5 mL) at RT (beige oil) and subsequently re-precipitated under excessive EtOH addition and stirring for 1 h. After filtration, washing, and drying in a vacuum oven, cellulose *tris*(3,5-dimethylphenyl carbamate) was obtained as a white solid (1.67 g, 89% yield).

Solid-state ¹³C NMR spectrum of *derivatized* Avicel: 152.4 (C=O), 137.6 (C-7, C-9, C-11) 124.6 (C-10, C-12), 115.3 (C-8), 102.5 (C-1), 73.0 (C-2, C-3, C-5), 64.1 (C-6), 20.8 (C-13, C-14).

EA of derivatized Avicel: C: 66.32 w-% ± 0.19; H: 6.34 w-% ± 0.00; N: 7.23 w-% ± 0.04; O: 20.29 w-% ± 0.41.

- Synthesis of cellulose *tris*(3,5-dimethylphenyl carbamate) using scH₂O-hydrolyzed cellulose

Pre-dried scH₂O-hydrolyzed cellulose (0.520 g, 3.2 mmol, 1.0 equiv.) was suspended in dry pyridine (10 mL) in an inert N₂ atmosphere and subsequently heated to 110°C, whereupon the solid partly dissolved. At this temperature, 3,5-dimethylphenyl isocyanate (2.50 mL, 17.8 mmol, 5.6 equiv.) was added to the reaction mixture and stirred at 110°C overnight. Due to educt accumulation on the stirring bar, the mixture was kept at this temperature for another 24 h. After 48 h, the dark brown viscous suspension was cooled to RT. The product was precipitated by adding EtOH (100 mL) and pouring the suspension into EtOH (1.0 L). Thereafter, it was isolated by filtration and multiple washing steps with EtOH (2 L) and H₂O (2 L) were conducted to remove byproducts. The product was dried in a vacuum oven overnight. For further purification, the crude product (light brown solid) was once more partly dissolved in pyridine (5 mL) at 90°C (brown suspension) and subsequently re-precipitated under excessive EtOH addition and stirring for 1h. After filtration, washing, and drying in a vacuum oven, cellulose *tris*-(3,5-dimethylphenyl carbamate) was obtained as a white solid (1.60 g, 80% yield). Product purity and characterization were determined using solid-state ¹³C NMR spectroscopy and EA.

Solid-state ¹³C NMR spectrum of derivatized scH₂O-hydrolyzed cellulose: 153.1 (C=O), 137.1 (C-7, C-9, C-11) 126.2 (C-12), 122.6 (C-12), 115.7 (C-8), 102.1 (C-1), 73.4 (C-2, C-3, C-5), 64.0 (C-6), 21.1 (C-13, C-14).

EA of derivatized scH₂O: C: 72.21 w-% ± 0.50; H: 7.13 w-% ± 0.04; N: 9.20 w-% ± 0.10; O: 11.25 w-% ± 0.25.

5.2.3. Derivatization of Silica Gel

Silica gel (10.00 g) for packaging materials for HPLC (Osaka SODA, cat No. 2303P, grade: SP-300-5P, lot# A1803261DQP) was suspended in HPLC grade toluene (200 mL) and the mixture was heated to refluxing temperature. A fraction of toluene (100 mL) was distilled off using a Dean-Stark apparatus to remove water azeotropically. To the colorless suspension, (3-aminopropyl)triethoxysilane (10 mL, 42.9 mmol) was added dropwise over 45 min and then stirred at 80°C overnight. Next, the mixture was cooled to RT and filtered. The reaction product was washed twice with toluene (100 mL), EtOH (100 mL), and H₂O (100 mL), respectively. After drying the product *in a vacuo*, it was further dried in a vacuum oven for 3 d, yielding (3-aminopropyl)-modified silica (10.47 g) as a white powder.

EA of silica: C: 1.55w-%±0.01; H: 0.527w-%±0.014; N:0.550w-%±0.011; S: <0.02w-%.

5.3. Synthesis of AQ-AX Stationary Phase

- Synthesis of (3-mercaptopropyl)-modified silica

Silica gel (SP-120-3P, 300 m²/g) was dried in a vacuum oven at 180°C for 5 h. To dry silica (12.00 g), (3-mercaptopropyl)trimethoxysilane (MPTMS, 10 mL, 53.8 mmol) was dissolved in anhydrous toluene (120 mL) was added. Subsequently, anhydrous pyridine (2.0 mL, 24.7 mmol) was added, and, in an inert atmosphere, the reaction mixture was stirred at refluxing temperature for 12 h. After multiple washing steps with MeOH, acetone, and *n*-hexane, the product was dried *in vacuo* at 60°C for 6 h yielding (3-mercaptopropyl)-modified silica gel as a white powder.

- Desalting of 3-aminoquinuclidine (AQ)

To obtain the free base, 3-aminoquinuclidine dihydrochloride (0.150 g, 0.8 mmol, 1.0 equiv.) was suspended in CHCl₃ (15 mL). A solution of NaOH (0.0600 g, 1.5 mmol, 2.0 equiv.) in deionized H₂O (0.70 mL) was added to the suspension. The colorless mixture was stirred for 5 min. Subsequently, anhydrous Na₂SO₄ (0.02 g) was added after phase separation, the suspension was stirred for another 30 min, and filtered to obtain the free base AQ after concentration *in vacuo* (646 mg, 67% yield).

- Synthesis of the AQ-AX selector

AQ (0.600 g, 5.1 mmol, 1.0 equiv) was dissolved in toluene (100 mL) and the solvent was azeotropically distilled at 84°C using a Dean-Stark apparatus to remove water. After cooling to RT, allyl isocyanate (0.600 mL, 0.500 g, 6.0 mmol, 1.2 equiv.) was added and stirred at 30°C overnight. After purification by flash column chromatography (eluent: DCM/MeOH 10/1 v/v), the product was obtained (840 mg, 79% yield).

¹H NMR (400.13 MHz, CDCl₃): 5.82 (ddt, *J* = 17.2, 10.4, 5.3 Hz, 1H, H-14), 5.19-5.04 (m, 2H, H-15), 3.78-3.75 (m, 2H, C-13), 3.74 (t, *J* = 1.7 Hz, 1H, H-5), 3.27 (s, 2H, H-4), 2.79 (ddq, *J* = 12.0, 6.3, 3.1 Hz, 4H, H-2, H-8), 1.86 (q, *J* = 3.1 Hz, 2H, H-6), 1.80-1.51 (m, 4H, H-1, H-7).

^{13}C NMR spectrum of the selector (100.26 MHz, CDCl_3): 158.5 (C=O), 135.6 (C14), 115.3 (C15), 56.4 (C4), 47.3 (C2), 47.0 (C5), 46.5 (C8), 42.7 (C13), 26.1 (C6), 25.6 (C1, C7).

- Immobilization by thiol-ene addition

In a round bottom flask equipped with a mechanical stirrer, 3-mercaptopropyl-modified silica (6.00 g) and the AQ-AX selector (0.460 g, 2.2 mmol) were suspended in MeOH (90 mL). AIBN (0.520 g, 3.2 mmol, 1.5 equiv., 1.1 g/mL) was added and the mixture was stirred under an inert atmosphere at 70°C for 18 h. The mixture was thoroughly washed with MeOH and CH_2Cl_2 . After drying, the product was obtained (6.25 g).

EA of AQ-AX: C: 5.70w-% \pm 0.08; H: 1.17 w-% \pm 0.11; N: 0.64 w-% \pm 0.02; S: 2.03 w-% \pm 0.00.

5.4. Derivatization of Amino Acids

- Synthesis of (*R,S*)-*N*-acetyl- β -leucine

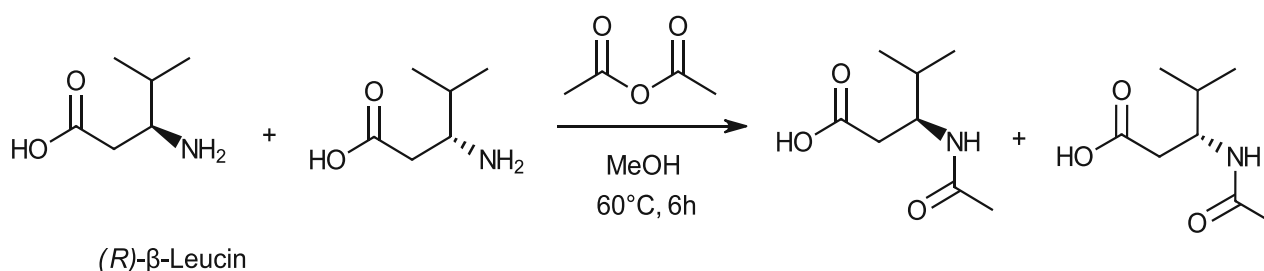


Figure 30: Derivatization of (*R,S*)- β -leucine with acetic anhydride.

Acetic anhydride (60 μL , 61.3 mg, 0.6 mmol, 2.8 equiv.) was added to a mixture (30.5 mg, 0.2 mmol) of (*R*)- β -leucine (20.6 mg) and (*S*)- β -leucine (9.9 mg). MeOH (200 μL) was added to the mixture, which was subsequently stirred at 60°C for 6 h. The volatiles were removed *in vacuo* yielding an oily product. The product was cooled to -18°C overnight. The cooled product was slowly warmed to RT, whereupon fine crystals formed yielding *N*-acetyl- β -leucine (28.2 mg, 70% yield).

^1H NMR spectrum of (*R,S*)-*N*-acetyl- β -leucine (400.3 MHz, CDCl_3): 4.04 (m, 1H, H-7), 2.57 (m, 2H, H-3), 2.01 (d, J = 12.8 Hz, 3H, H-15), 1.85 (ddd, J = 19.0, 14.2, 6.8 Hz, 1H, H-9), 0.94 (ddd, J = 12.8, 6.7, 2.6 Hz, 8H, H-10, H-11).

- Synthesis of (*R,S*)-*N*-benzoyl- β -leucine

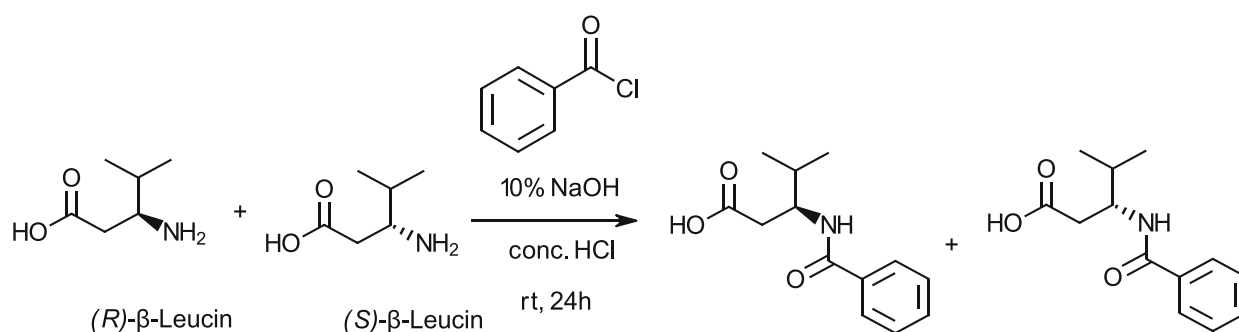


Figure 31: Derivatization of (*R,S*)- β -leucine with benzoyl chloride.

After combining (*R*)- β -leucine (20.5 mg) with (*S*)- β -leucine (9.50 mg) (30.0 mg, 0.2 mmol in total), the mixture was dissolved in 10 wt% aqueous NaOH (300 μ L). Subsequently, benzoyl chloride (37.5 μ L, 0.3 mmol, 1.4 equiv.) was added dropwise to the mixture under vigorous stirring. The mixture was acidified using conc. HCl before crushed ice was added. Under acidic conditions, the product precipitated (31.4 mg, 58% yield).

^1H NMR spectrum of (*R,S*)-*N*-benzoyl- β -leucine (400.13 MHz, CD_3OD): 7.89 – 7.25 (m, 5H, Ph), 4.54 – 4.09 (m, 1H, H-6), 2.72 – 2.50 (m, 2H, H-3), 2.01 – 1.88 (m, 1H, H-8), 0.99 (dd, $J = 6.8, 5.0$ Hz, 6H, H-9, H-10).

5.5. Evaluation of the AQ-AX Phase

- HPLC parameters

The AQ-AX phase was packed into an HPLC column (150 x 4 mm, i.d.) using a slurry packing method according to standard procedures. All measurements were done at 22°C, with a flow rate of 1 mL/min and a pressure limit of 400 bar. As a dead time marker (t_0), *p*-cymene was used.

The Agilent 1100 HPLC system was purchased from Agilent Technologies, Inc. and was equipped with a degasser (G1322A), a quaternary pump (G1311A), an ALS autosampler (G1313A), and a DAD detector (G1315A). Mobile phases consisting of ACN/ H_2O (9/1, 8/2, 7/3 v/v) or MeOH/ H_2O (10/0, 9/1, 8/2 v/v) without and with NH_4OAc (1.93 g/L) were used.

- Analytes

Eight different *N*-protected amino acids (1 mg/mL) were used (**Figure 33**) for stationary phase evaluation. As a control, one neutral reference and one cationic reference were used. Chiral and achiral analytes were available in the house from previous projects.

6. References

- Abate, A., Brenna, E., Fuganti, C., Gatti, F. G., Giovenzana, T., Malpezzi, L., & Serra, S. (2005). Chirality and Fragrance Chemistry: Stereoisomers of the Commercial Chiral Odorants Muguesia and Pamplefleuer. *The Journal of Organic Chemistry*, 70(4), 1281–1290. <https://doi.org/10.1021/jo048445j>
- Abdulbagi, M., Wang, L., Siddig, O., Di, B., & Li, B. (2021). D-Amino Acids and D-Amino Acid-Containing Peptides: Potential Disease Biomarkers and Therapeutic Targets? *Biomolecules*, 11(11), 1716. <https://doi.org/10.3390/biom11111716>
- Aburatani, R., Okamoto, Y., & Hatada, K. (1990). Optical Resolving Ability of 3,5-Dimethylphenylcarbamates of Oligosaccharides and Cyclodextrins. *Bulletin of the Chemical Society of Japan*, 63(12), 3606–3610. <https://doi.org/10.1246/bcsj.63.3606>
- Ahuja, S. (2010). Chirality of Biomolecules and Biotechnology Products. In *Chiral Separation Methods for Pharmaceutical and Biotechnological Products* (pp. 441–467). John Wiley & Sons, Inc. <https://doi.org/10.1002/9780470608661.ch15>
- Allen, D. A., Tomaso, A. E., Priest, O. P., Hindson, D. F., & Hurlburt, J. L. (2008). Mosher Amides: Determining the Absolute Stereochemistry of Optically-Active Amines. *Journal of Chemical Education*, 85(5), 698. <https://doi.org/10.1021/ed085p698>
- Arenas, M., Martín, J., Santos, J. L., Aparicio, I., & Alonso, E. (2021). An overview of analytical methods for enantiomeric determination of chiral pollutants in environmental samples and biota. *TrAC Trends in Analytical Chemistry*, 143, 116370. <https://doi.org/10.1016/j.trac.2021.116370>
- Armstrong, D. W., Tang, Yubing., Chen, Shushi., Zhou, Yiwen., Bagwill, Christina., & Chen, J.-Ran. (1994). Macrocyclic Antibiotics as a New Class of Chiral Selectors for Liquid Chromatography. *Analytical Chemistry*, 66(9), 1473–1484. <https://doi.org/10.1021/ac00081a019>
- Bajtai, A., Lajkó, G., Szatmári, I., Fülöp, F., Lindner, W., Ilisz, I., & Péter, A. (2018). Dedicated comparisons of diverse polysaccharide- and zwitterionic Cinchona alkaloid-based chiral stationary phases probed with basic and ampholytic indole analogs in liquid and subcritical fluid chromatography mode. *Journal of Chromatography A*, 1563, 180–190. <https://doi.org/10.1016/j.chroma.2018.05.064>
- Balzano, F., Uccello-Barretta, G., & Aiello, F. (2018). Chiral Analysis by NMR Spectroscopy: Chiral Solvating Agents. In *Chiral Analysis* (pp. 367–427). Elsevier. <https://doi.org/10.1016/B978-0-444-64027-7.00009-4>

- Bargmann-Leyder, N., Caude, M., & Tambute, A. (2000). CHIRAL SEPARATIONS | Supercritical Fluid Chromatography. In *Encyclopedia of Separation Science* (pp. 2406–2418). Elsevier. <https://doi.org/10.1016/B0-12-226770-2/03221-X>
- Barth G. H. (2018). Chromatography Fundamentals, Part II: Thermodynamics of Liquid Chromatography: Energetics. *LCGC North America*, 36(6), 394–396.
- Baykusheva, D., Zindel, D., Svoboda, V., Bommeli, E., Ochsner, M., Tehlar, A., & Wörner, H. J. (2019). Real-time probing of chirality during a chemical reaction. *Proceedings of the National Academy of Sciences*, 116(48), 23923–23929. <https://doi.org/10.1073/pnas.1907189116>
- Berthod, A. (2010a). *Chiral Recognition in Separation Methods* (A. Berthod, Ed.). Springer Berlin Heidelberg. <https://doi.org/10.1007/978-3-642-12445-7>
- Berthod, A. (2010b). Chiral Recognition Mechanisms in Enantiomers Separations: A General View. In *Chiral Recognition in Separation Methods* (pp. 1–32). Springer Berlin Heidelberg. https://doi.org/10.1007/978-3-642-12445-7_1
- Betzenbichler, G., Huber, L., Kräh, S., Morkos, M. K., Siegle, A. F., & Trapp, O. (2022). Chiral stationary phases and applications in gas chromatography. *Chirality*, 34(5), 732–759. <https://doi.org/10.1002/chir.23427>
- Bingyun Li, & Donald T. Haynie. (2005). *Chiral Drug Separation*.
- Blackmond, D. G. (2019). The Origin of Biological Homochirality. *Cold Spring Harbor Perspectives in Biology*, 11(3), a032540. <https://doi.org/10.1101/cshperspect.a032540>
- Boratyński, P. J., Zielińska-Błajet, M., & Skarzewski, J. (2019). *Cinchona Alkaloids—Derivatives and Applications* (pp. 29–145). <https://doi.org/10.1016/bs.alkal.2018.11.001>
- Bougas, L., Byron, J., Budker, D., & Williams, J. (2022). Absolute optical chiral analysis using cavity-enhanced polarimetry. *Science Advances*, 8(22). <https://doi.org/10.1126/sciadv.abm3749>
- Buffiere, J., Ahvenainen, P., Borrega, M., Svedström, K., & Sixta, H. (2016). Supercritical water hydrolysis: a green pathway for producing low-molecular-weight cellulose. *Green Chemistry*, 18(24), 6516–6525. <https://doi.org/10.1039/C6GC02544G>
- Bui, C. V., Rosenau, T., & Hettegger, H. (2021). Polysaccharide- and β -Cyclodextrin-Based Chiral Selectors for Enantiomer Resolution: Recent Developments and Applications. *Molecules*, 26(14), 4322. <https://doi.org/10.3390/molecules26144322>

- Bui, C. V., Rosenau, T., & Hettegger, H. (2022a). Synthesis of Polyanionic Cellulose Carbamates by Homogeneous Aminolysis in an Ionic Liquid/DMF Medium. *Molecules*, 27(4), 1384. <https://doi.org/10.3390/molecules27041384>
- Bui, C. V., Rosenau, T., & Hettegger, H. (2022b). Synthesis by carbonate aminolysis and chiral recognition ability of cellulose 2,3-bis(3,5-dimethylphenyl carbamate)-6-(α -phenylethyl carbamate) selectors. *Cellulose*. <https://doi.org/10.1007/s10570-022-04898-8>
- Calvello, S., & Soncini, A. (2020). Effect of magnetic anisotropy on direct chiral discrimination in paramagnetic NMR spectroscopy. *Physical Chemistry Chemical Physics*, 22(16), 8427–8441. <https://doi.org/10.1039/D0CP00539H>
- Castells, C. B., & Carr, P. W. (2000). A study of the thermodynamics and influence of temperature on chiral high-performance liquid chromatographic separations using cellulosetris(3,5-dimethylphenylcarbamate) coated zirconia stationary phases. *Chromatographia*, 52(9–10), 535–542. <https://doi.org/10.1007/BF02789747>
- Cavazzini, A., Pasti, L., Massi, A., Marchetti, N., & Dondi, F. (2011). Recent applications in chiral high performance liquid chromatography: A review. *Analytica Chimica Acta*, 706(2), 205–222. <https://doi.org/10.1016/j.aca.2011.08.038>
- Chankvetadze, B. (2012). Recent developments on polysaccharide-based chiral stationary phases for liquid-phase separation of enantiomers. *Journal of Chromatography A*, 1269, 26–51. <https://doi.org/10.1016/j.chroma.2012.10.033>
- Chhabra, N., Aseri, M., & Padmanabhan, D. (2013). A review of drug isomerism and its significance. *International Journal of Applied and Basic Medical Research*, 3(1), 16. <https://doi.org/10.4103/2229-516X.112233>
- Cossy, J. R. (2012). 1.1 Introduction: The Importance of Chirality in Drugs and Agrochemicals. In *Comprehensive Chirality* (pp. 1–7). Elsevier. <https://doi.org/10.1016/B978-0-08-095167-6.00101-4>
- Czerwenka, C., Zhang, M. M., Kählig, H., Maier, N. M., Lipkowitz, K. B., & Lindner, W. (2003). Chiral Recognition of Peptide Enantiomers by Cinchona Alkaloid Derived Chiral Selectors: Mechanistic Investigations by Liquid Chromatography, NMR Spectroscopy, and Molecular Modeling. *The Journal of Organic Chemistry*, 68(22), 8315–8327. <https://doi.org/10.1021/jo0346914>
- Davankov V.A. (1997). Analytical chiral separation methods. *International Union of Pure and Applied Chemistry*, 69(7), 1469–1474.

- Didier, D., Tylleman, B., Lambert, N., vande Velde, C. M. L., Blockhuys, F., Collas, A., & Sergeev, S. (2008). Functionalized analogues of Tröger's base: scope and limitations of a general synthetic procedure and facile, predictable method for the separation of enantiomers. *Tetrahedron*, *64*(27), 6252–6262. <https://doi.org/10.1016/j.tet.2008.04.111>
- Evans, A. M. (2001). Comparative Pharmacology of S(+)-Ibuprofen and (RS)-Ibuprofen. *Clinical Rheumatology*, *20*(S1), 9–14. <https://doi.org/10.1007/BF03342662>
- Fassihi, A. (1993). Racemates and enantiomers in drug development. *International Journal of Pharmaceutics*, *92*(1–3), 1–14. [https://doi.org/10.1016/0378-5173\(93\)90257-G](https://doi.org/10.1016/0378-5173(93)90257-G)
- Fernandes, C., Teixeira, J., Pinto, M. M. M., & Tiritan, M. E. (2021). Strategies for Preparation of Chiral Stationary Phases: Progress on Coating and Immobilization Methods. *Molecules*, *26*(18), 5477. <https://doi.org/10.3390/molecules26185477>
- Finefield, J. M., Sherman, D. H., Kreitman, M., & Williams, R. M. (2012). Enantiomeric Natural Products: Occurrence and Biogenesis. *Angewandte Chemie International Edition*, *51*(20), 4802–4836. <https://doi.org/10.1002/anie.201107204>
- Geoffrey B. Cox. (2005). *Preparative Enantioselective Chromatography* (G. B. Cox, Ed.). Wiley. <https://doi.org/10.1002/9780470988428>
- Gogoi, A., Konwer, S., & Zhuo, G.-Y. (2021). Polarimetric Measurements of Surface Chirality Based on Linear and Nonlinear Light Scattering. *Frontiers in Chemistry*, *8*. <https://doi.org/10.3389/fchem.2020.611833>
- Grinberg, N., & Carr, W. P. (2017). *Advances in Chromatography* (N. Grinberg, Ed.). CRC Press. <https://doi.org/10.1201/9781315158075>
- Grybinik, S., & Bosakova, Z. (2021a). An overview of chiral separations of pharmaceutically active substances by HPLC (2018–2020). *Monatshefte Für Chemie - Chemical Monthly*, *152*(9), 1033–1043. <https://doi.org/10.1007/s00706-021-02832-5>
- Grybinik, S., & Bosakova, Z. (2021b). An overview of chiral separations of pharmaceutically active substances by HPLC (2018–2020). *Monatshefte Für Chemie - Chemical Monthly*, *152*(9), 1033–1043. <https://doi.org/10.1007/s00706-021-02832-5>
- Guo, J., Wang, Q., Xu, D., Crommen, J., & Jiang, Z. (2020). Recent advances in preparation and applications of monolithic chiral stationary phases. *TrAC Trends in Analytical Chemistry*, *123*, 115774. <https://doi.org/10.1016/j.trac.2019.115774>

- Guo, P., An, X., Chen, W., Pan, X., Li, R., Xu, J., Wu, X., Zheng, Y., & Dong, F. (2022). Separation and determination of fluindapyr enantiomers in cucumber and tomato and by supercritical fluid chromatography tandem mass spectrometry. *Food Chemistry*, 395, 133571. <https://doi.org/10.1016/j.foodchem.2022.133571>
- Guo-Qiang Lin, Q.-D. Y. J.-F. C. (2011). *Chiral Drugs: Chemistry and Biological Action*.
- Hancu, G., & Modroiu, A. (2022). Chiral Switch: Between Therapeutical Benefit and Marketing Strategy. *Pharmaceuticals*, 15(2), 240. <https://doi.org/10.3390/ph15020240>
- Harada, N. (2016). HPLC Separation of Diastereomers: Chiral Molecular Tools Useful for the Preparation of Enantiopure Compounds and Simultaneous Determination of Their Absolute Configurations. *Molecules*, 21(10), 1328. <https://doi.org/10.3390/molecules21101328>
- Haslinger, S., Hietala, S., Hummel, M., Maunu, S. L., & Sixta, H. (2019). Solid-state NMR method for the quantification of cellulose and polyester in textile blends. *Carbohydrate Polymers*, 207, 11–16. <https://doi.org/10.1016/j.carbpol.2018.11.052>
- Hellwich, K.-H. (2002). Stereochemie. In *Stereochemie — Grundbegriffe* (pp. 76–76). Springer Berlin Heidelberg. https://doi.org/10.1007/978-3-662-10051-6_48
- Hettegger, H., Lindner, W., & Rosenau, T. (2020). Derivatized polysaccharides on silica and hybridized with silica in chromatography and separation—A mini review. In *Recent Trends in Carbohydrate Chemistry* (pp. 441–462). Elsevier. <https://doi.org/10.1016/B978-0-12-817467-8.00012-8>
- Heuberger, E. (2001). Effects of Chiral Fragrances on Human Autonomic Nervous System Parameters and Self-evaluation. *Chemical Senses*, 26(3), 281–292. <https://doi.org/10.1093/chemse/26.3.281>
- Hoffmann, C. v., Laemmerhofer, M., & Lindner, W. (2007). Novel strong cation-exchange type chiral stationary phase for the enantiomer separation of chiral amines by high-performance liquid chromatography. *Journal of Chromatography A*, 1161(1–2), 242–251. <https://doi.org/10.1016/j.chroma.2007.05.092>
- Hoffmann, C. v., Reischl, R., Maier, N. M., Lämmerhofer, M., & Lindner, W. (2009). Stationary phase-related investigations of quinine-based zwitterionic chiral stationary phases operated in anion-, cation-, and zwitterion-exchange modes. *Journal of Chromatography A*, 1216(7), 1147–1156. <https://doi.org/10.1016/j.chroma.2008.12.045>

- Holtzapfle, M. T., & Humphrey, A. E. (1983). Determination of soluble and insoluble glucose oligomers with chromotropic acid. *Analytical Chemistry*, 55(3), 584–585. <https://doi.org/10.1021/ac00254a040>
- Ikai, T., & Okamoto, Y. (2009). Structure Control of Polysaccharide Derivatives for Efficient Separation of Enantiomers by Chromatography. *Chemical Reviews*, 109(11), 6077–6101. <https://doi.org/10.1021/cr8005558>
- Ikegami, W., Kamitakahara, H., Teramoto, Y., & Takano, T. (2021). Synthesis of optically inactive cellulose via cationic ring-opening polymerization. *Cellulose*, 28(10), 6125–6132. <https://doi.org/10.1007/s10570-021-03970-z>
- Isac-García, J., Dobado, J. A., Calvo-Flores, F. G., & Martínez-García, H. (2016). Basic Operation Experiments. In *Experimental Organic Chemistry* (pp. 207–238). Elsevier. <https://doi.org/10.1016/B978-0-12-803893-2.50007-3>
- José, C., Toledo, M. V., & Briand, L. E. (2016). Enzymatic kinetic resolution of racemic ibuprofen: past, present and future. *Critical Reviews in Biotechnology*, 36(5), 891–903. <https://doi.org/10.3109/07388551.2015.1057551>
- Kamitakahara, H., Hori, M., & Nakatsubo, F. (1996). Substituent Effect on Ring-Opening Polymerization of Regioselectively Acylated α -D-Glucopyranose 1,2,4-Orthopivalate Derivatives. *Macromolecules*, 29(19), 6126–6131. <https://doi.org/10.1021/ma960488h>
- Kasuya, N., Kusaka, Y., Habu, N., & Ohnishi, A. (2002). Development of chiral stationary phases consisting of low-molecular-weight cellulose derivatives covalently bonded to silica gel. *Cellulose*, 9(3/4), 263–269. <https://doi.org/10.1023/A:1021188610098>
- Katoh, Y., Tsujimoto, Y., Yamamoto, C., Ikai, T., Kamigaito, M., & Okamoto, Y. (2011). Chiral recognition ability of cellulose derivatives bearing pyridyl and bipyridyl residues as chiral stationary phases for high-performance liquid chromatography. *Polymer Journal*, 43(1), 84–90. <https://doi.org/10.1038/pj.2010.108>
- Kaushik, M., Basu, K., Benoit, C., Cirtiu, C. M., Vali, H., & Moores, A. (2015). Cellulose Nanocrystals as Chiral Inducers: Enantioselective Catalysis and Transmission Electron Microscopy 3D Characterization. *Journal of the American Chemical Society*, 137(19), 6124–6127. <https://doi.org/10.1021/jacs.5b02034>
- Khandelwal, M., & Windle, A. (2014). Origin of chiral interactions in cellulose supra-molecular microfibrils. *Carbohydrate Polymers*, 106, 128–131. <https://doi.org/10.1016/j.carbpol.2014.01.050>

- Kobayashi, S., Kashiwa, K., Kawasaki, T., & Shoda, S. (1991). Novel method for polysaccharide synthesis using an enzyme: the first in vitro synthesis of cellulose via a nonbiosynthetic path utilizing cellulase as catalyst. *Journal of the American Chemical Society*, *113*(8), 3079–3084. <https://doi.org/10.1021/ja00008a042>
- Kohout, M., Wernisch, S., Tůma, J., Hettegger, H., Pícha, J., & Lindner, W. (2018). Effect of different immobilization strategies on chiral recognition properties of *Cinchona* -based anion exchangers. *Journal of Separation Science*, *41*(6), 1355–1364. <https://doi.org/10.1002/jssc.201701213>
- Lämmerhofer, M. (2010). Chiral recognition by enantioselective liquid chromatography: Mechanisms and modern chiral stationary phases. *Journal of Chromatography A*, *1217*(6), 814–856. <https://doi.org/10.1016/j.chroma.2009.10.022>
- Lämmerhofer, M., & Lindner, W. (1996). Quinine and quinidine derivatives as chiral selectors I. Brush type chiral stationary phases for high-performance liquid chromatography based on cinchonan carbamates and their application as chiral anion exchangers. *Journal of Chromatography A*, *741*(1), 33–48. [https://doi.org/10.1016/0021-9673\(96\)00137-9](https://doi.org/10.1016/0021-9673(96)00137-9)
- Lämmerhofer, M., Nogueira, R., & Lindner, W. (2011). Multi-modal applicability of a reversed-phase/weak-anion exchange material in reversed-phase, anion-exchange, ion-exclusion, hydrophilic interaction and hydrophobic interaction chromatography modes. *Analytical and Bioanalytical Chemistry*, *400*(8), 2517–2530. <https://doi.org/10.1007/s00216-011-4755-3>
- Lehrhofer, A. F., Goto, T., Kawada, T., Rosenau, T., & Hettegger, H. (2022). The in vitro synthesis of cellulose – A mini-review. *Carbohydrate Polymers*, *285*, 119222. <https://doi.org/10.1016/j.carbpol.2022.119222>
- Li, B., & Haynie, D. T. (2005). Chiral Drug Separation. *Encyclopedia of Chemical Processing*, 449–458. <https://doi.org/10.1081/E-ECHP-120039232>
- Li, L., Yuan, X., Shi, Z., & Xu, L. (2020). Chiral stationary phase based on cellulose derivative coated polymer microspheres and its separation performance. *Journal of Chromatography A*, *1623*, 461154. <https://doi.org/10.1016/j.chroma.2020.461154>
- Liu, R.-Q., Bai, L., Zhang, Y.-J., & Zhang, Y.-P. (2013). Green synthesis of a typical chiral stationary phase of cellulose-tris(3, 5-dimethylphenylcarbamate). *Chemistry Central Journal*, *7*(1), 129. <https://doi.org/10.1186/1752-153X-7-129>
- Liu, Y., Xu, F., Wu, F., Wang, H., Liang, Z., & Ding, C.-F. (2022). Chiral distinction of phenyl-substituted ethanediol enantiomers by measuring the ion

mobility of their ternary complexes. *Microchemical Journal*, **178**, 107389.
<https://doi.org/10.1016/j.microc.2022.107389>

Long, A. S., Zhang, A. D., Meyer, C. E., Egilman, A. C., Ross, J. S., & Wallach, J. D. (2021). Evaluation of Trials Comparing Single-Enantiomer Drugs to Their Racemic Precursors. *JAMA Network Open*, **4**(5), e215731.

<https://doi.org/10.1001/jamanetworkopen.2021.5731>

López, R., & Palomo, C. (2022). Planar Chirality: A Mine for Catalysis and Structure Discovery. *Angewandte Chemie International Edition*, **61**(13).

<https://doi.org/10.1002/anie.202113504>

Lough, W. J. (2014). Classification of LC chiral stationary phases: Wainer Types I–V revisited. *Journal of Chromatography B*, **968**, 1–7.

<https://doi.org/10.1016/j.jchromb.2014.04.044>

Lowe, A. B. (2010). Thiol-ene “click” reactions and recent applications in polymer and materials synthesis. *Polym. Chem.*, **1**(1), 17–36.

<https://doi.org/10.1039/B9PY00216B>

Maier, N. M., Nicoletti, L., Lämmerhofer, M., & Lindner, W. (1999). Enantioselective anion exchangers based on cinchona alkaloid-derived carbamates: Influence of C8/C9 stereochemistry on chiral recognition.

Chirality, **11**(7), 522–528. [https://doi.org/10.1002/\(SICI\)1520-636X\(1999\)11:7<522::AID-CHIR2>3.0.CO;2-U](https://doi.org/10.1002/(SICI)1520-636X(1999)11:7<522::AID-CHIR2>3.0.CO;2-U)

Mandl, A., Nicoletti, L., Lämmerhofer, M., & Lindner, W. (1999). Quinine- versus carbamoylated quinine-based chiral anion exchangers. *Journal of Chromatography A*, **858**(1), 1–11.

[https://doi.org/10.1016/S0021-9673\(99\)00803-1](https://doi.org/10.1016/S0021-9673(99)00803-1)

McCalley V. D. (2019). Hydrophilic Interaction Liquid Chromatography: An Update. *LCGC Europe*, **32**(3), 114–125.

McConathy, J., & Owens, M. J. (2003). Stereochemistry in Drug Action. *The Primary Care Companion to The Journal of Clinical Psychiatry*, **05**(02), 70–73.

<https://doi.org/10.4088/PCC.v05n0202>

Metcalfe, S., & Reilly, I. (2010). Local Anaesthetics. In *Foot and Ankle Injection Techniques* (pp. 1–22). Elsevier.

<https://doi.org/10.1016/B978-0-7020-3107-6.00001-6>

Metier, C., Dow, J., Wootton, H., Lynham, S., Wren, B., & Wagner, G. K. (2021). Profiling of Haemophilus influenzae strain R2866 with carbohydrate-based covalent probes. *Organic & Biomolecular Chemistry*, **19**(2), 476–485.

<https://doi.org/10.1039/D0OB01971B>

- Nakano, T. (2001). Optically active synthetic polymers as chiral stationary phases in HPLC. *Journal of Chromatography A*, 906(1–2), 205–225. [https://doi.org/10.1016/S0021-9673\(00\)00944-4](https://doi.org/10.1016/S0021-9673(00)00944-4)
- Nakatsubo, F., Kamitakahara, H., & Hori, M. (1996). Cationic Ring-Opening Polymerization of 3,6-Di- O -benzyl- α -D-glucose 1,2,4-Orthopivalate and the First Chemical Synthesis of Cellulose. *Journal of the American Chemical Society*, 118(7), 1677–1681. <https://doi.org/10.1021/ja953286u>
- Naturale, G., Lamblin, M., Commandeur, C., Felpin, F.-X., & Dessolin, J. (2012). Direct C-H Alkylation of Naphthoquinones with Amino Acids Through a Revisited Kochi-Anderson Radical Decarboxylation: Trends in Reactivity and Applications. *European Journal of Organic Chemistry*, 2012(29), 5774–5788. <https://doi.org/10.1002/ejoc.201200722>
- Nguyen, L. A., He, H., & Pham-Huy, C. (2006). Chiral drugs: an overview. *International Journal of Biomedical Science : IJBS*, 2(2), 85–100.
- Nogueira, R., Lämmerhofer, M., & Lindner, W. (2005). Alternative high-performance liquid chromatographic peptide separation and purification concept using a new mixed-mode reversed-phase/weak anion-exchange type stationary phase. *Journal of Chromatography A*, 1089(1–2), 158–169. <https://doi.org/10.1016/j.chroma.2005.06.093>
- Nuyken, O., & Pask, S. (2013). Ring-Opening Polymerization—An Introductory Review. *Polymers*, 5(2), 361–403. <https://doi.org/10.3390/polym5020361>
- Oberleitner, W. R., Maier, N. M., & Lindner, W. (2002). Enantioseparation of various amino acid derivatives on a quinine based chiral anion-exchange selector at variable temperature conditions. Influence of structural parameters of the analytes on the apparent retention and enantioseparation characteristics. *Journal of Chromatography A*, 960(1–2), 97–108. [https://doi.org/10.1016/S0021-9673\(02\)00244-3](https://doi.org/10.1016/S0021-9673(02)00244-3)
- Okada, Y., Yamamoto, C., Kamigaito, M., Gao, Y., Shen, J., & Okamoto, Y. (2016). Enantioseparation Using Cellulose Tris(3,5-dimethylphenylcarbamate) as Chiral Stationary Phase for HPLC: Influence of Molecular Weight of Cellulose. *Molecules*, 21(11), 1484. <https://doi.org/10.3390/molecules21111484>
- Okamoto, Y., Aburatani, R., & Hatada, K. (1987). Chromatographic chiral resolution. *Journal of Chromatography A*, 389, 95–102. [https://doi.org/10.1016/S0021-9673\(01\)94414-0](https://doi.org/10.1016/S0021-9673(01)94414-0)
- Okamoto, Y., & Kaida, Y. (1994). Resolution by high-performance liquid chromatography using polysaccharide carbamates and benzoates as chiral

stationary phases. *Journal of Chromatography A*, 666(1–2), 403–419.
[https://doi.org/10.1016/0021-9673\(94\)80400-1](https://doi.org/10.1016/0021-9673(94)80400-1)

Orofino, T. A., & Wenger, F. (1961). The Effect of Impurities on the Molecular Weight Distributions of Anionic Polymers. *The Journal of Chemical Physics*, 35(2), 532–538. <https://doi.org/10.1063/1.1731963>

Ouellette, R. J., & Rawn, J. D. (2015). Stereochemistry. In *Organic Chemistry Study Guide* (pp. 117–133). Elsevier. <https://doi.org/10.1016/B978-0-12-801889-7.00008-X>

Patil, R. A., Weatherly, C. A., & Armstrong, D. W. (2018). Chiral Gas Chromatography. In *Chiral Analysis* (pp. 468–505). Elsevier.
<https://doi.org/10.1016/B978-0-444-64027-7.00012-4>

Peluso, P., Mamane, V., Dallochio, R., Dessì, A., & Cossu, S. (2020). Noncovalent interactions in high-performance liquid chromatography enantioseparations on polysaccharide-based chiral selectors. *Journal of Chromatography A*, 1623, 461202.
<https://doi.org/10.1016/j.chroma.2020.461202>

Petrie, B., Camacho Muñoz, M. D., & Martín, J. (2019). Stereoselective LC–MS/MS methodologies for environmental analysis of chiral pesticides. *TrAC Trends in Analytical Chemistry*, 110, 249–258.
<https://doi.org/10.1016/j.trac.2018.11.010>

Piette, V., Lämmerhofer, M., Lindner, W., & Crommen, J. (2003). Enantiomer separation of N-protected amino acids by non-aqueous capillary electrophoresis and high-performance liquid chromatography with tert.-butyl carbamoylated quinine in either the background electrolyte or the stationary phase. *Journal of Chromatography A*, 987(1–2), 421–427.
[https://doi.org/10.1016/S0021-9673\(02\)01465-6](https://doi.org/10.1016/S0021-9673(02)01465-6)

Piette, V., Lindner, W., & Crommen, J. (2002). Enantiomeric separation of N-protected amino acids by non-aqueous capillary electrophoresis with dimeric forms of quinine and quinidine derivatives serving as chiral selectors. *Journal of Chromatography A*, 948(1–2), 295–302.
[https://doi.org/10.1016/S0021-9673\(01\)01591-6](https://doi.org/10.1016/S0021-9673(01)01591-6)

Pirkle, W. H., Finn, J. M., Schreiner, J. L., & Hamper, B. C. (1981). A widely useful chiral stationary phase for the high-performance liquid chromatography separation of enantiomers. *Journal of the American Chemical Society*, 103(13), 3964–3966. <https://doi.org/10.1021/ja00403a076>

Pirrung C. M. (2017). Recipes for TLC Stains. In *Handbook of Synthetic Organic Chemistry* (pp. 243–244). Elsevier. <https://doi.org/10.1016/B978-0-12-809504-1.15006-X>

- Qiu, J., Dai, S., Chai, T., Yang, W., Yang, S., & Zhao, H. (2013). The Development and Application of Cellulose-Based Stationary Phases in Stereoselective Separation of Chiral Pesticides. In *Cellulose - Medical, Pharmaceutical and Electronic Applications*. InTech. <https://doi.org/10.5772/56575>
- Ribeiro, J., Tiritan, M., Pinto, M., & Fernandes, C. (2017). Chiral Stationary Phases for Liquid Chromatography Based on Chitin- and Chitosan-Derived Marine Polysaccharides. *Symmetry*, 9(9), 190. <https://doi.org/10.3390/sym9090190>
- Robards, K., Haddad, P. R., & Jackson, P. E. (2004). High-performance Liquid Chromatography—Separations. In *Principles and Practice of Modern Chromatographic Methods* (pp. 305–380). Elsevier. <https://doi.org/10.1016/B978-0-08-057178-2.50009-1>
- Roos, G., & Roos, C. (2015). Isomers and Stereochemistry. In *Organic Chemistry Concepts* (pp. 43–54). Elsevier. <https://doi.org/10.1016/B978-0-12-801699-2.00003-1>
- Rosanoff, M. A. (1906). ON FISCHER'S CLASSIFICATION OF STEREO-ISOMERS. 1. *Journal of the American Chemical Society*, 28(1), 114–121. <https://doi.org/10.1021/ja01967a014>
- Sanganyado, E., Lu, Z., Fu, Q., Schlenk, D., & Gan, J. (2017). Chiral pharmaceuticals: A review on their environmental occurrence and fate processes. *Water Research*, 124, 527–542. <https://doi.org/10.1016/j.watres.2017.08.003>
- Sarasamkan, J., Scheunemann, M., Apaijai, N., Palee, S., Parichatikanond, W., Arunrungvichian, K., Fischer, S., Chattipakorn, S., Deuther-Conrad, W., Schüürmann, G., Brust, P., & Vajragupta, O. (2016). Varying Chirality Across Nicotinic Acetylcholine Receptor Subtypes: Selective Binding of Quinuclidine Triazole Compounds. *ACS Medicinal Chemistry Letters*, 7(10), 890–895. <https://doi.org/10.1021/acsmchemlett.6b00146>
- Scriba, G. K. E. (2019). Chiral recognition in separation sciences. Part I: Polysaccharide and cyclodextrin selectors. *TrAC Trends in Analytical Chemistry*, 120, 115639. <https://doi.org/10.1016/j.trac.2019.115639>
- Sekhon. (2013). Exploiting the Power of Stereochemistry in Drugs: An Overview of Racemic and Enantiopure Drugs. *Journal of Modern Medicinal Chemistry*. <https://doi.org/10.12970/2308-8044.2013.01.01.2>
- Sharma, S., & Anand, N. (1997). *Natural Products* (pp. 347–383). [https://doi.org/10.1016/S0165-7208\(97\)80036-0](https://doi.org/10.1016/S0165-7208(97)80036-0)
- Sharp, V. S., Stafford, J. D., Forbes, R. A., Gokey, M. A., & Cooper, M. R. (2014). Stereoselective high-performance liquid chromatography and analytical

method characterization of evacetrapib using a brush-type chiral stationary phase: A challenging isomeric separation requiring a unique eluent system. *Journal of Chromatography A*, 1363, 183–190.

<https://doi.org/10.1016/j.chroma.2014.03.048>

Shen, J., Ikai, T., & Okamoto, Y. (2014). Synthesis and application of immobilized polysaccharide-based chiral stationary phases for enantioseparation by high-performance liquid chromatography. *Journal of Chromatography A*, 1363, 51–61.

<https://doi.org/10.1016/j.chroma.2014.06.042>

Shinoda, S., Miyake, H., & Tsukube, H. (2005). *Molecular recognition and sensing via rare earth complexes* (pp. 273–335).

[https://doi.org/10.1016/S0168-1273\(05\)35004-5](https://doi.org/10.1016/S0168-1273(05)35004-5)

Sinhababu, A., Basu, S., & Dey, H. (2015). Modified ninhydrin reagents to detect amino acids on TLC plates. *Research on Chemical Intermediates*, 41(5), 2785–2792. <https://doi.org/10.1007/s11164-013-1388-5>

Sun, S., Oliveira, B. L., Jiménez-Osés, G., & Bernardes, G. J. L. (2018). Radical-Mediated Thiol-Ene Strategy: Photoactivation of Thiol-Containing Drugs in Cancer Cells. *Angewandte Chemie International Edition*, 57(48), 15832–15835. <https://doi.org/10.1002/anie.201811338>

Takasu, A., & Hayashi, T. (2015). Cationic Ring-Opening Polymerization. In *Encyclopedia of Polymeric Nanomaterials* (pp. 324–329). Springer Berlin Heidelberg. https://doi.org/10.1007/978-3-642-29648-2_176

Tanács, D., Orosz, T., Ilisz, I., Péter, A., & Lindner, W. (2021). Unexpected effects of mobile phase solvents and additives on retention and resolution of N-acyl-D,L-leucine applying Cinchonane-based chiral ion exchangers. *Journal of Chromatography A*, 1648, 462212.

<https://doi.org/10.1016/j.chroma.2021.462212>

Teixeira, J., Tiritan, M. E., Pinto, M. M. M., & Fernandes, C. (2019). Chiral Stationary Phases for Liquid Chromatography: Recent Developments. *Molecules*, 24(5), 865. <https://doi.org/10.3390/molecules24050865>

Usov, I., Nyström, G., Adamcik, J., Handschin, S., Schütz, C., Fall, A., Bergström, L., & Mezzenga, R. (2015). Understanding nanocellulose chirality and structure–properties relationship at the single fibril level. *Nature Communications*, 6(1), 7564. <https://doi.org/10.1038/ncomms8564>

Viedma, C., Coquerel, G., & Cintas, P. (2015). Crystallization of Chiral Molecules. In *Handbook of Crystal Growth* (pp. 951–1002). Elsevier. <https://doi.org/10.1016/B978-0-444-56369-9.00022-8>

- Wahab, M. F., Weatherly, C. A., Patil, R. A., & Armstrong, D. W. (2018). Chiral Liquid Chromatography. In *Chiral Analysis* (pp. 507–564). Elsevier.
<https://doi.org/10.1016/B978-0-444-64027-7.00014-8>
- Wang, Y., Xiang, S., & Tan, B. (2021). Introduction and Characteristics. In *Axially Chiral Compounds* (pp. 1–12). Wiley.
<https://doi.org/10.1002/9783527825172.ch1>
- Wei, Y., Zhou, M., Yao, A., & Zhu, P. (2020). Preparation of Microfibrillated Cellulose from Wood Pulp through Carbamate Modification and Colloid Milling. *Applied Sciences*, 10(6), 1977. <https://doi.org/10.3390/app10061977>
- Witte, D. T., Bruggeman, F. J., Franke, J. P., Coppinga, S., Jansen, J. M., & de Zeeuw, R. A. (1993). Comparison between cellulose and amylose tris(3,5-dimethylphenylcarbamate) chiral stationary phases for enantiomeric separation of 17 amidotetralins. *Chirality*, 5(7), 545–553.
<https://doi.org/10.1002/chir.530050711>
- Wolrab, D., Frühauf, P., Kolderová, N., & Kohout, M. (2021). Strong cation- and zwitterion-exchange-type mixed-mode stationary phases for separation of pharmaceuticals and biogenic amines in different chromatographic modes. *Journal of Chromatography A*, 1635, 461751.
<https://doi.org/10.1016/j.chroma.2020.461751>
- Xiao, R., & Grinstaff, M. W. (2017). Chemical synthesis of polysaccharides and polysaccharide mimetics. *Progress in Polymer Science*, 74, 78–116.
<https://doi.org/10.1016/j.progpolymsci.2017.07.009>
- Xin, F., & Pope, M. T. (1996). Lone-Pair-Induced Chirality in Polyoxotungstate Structures: Tin(II) Derivatives of A-Type XW₉O_{34n}- (X = P, Si). Interaction with Amino Acids. *Journal of the American Chemical Society*, 118(33), 7731–7736. <https://doi.org/10.1021/ja954045p>
- Yagura, T., Ikegami, W., Kamitakahara, H., & Takano, T. (2020). Synthesis of an enantiomer of cellulose via cationic ring-opening polymerization. *Cellulose*, 27(17), 9755–9766. <https://doi.org/10.1007/s10570-020-03512-z>
- Yu, R. B., & Quirino, J. P. (2019). Chiral liquid chromatography and capillary electrochromatography: Trends from 2017 to 2018. *TrAC Trends in Analytical Chemistry*, 118, 779–792.
<https://doi.org/10.1016/j.trac.2019.07.011>
- Zhang, J., Xie, S., & Yuan, L. (2022). Recent progress in the development of chiral stationary phases for high-performance liquid chromatography. *Journal of Separation Science*, 45(1), 51–77.
<https://doi.org/10.1002/jssc.202100593>

- Zhang, K., & Liu, X. (2016). Mixed-mode chromatography in pharmaceutical and biopharmaceutical applications. *Journal of Pharmaceutical and Biomedical Analysis*, 128, 73–88. <https://doi.org/10.1016/j.jpba.2016.05.007>
- Zhou, J., Yang, Y., Wei, F., & Wu, P. (2007). Comparison of the performance of chiral stationary phase for separation of fluoxetine enantiomers. *Journal of Zhejiang University SCIENCE B*, 8(1), 56–59. <https://doi.org/10.1631/jzus.2007.B0056>
- Zhou, Y., Ma, C., Wang, Y., Zhang, Q.-M., Zhang, Y.-Y., Fu, J., Gao, H., & Zhao, L.-X. (2012). High performance liquid chromatographic separation of thirteen drugs collected in Chinese Pharmacopoeia 2010(Ch.P2010) on cellulose ramification chiral stationary phase. *Journal of Pharmaceutical Analysis*, 2(1), 48–55. <https://doi.org/10.1016/j.jpha.2011.11.007>

7. Appendix

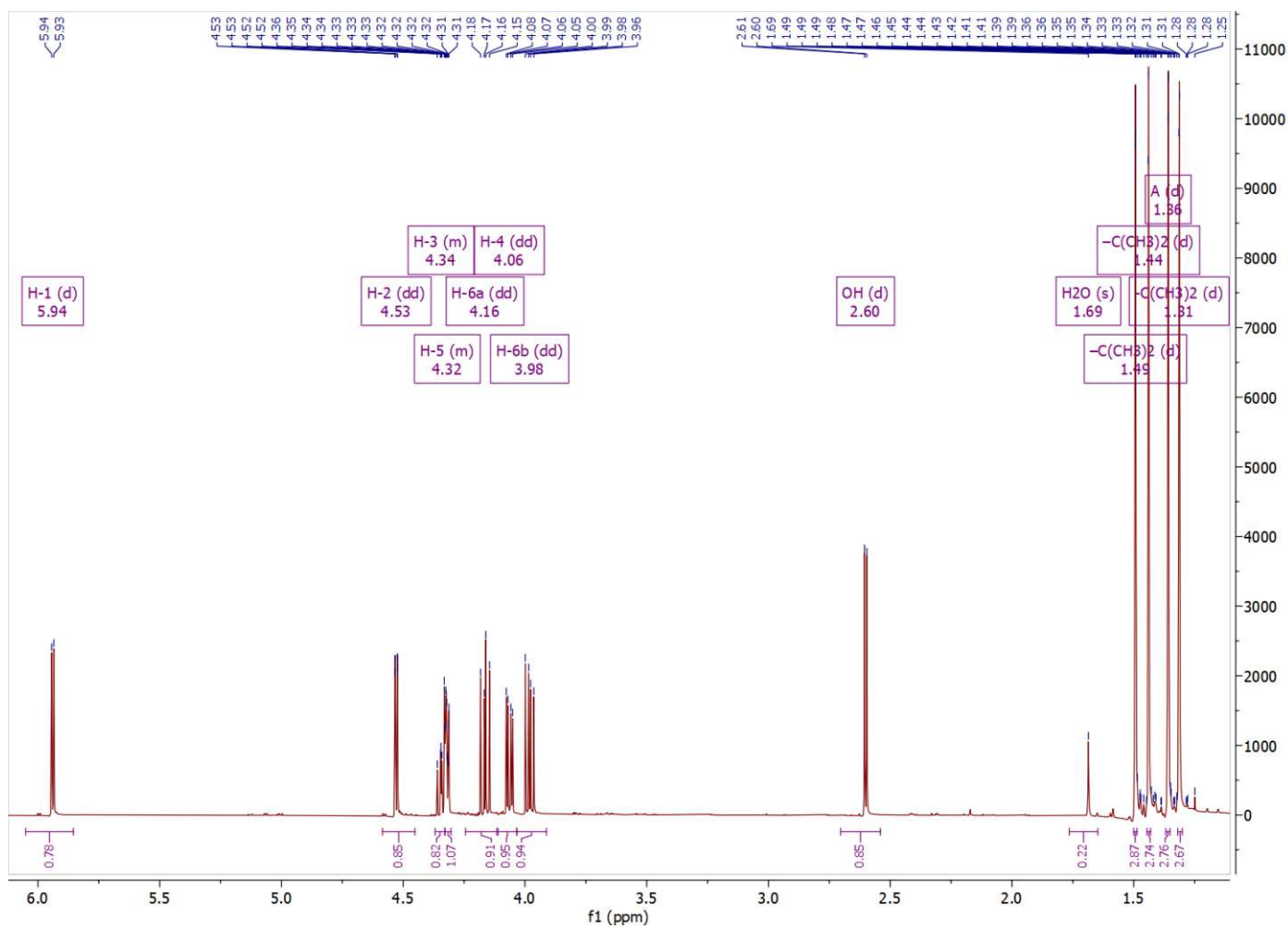


Figure 12: ¹H NMR spectrum of 2D.

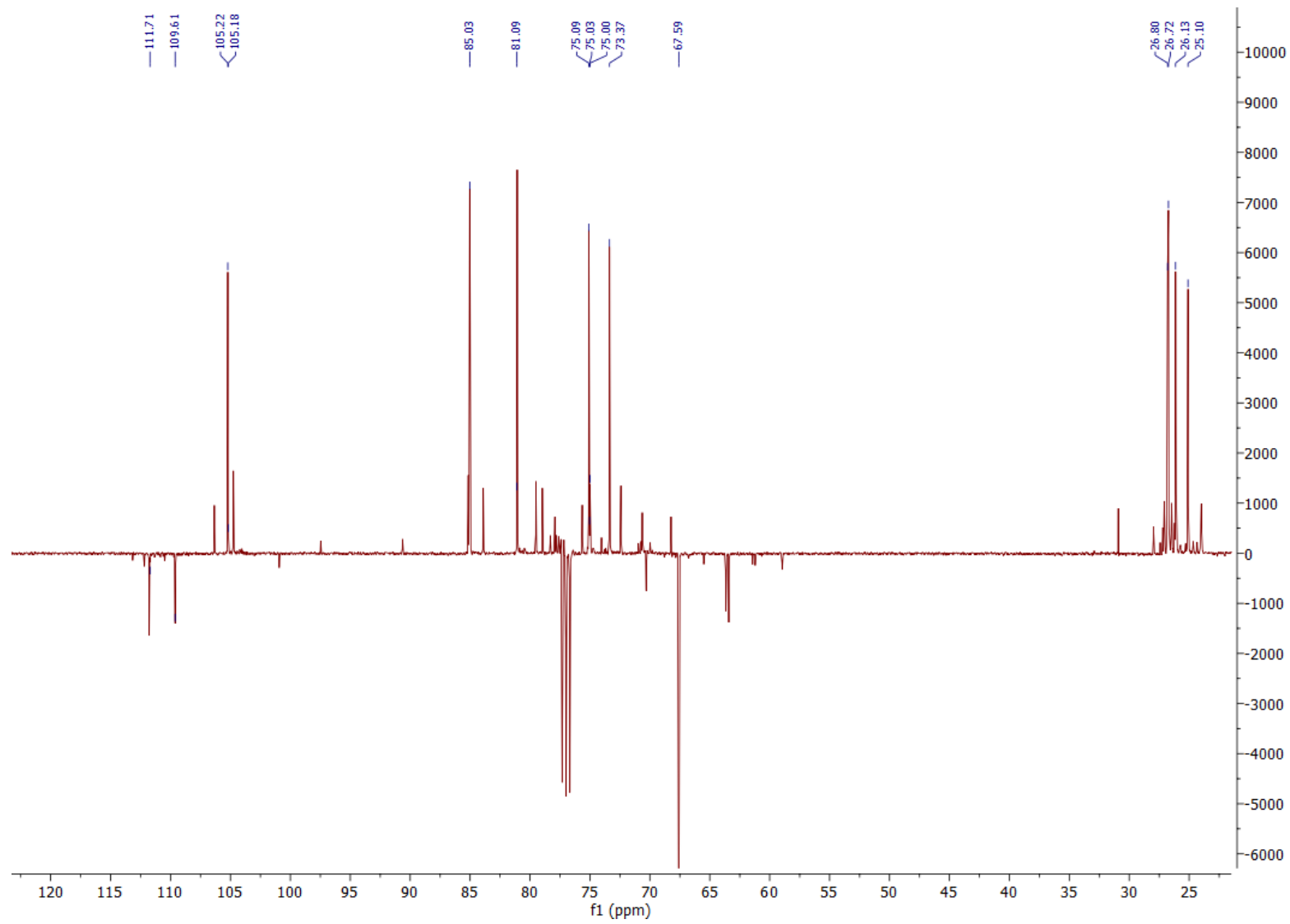


Figure 13: ^{13}C NMR spectrum of 2D.

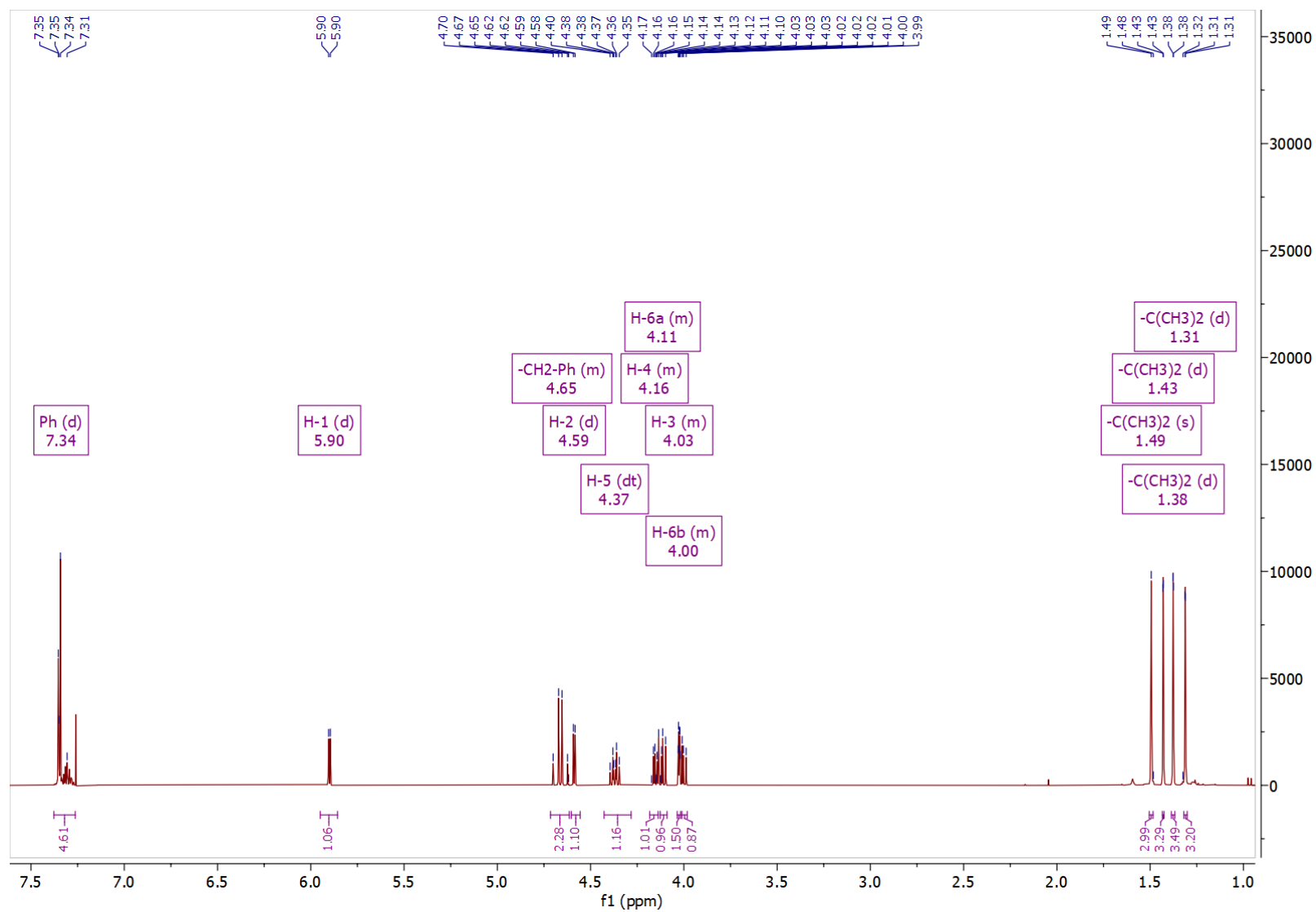


Figure 14: ¹H NMR spectrum of 3D.

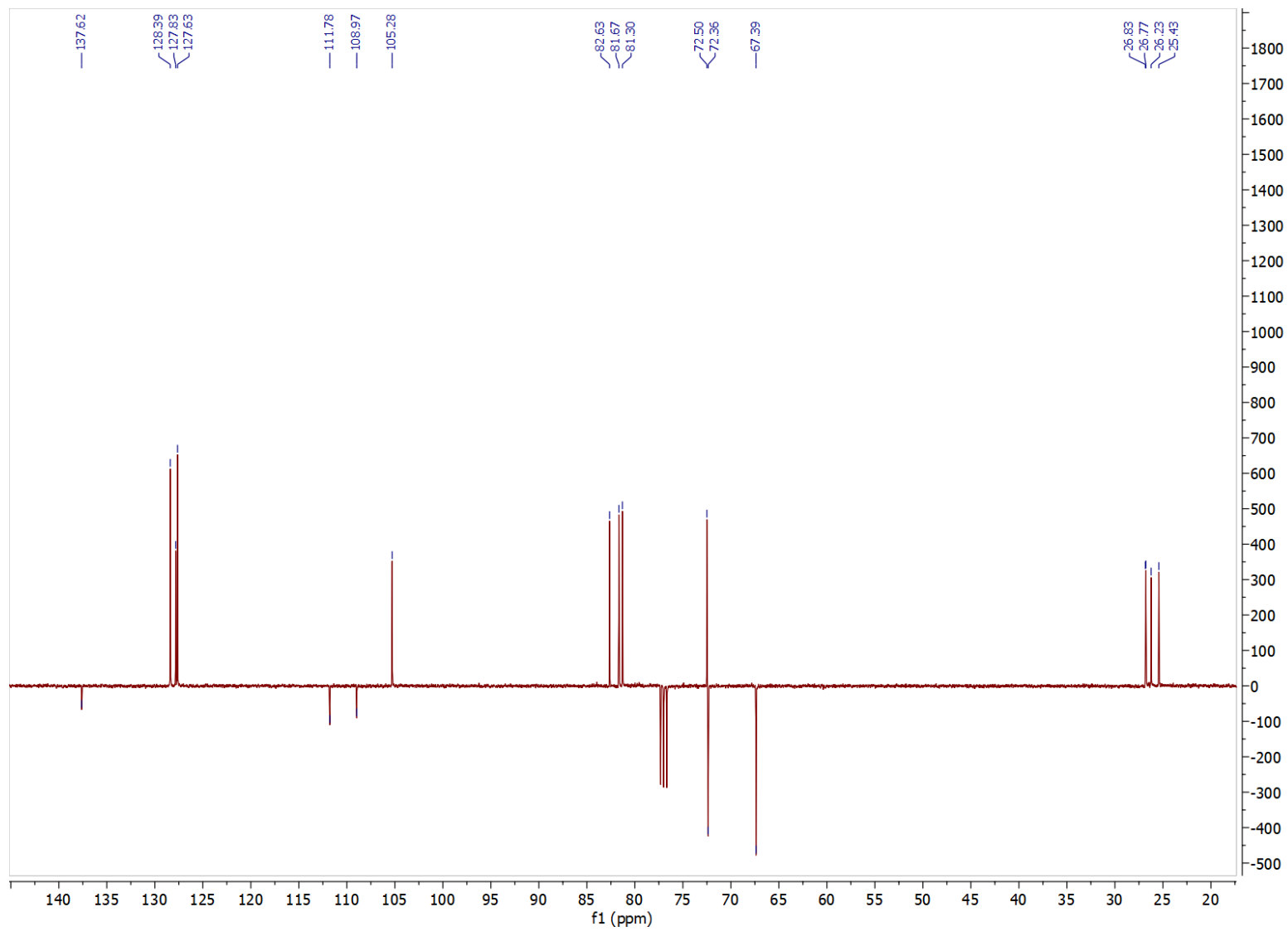


Figure 15: ^{13}C NMR spectrum of 3D.

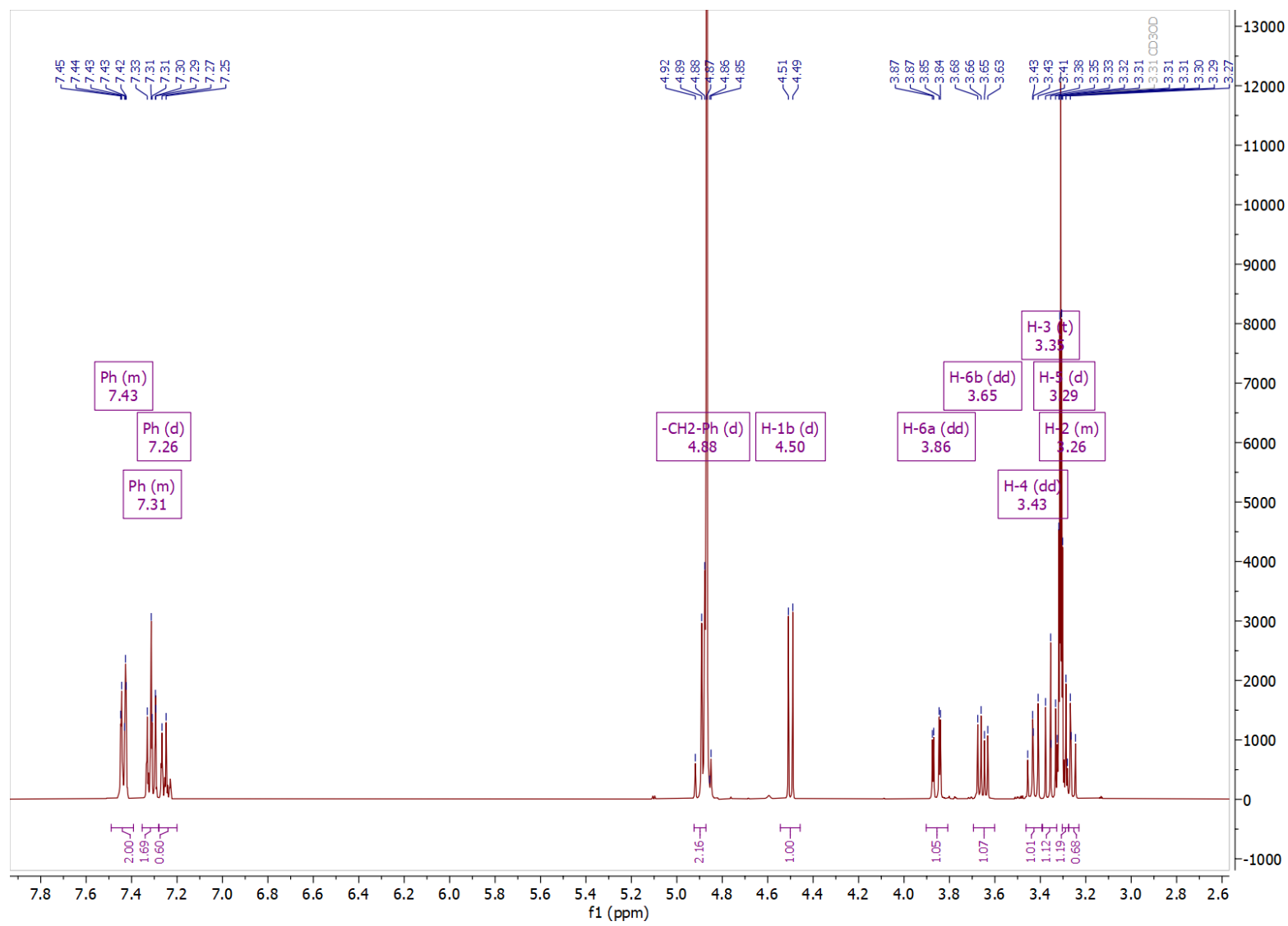


Figure 16: ¹H NMR spectrum of 4D.

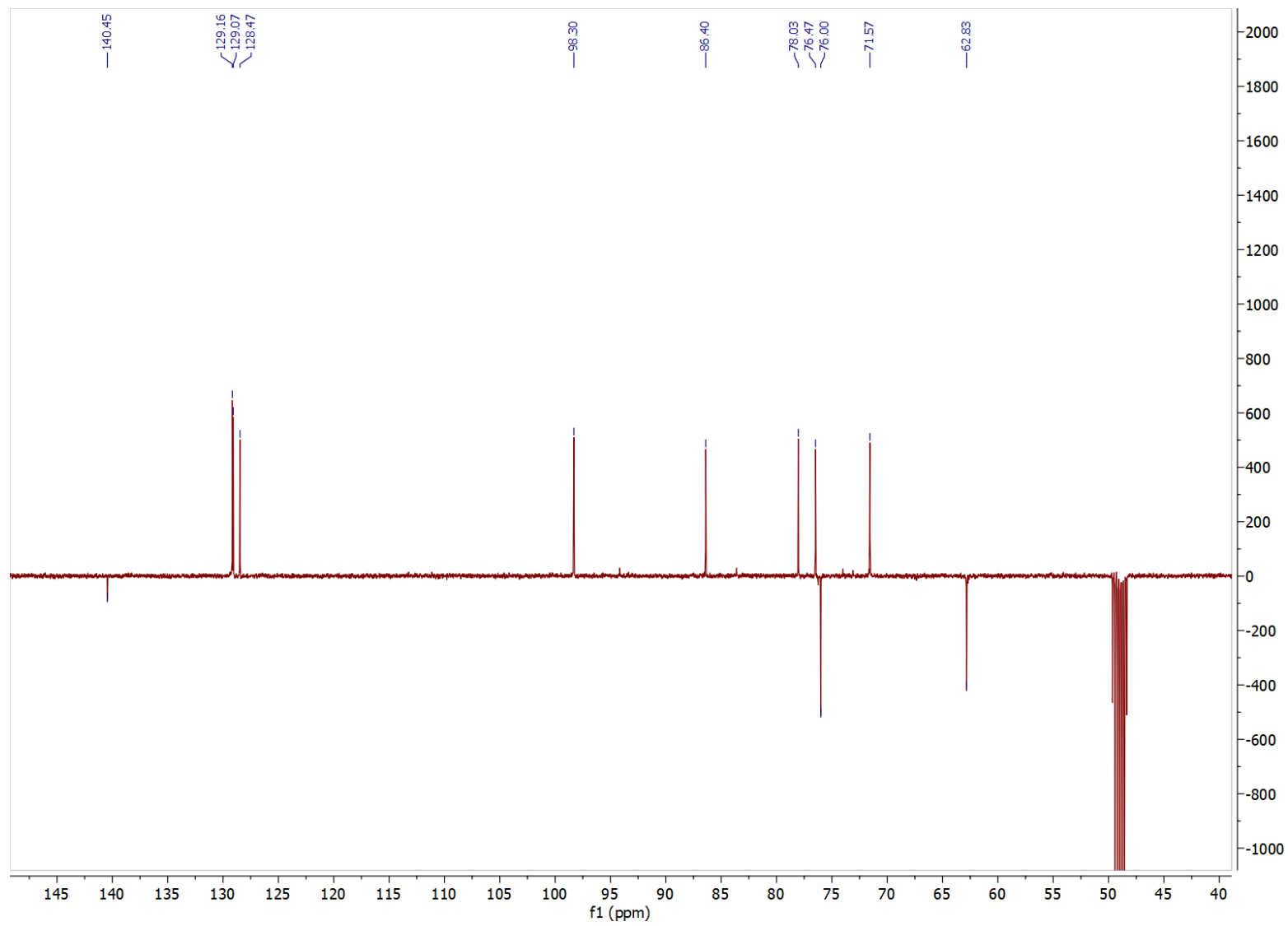


Figure 17: ^{13}C NMR spectrum of 4D.

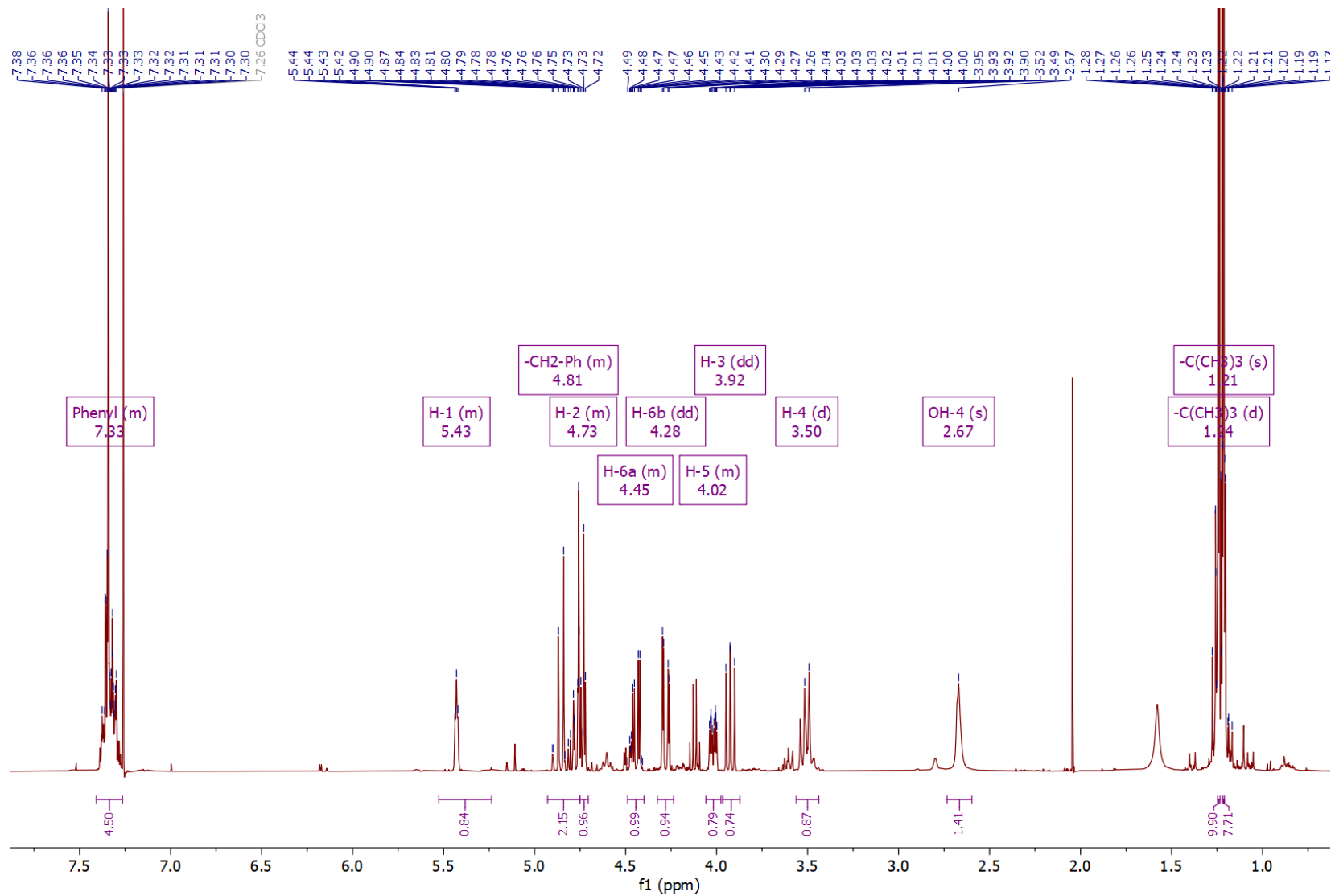


Figure 18: ¹H NMR spectrum of 5D.

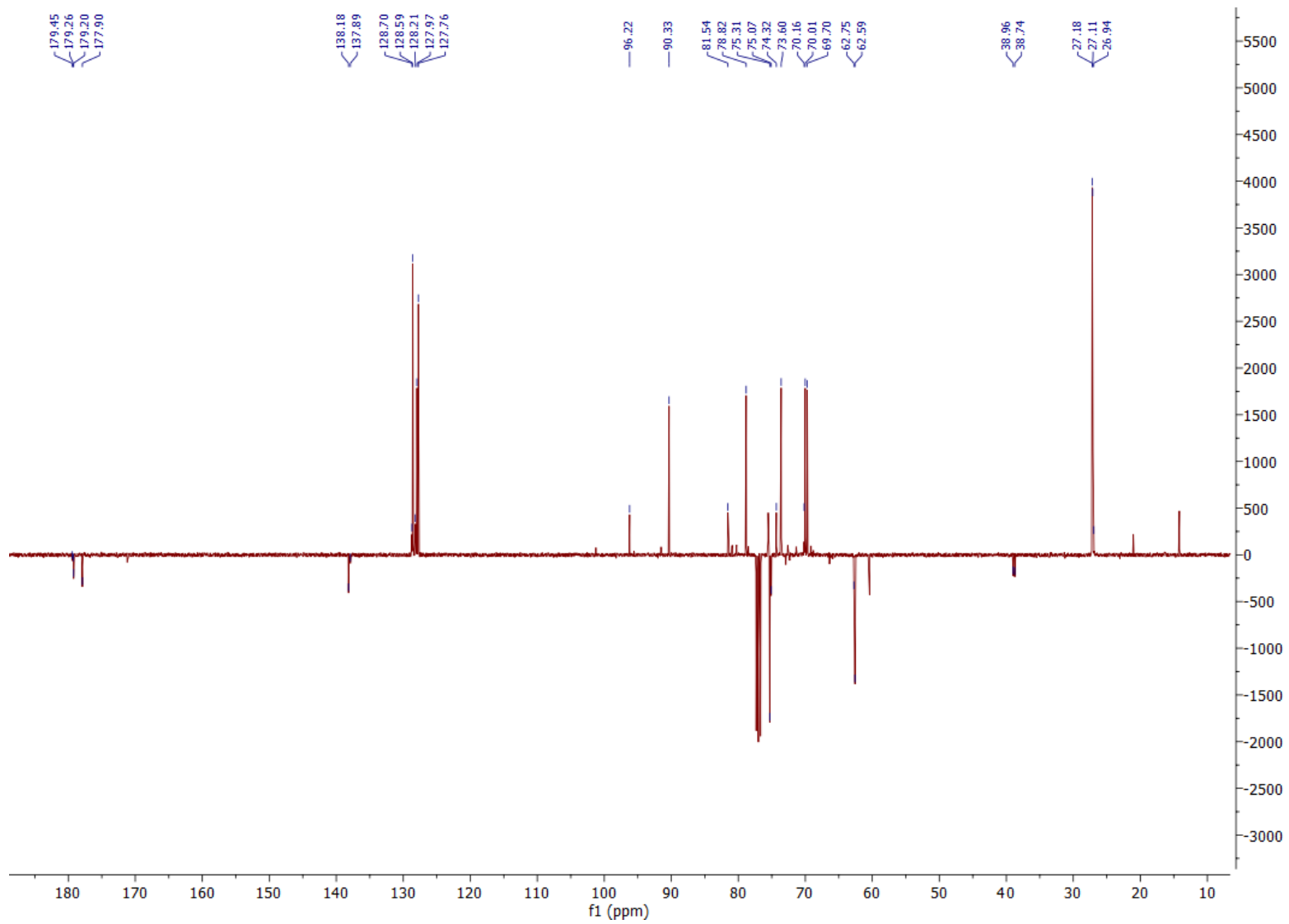


Figure 19: ^{13}C NMR spectrum of 5D.

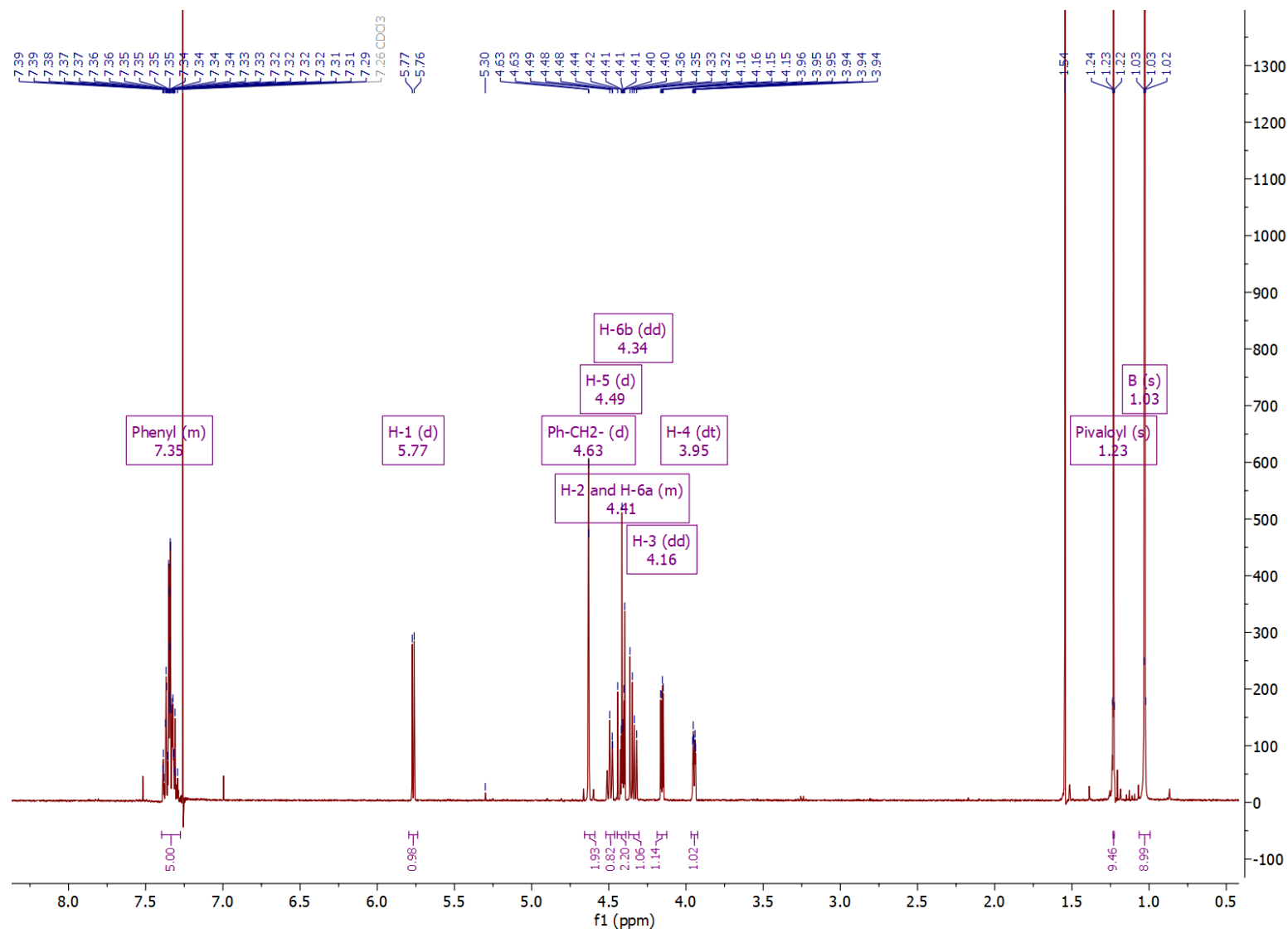


Figure 20: ¹H NMR spectrum of 6D.

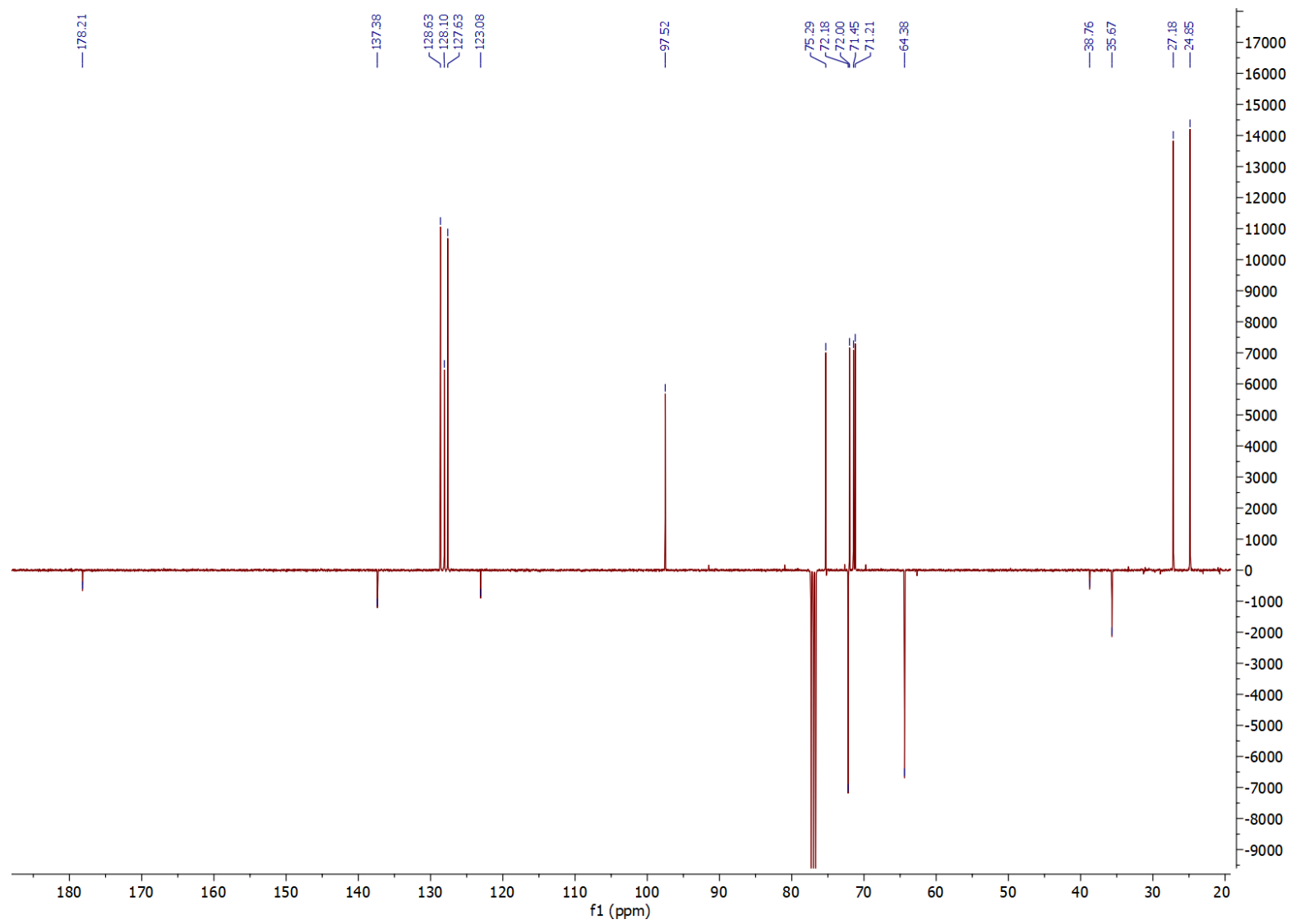


Figure 21: ^{13}C NMR spectrum of 6D.

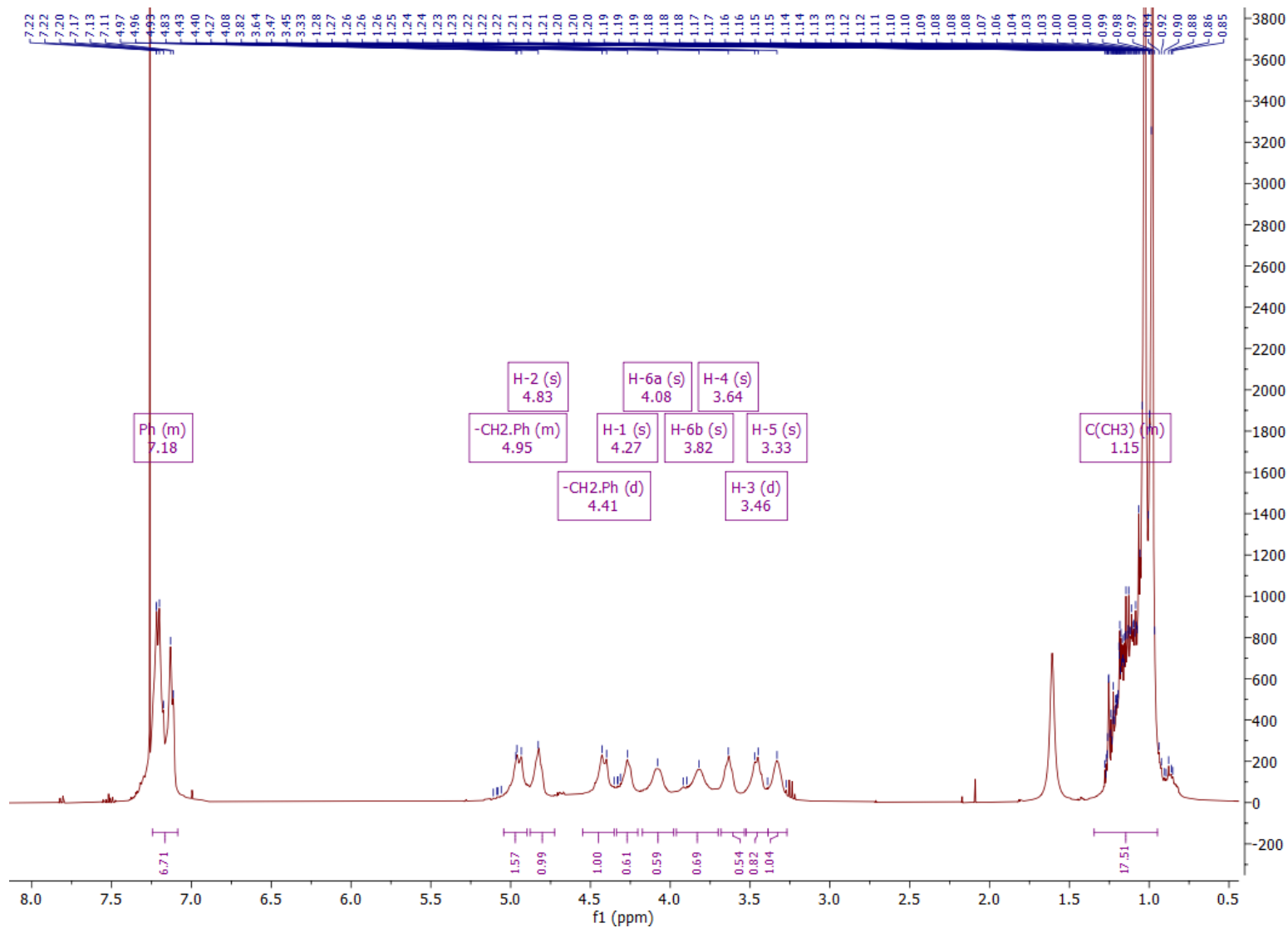


Figure 22: ^1H NMR spectrum of protected 7D.

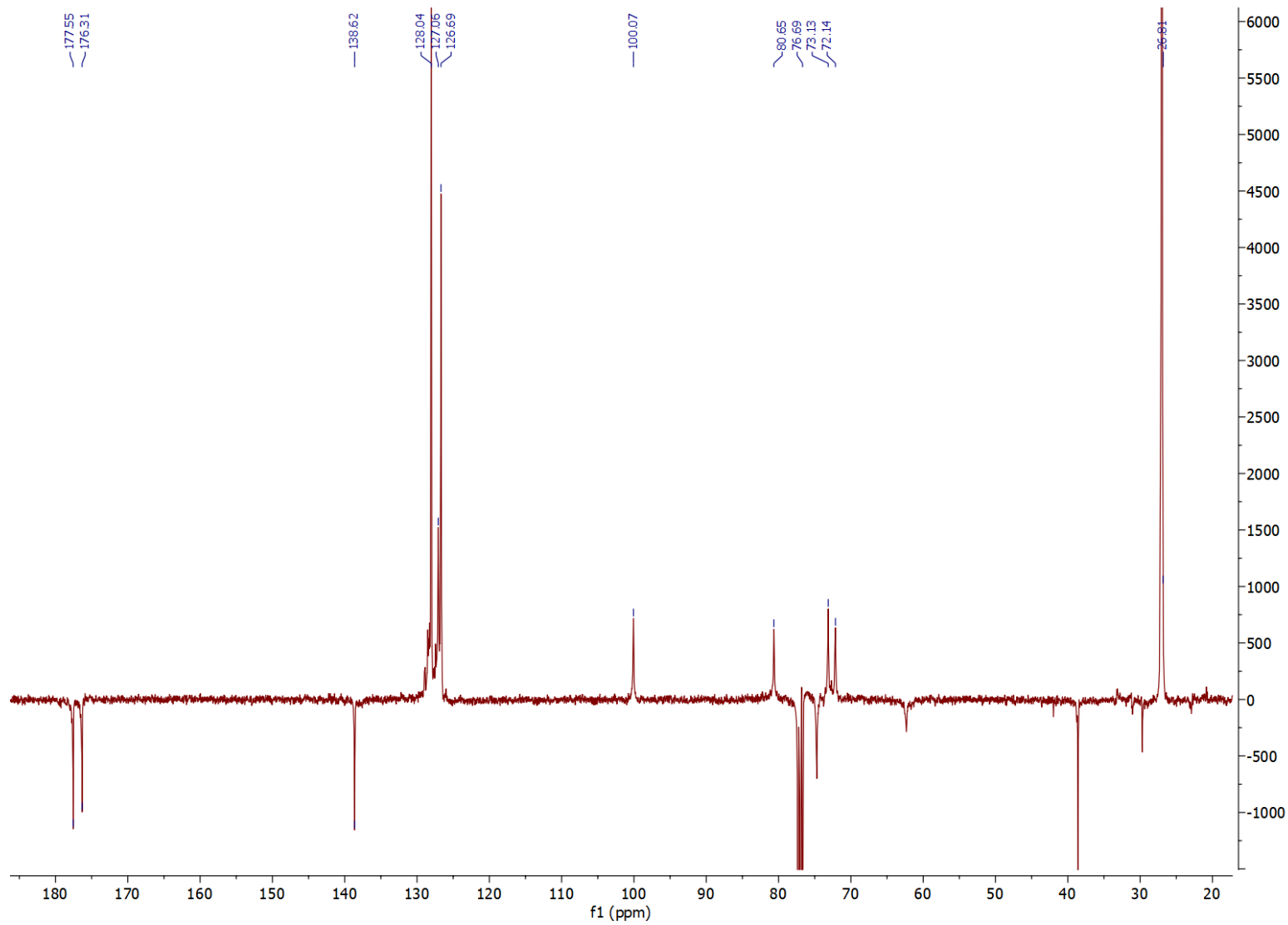


Figure 23: ^{13}C NMR spectrum of protected 7D.

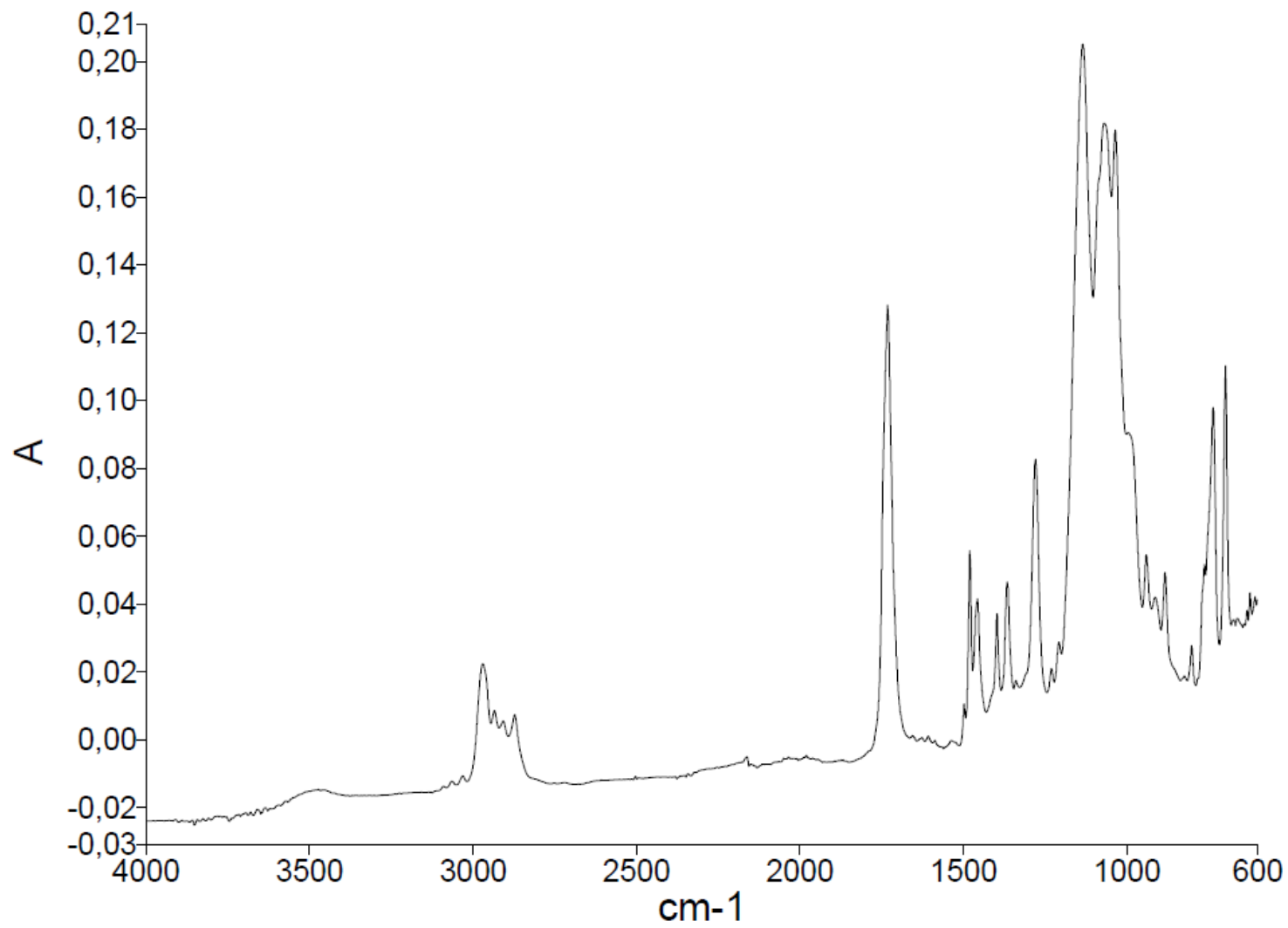


Figure 24: IR spectrum of protected 7D.

AK_016_20001, AK_016_2_weniger E0001
Shimadzu Biotech Axima Performance 2.9.4.1
%Int. 1142 mV 362 mV

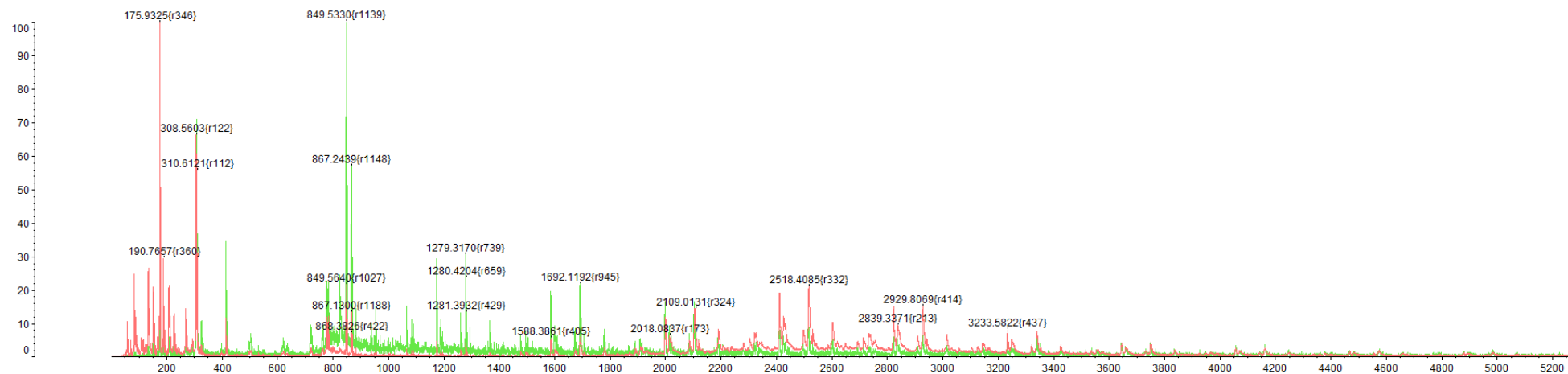


Figure 25: MALDI-TOF spectrum of protected 7D.

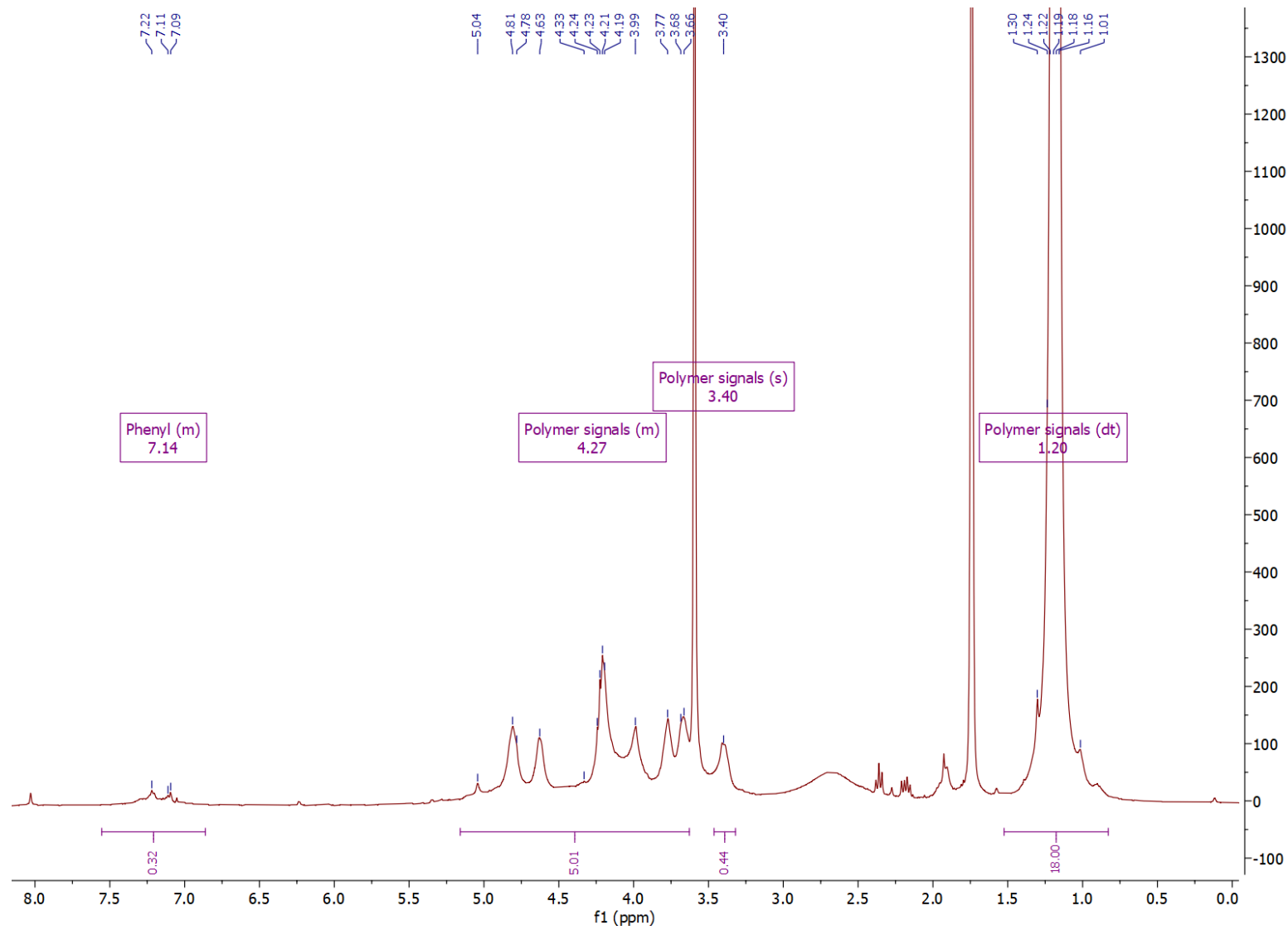


Figure 26: ¹H NMR spectrum of 7D after 1st O-debenzylation.

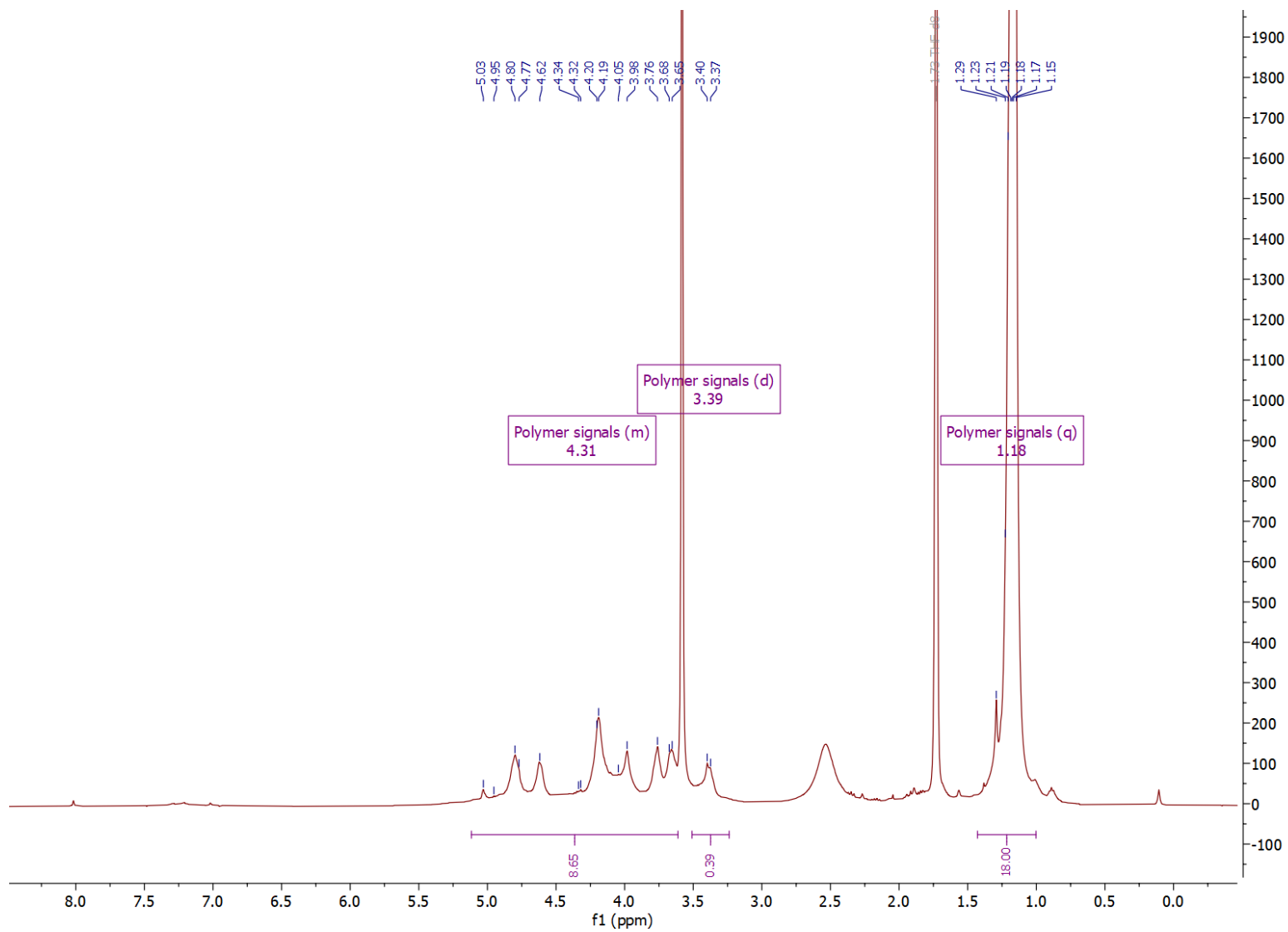


Figure 27: ^1H NMR spectrum of 7D after 2nd O-debenzylation.

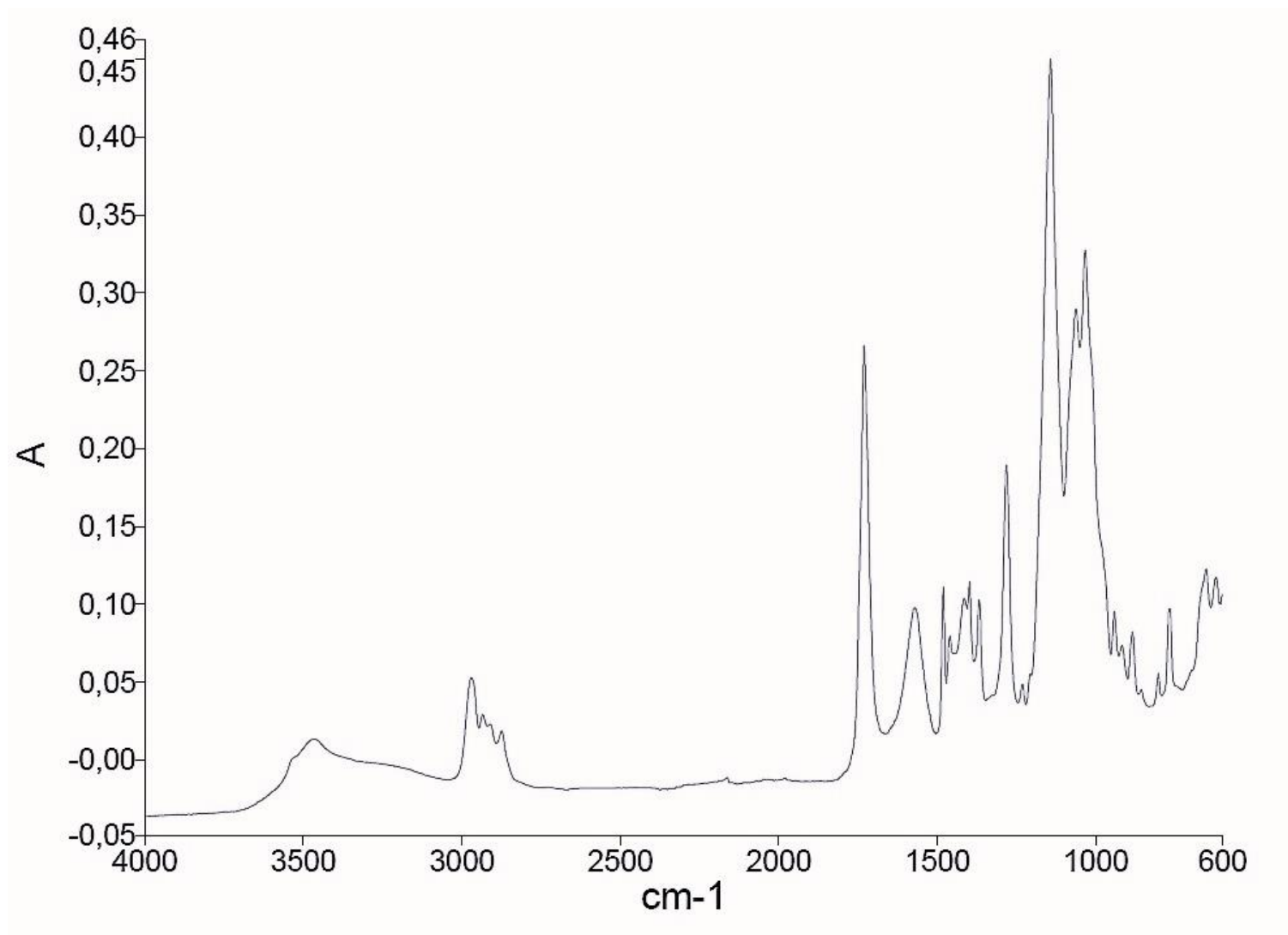


Figure 28: IR spectrum of 7D-2.

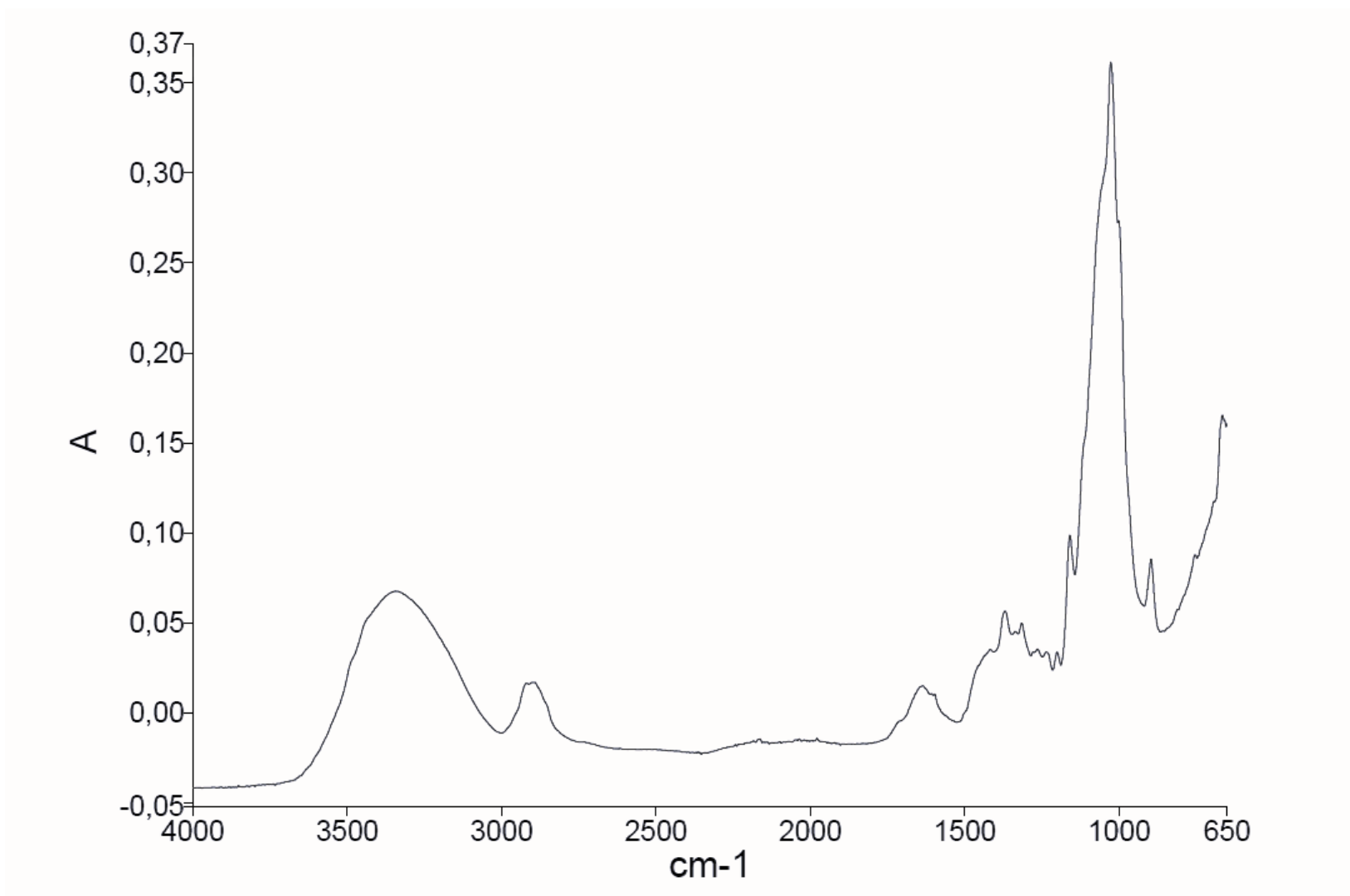


Figure 29: IR spectrum of 8D.

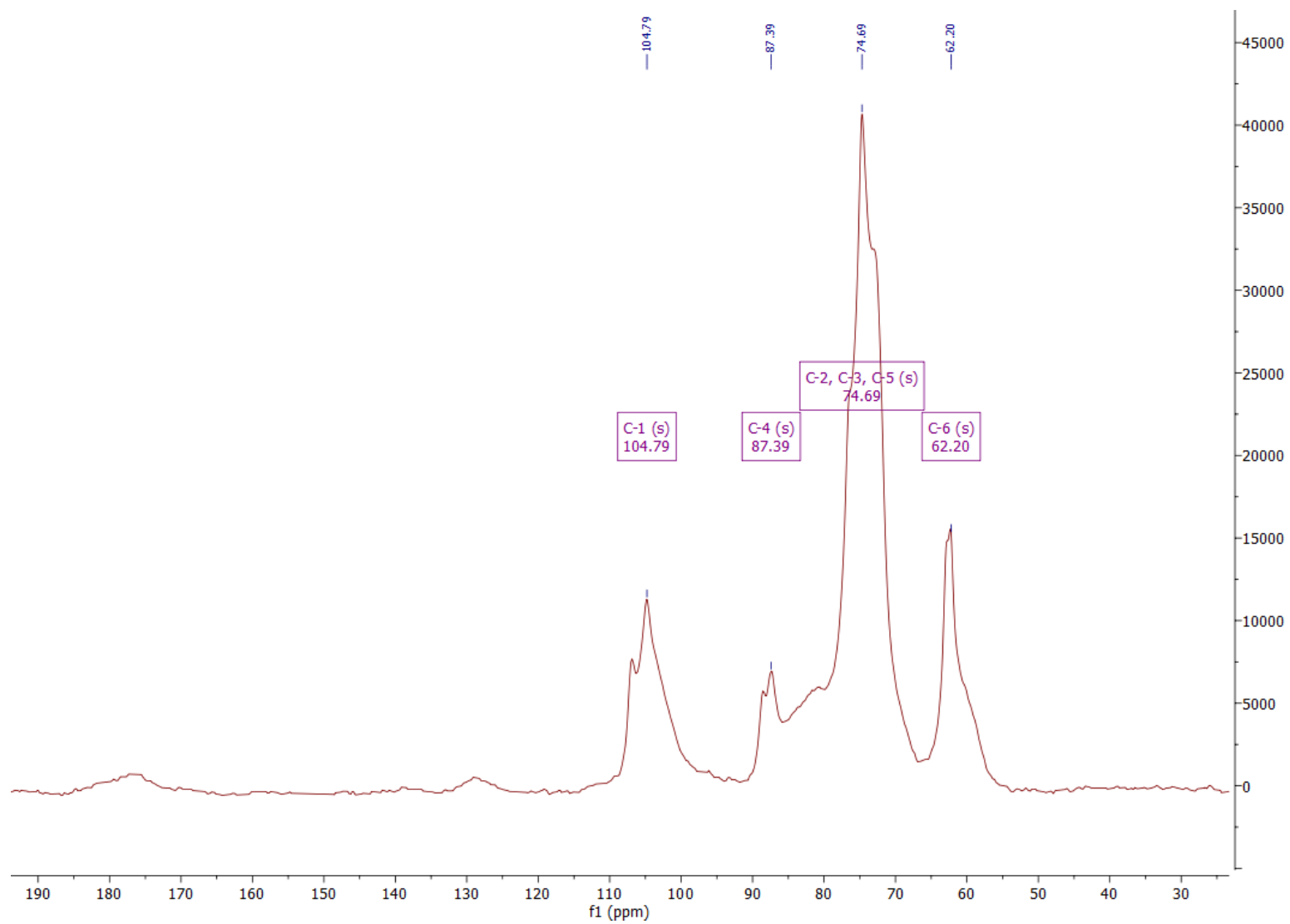


Figure 30: Solid-state ^{13}C NMR spectrum of 8D.

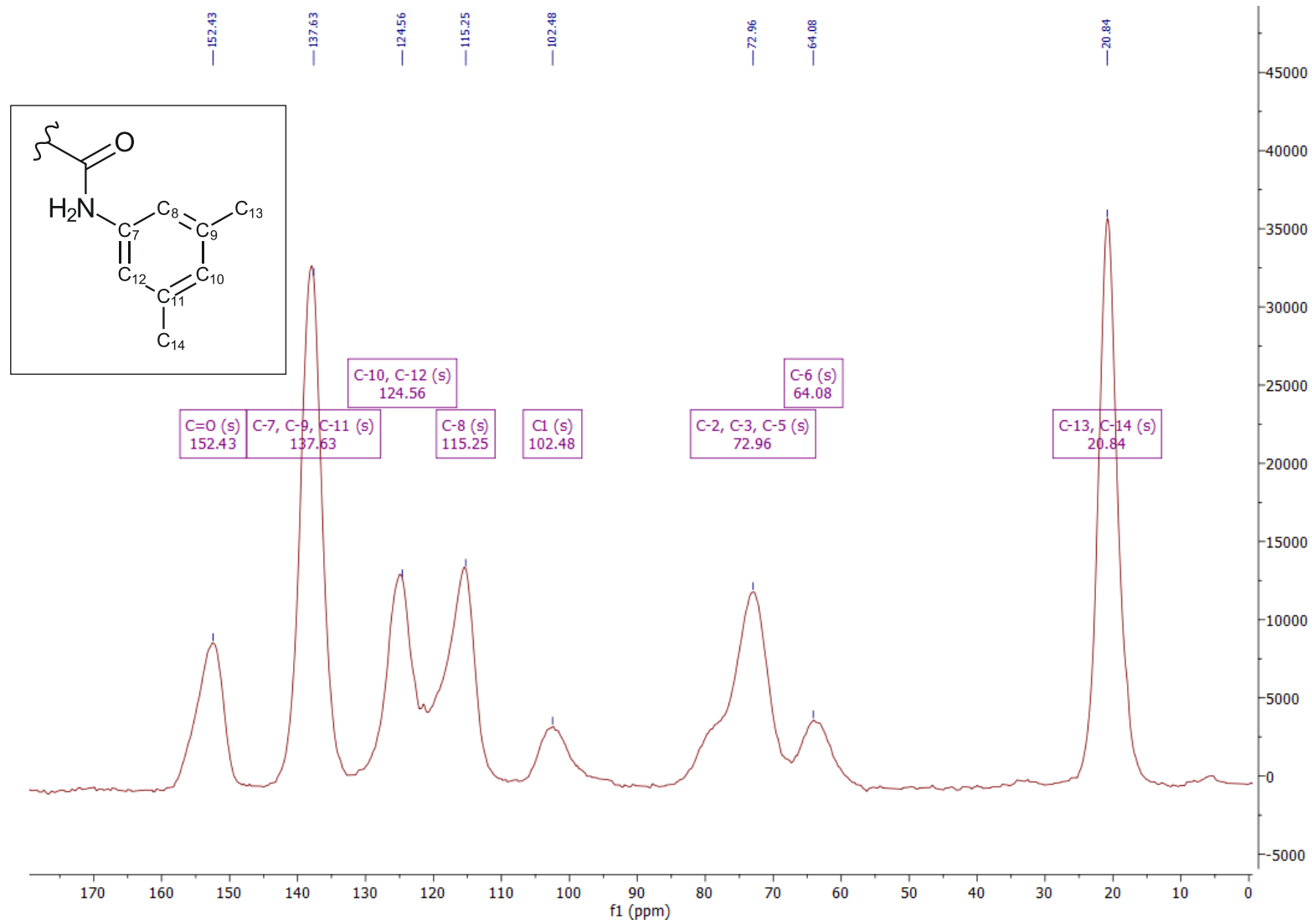


Figure 31: Solid-state ^{13}C NMR spectrum of derivatized Avicel[®].

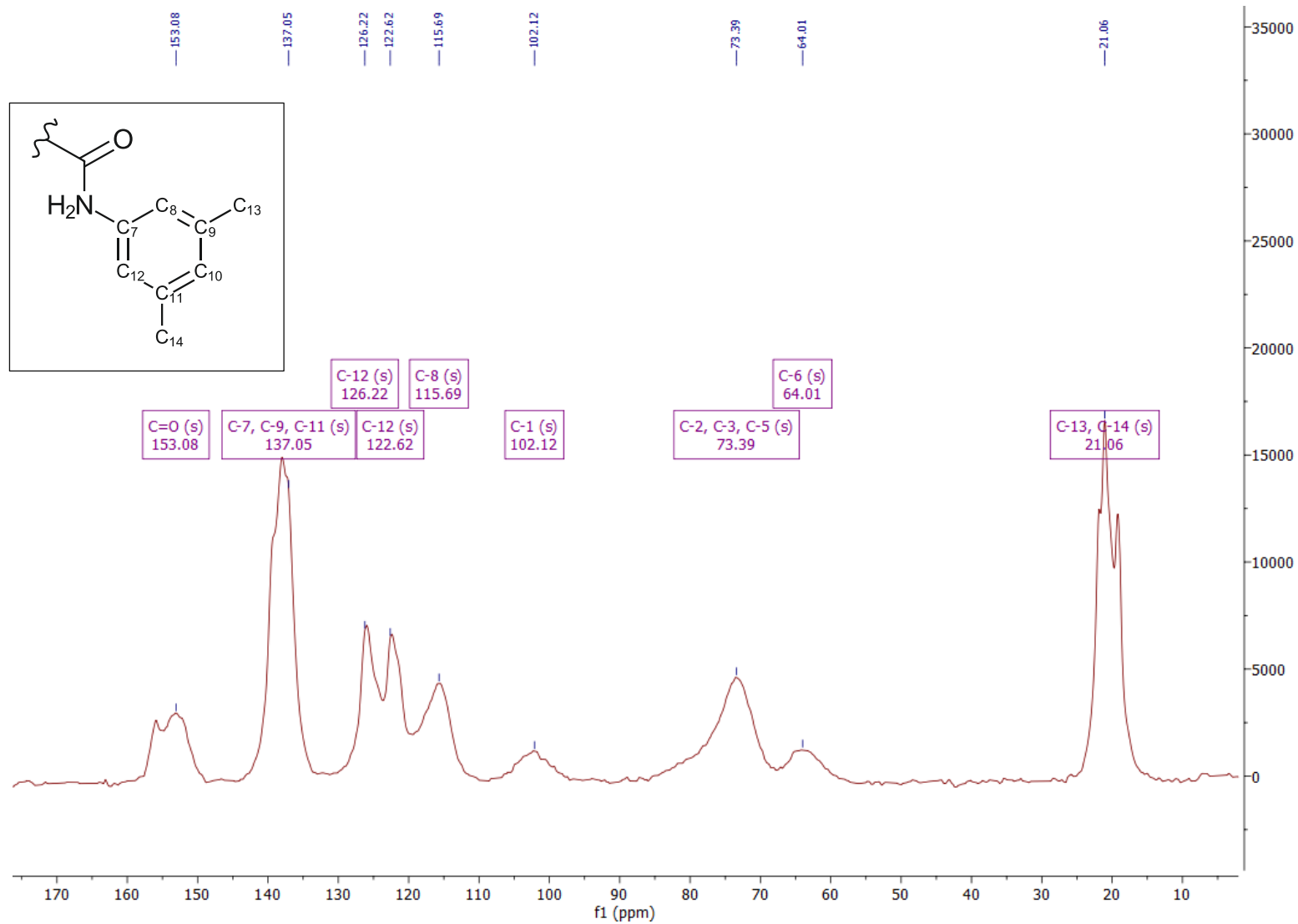


Figure 32: Solid-state ^{13}C NMR spectrum of derivatized scH₂O-hydrolyzed cellulose.

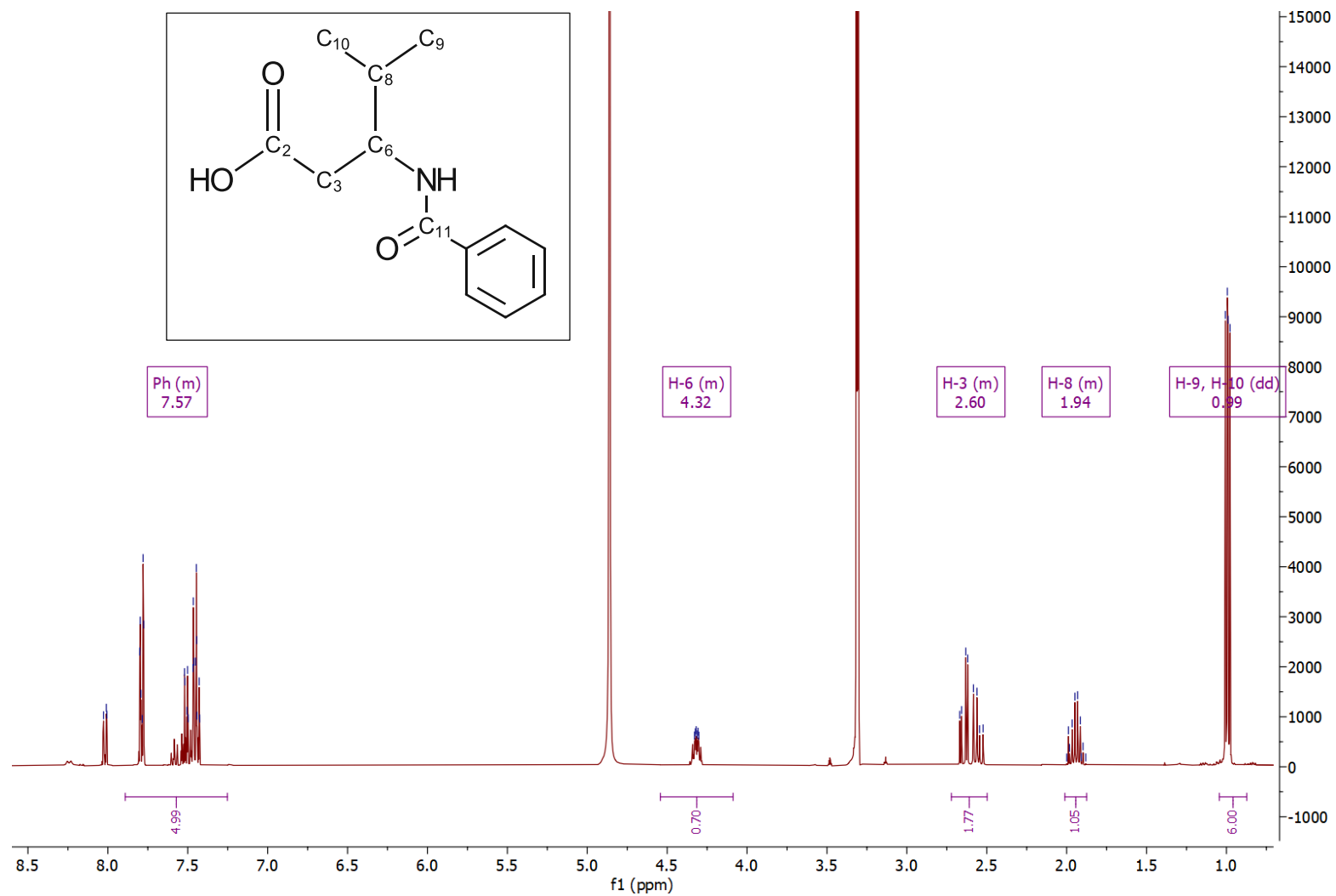


Figure 33: ^1H NMR spectrum of (R,S) -*N*-benzoyl- β -leucine.

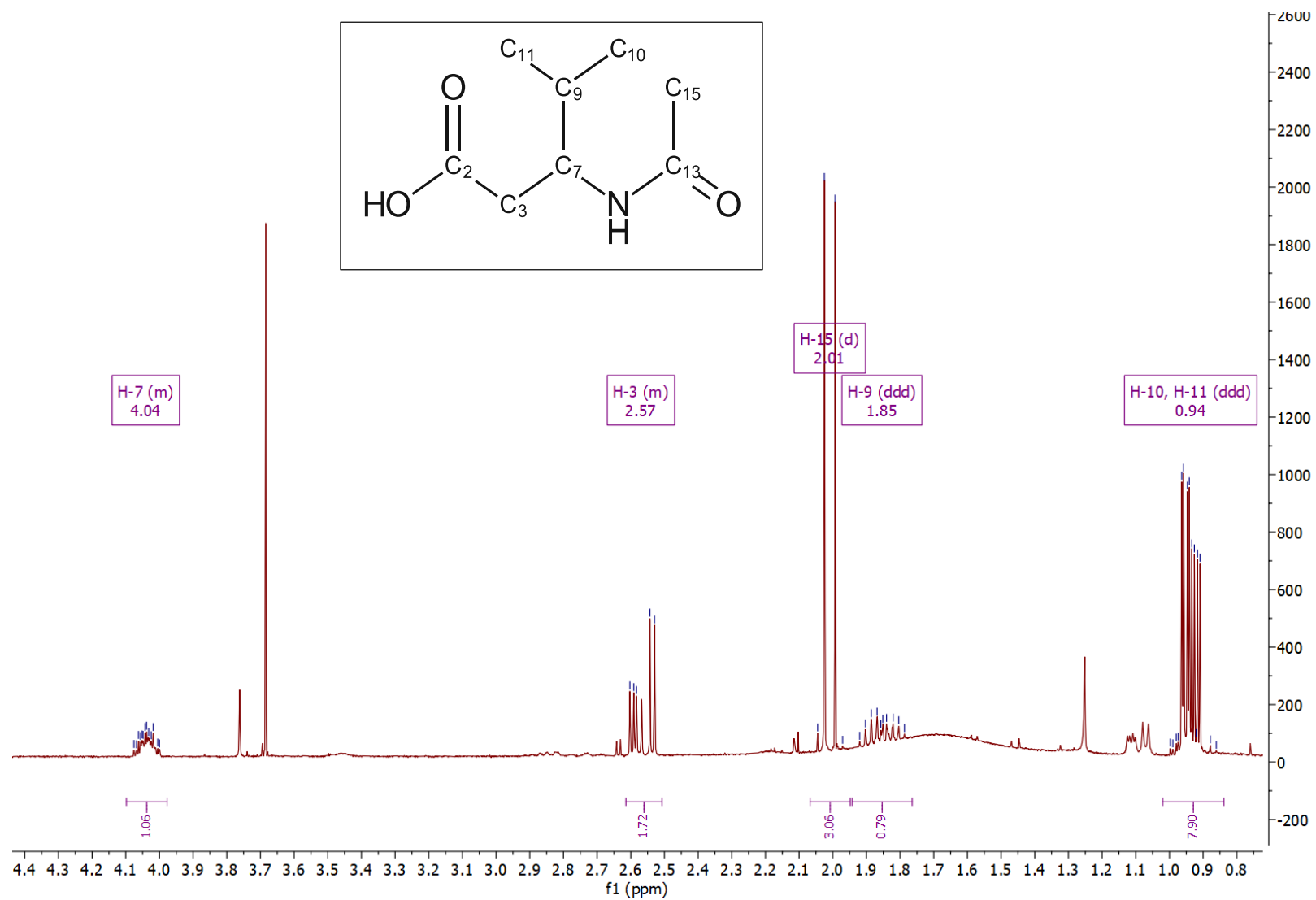


Figure 34: ¹H NMR spectrum of (R,S)-N-acetyl-β-leucine.

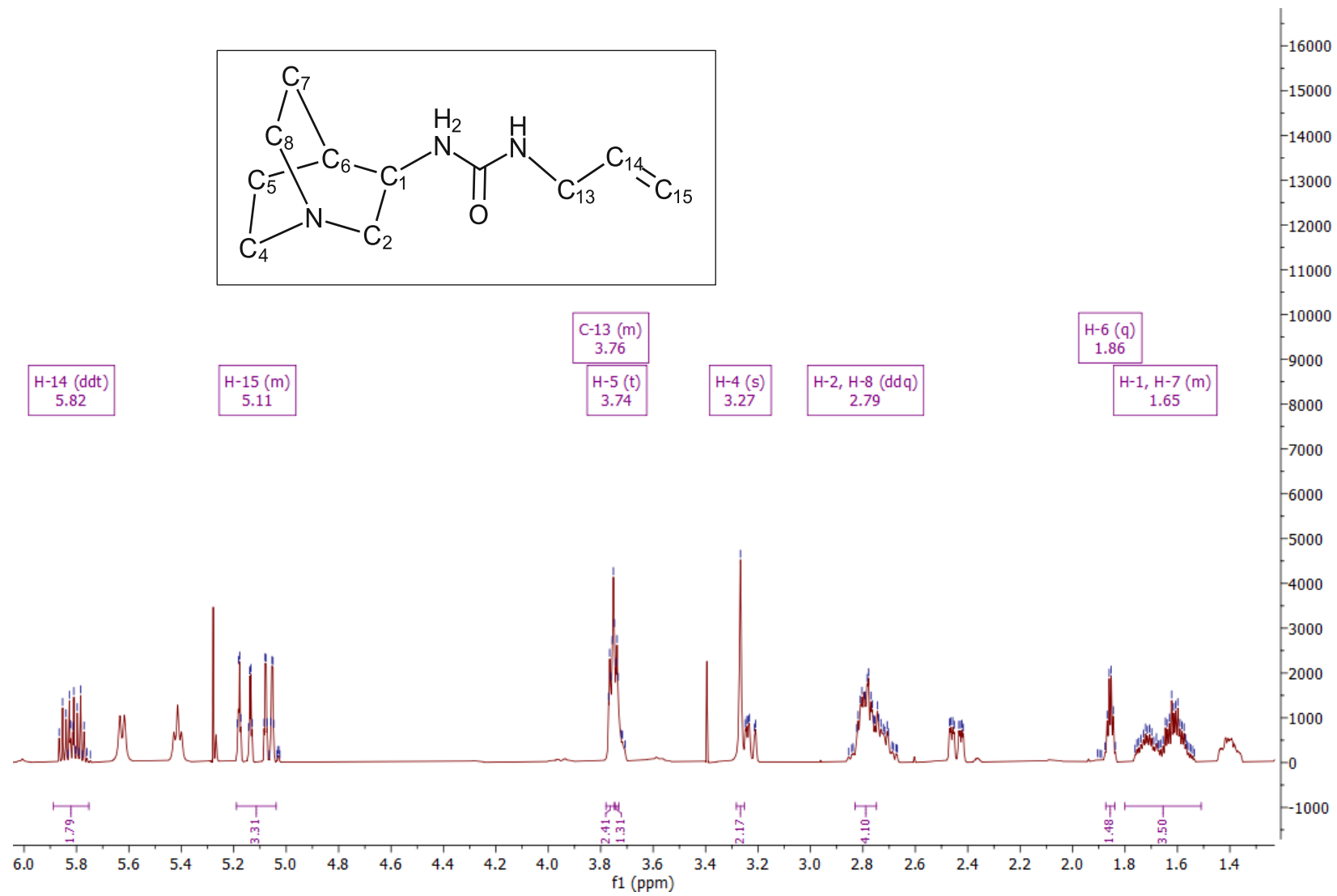


Figure 35: ¹H NMR spectrum of AQ-AX.

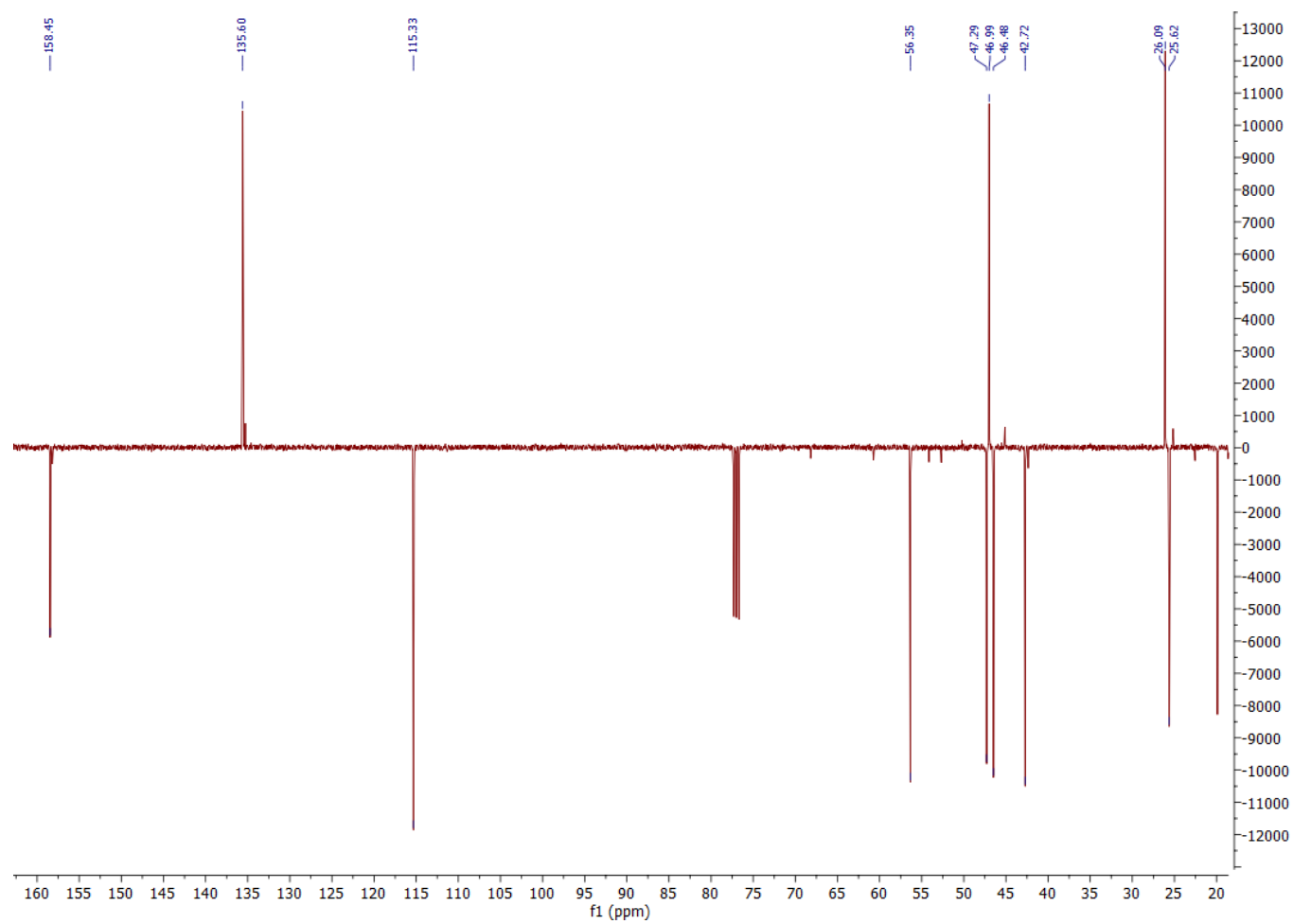


Figure 36: ^{13}C NMR spectrum of AQ-AX.

Curriculum Vitae

Personal Data

Name: Agop Kabrelian
Date of Birth: ■■■■■■■■
Sex: Male
Residence: Vienna, Austria



Technical Skills

Chemistry: HPLC, NMR, Synthesis, Schlenk technique, UV-Vis, GC, MALDI-TOF, IR, GPC
Biochemistry: PCR, electrophoresis, vector cloning, primer design, western blotting
Molecular Biology: Bioassays, Immunoassays, flow cytometry, small animal handling, h1 synergy plate reader, cell culture, DNA, RNA, and protein extraction
Material Science: Polymer coatings, tensiometer, tensile tests, heat sealing tests, colorimetry, pulp analysis
Software & Tools: Mnova Mestrelab, SciFinder®, Design-Expert®, OriginLab®, NCBI, R Studio®, VectorBase, MEGA sequence alignment, BioEdit, Microsoft Office
Character, skills: Curious, communicative, problem-solving, flexible, innovative, fast learner

Education & Qualification

2019 – 2023 **MSc in technical chemistry**, Technical University of Vienna
Thesis: *“Synthesis and evaluation of chiral stationary phases derived from natural compounds for enantiomer separation”*

2015 – 2019 **BSc., Bc in biological chemistry (double degree)**, JKU Linz and University of South Bohemia, Czech Republic
Thesis 1: *“Investigations on the hydrophobization and heat sealing of biogenic fiber materials”*
Thesis 2: *“Reverse pharmacology: Searching for novel drugs in ticks”*

2002 – 2014 **Scientific Baccalaureate according to French education standards** equivalent to Austrian “mit Auszeichnung”, AGBU high school, Aleppo, Syria

Work Experience

10/2021 – 07/2022 Analytical methods development, IMC Krems
10/2020 – 07/2022 Co-lecturer in the organic and advanced organic chemistry laboratory, IMC FH Krems
02/2020 – 03/2020 Internship at the Chemistry of Renewable Resources Institute, BOKU, Tulln

02/2019 Internship in Small Scale & Process Dev. Pulp department, Lenzing AG
09/2018 Home office, literature research, Lenzing AG
02/2018 – 01/2019 Research Assistant, Kompetenzzentrum Holz GmbH, Linz
10/2017 – 06/2019 Teaching assistant in analytical, inorganic, and general laboratories, JKU Linz
 Tutoring chemical calculations and mathematics for chemists, JKU, Linz
09/2017 Research assistant, Pharma. and Toxicology Department, VetMedUni, Vienna

Grants, Awards & Honors

2017 JKU study abroad excellence award for an exchange year in the Czech Republic
2015 – 2018 AGBU international scholarship
2016 – 2017 Erasmus+ exchange program at the University of South Bohemia by OEAD
2016 – 2017 Student grant agency (SGA) scientific award in Science Faculty of the University of South Bohemia, for the research project, “*Reverse pharmacology: Searching for novel drugs in ticks*” supporting bachelor thesis research in the University of South Bohemia

Languages

Armenian:	Native speaker	Arabic:	Native speaker
English:	Fluent C1	German:	Fluent C1
French:	Basic A2		

Interests & Hobbies:

Hobbies: Table tennis, acting, chess, violin
Interests: History, science, geography

Date: January 2023

Signature:

